Faculdade de Ciências e Tecnologia da Universidade de Coimbra

Raw Paper Functionalization for the development of a security paper

MARIA PASCOAL RODRIGUES DE TÒVAR FARO

Dissertação no âmbito do Mestrado em Química Forense, orientada pelo Professor Doutor Artur José Monteiro Valente, coorientada pelo Professor Doutor Alberto António Caria Canelas Pais e pela Professora Doutora Dina Maria Bairrada Murtinho e apresentada ao Departamento de Química da Faculdade de Ciências e Tecnologia da Universidade de Coimbra.

1 2 9 0

UNIVERSIDADE D COIMBRA

Setembro de 2019

"The world of fluorescence is a world of beautiful colour. In the darkness all the ordinary colours of our daylight world disappear. Only the intensely glowing hues of fluorescent substances touched by the ultraviolet beam shine out with striking clarity."

(Sterling Gleason, 1960)

Agradecimentos

A realização desta tese de Mestrado teve muitos apoios a quem devo o meu especial agradecimento.

Em primeiro lugar, gostaria de agradecer ao Professor Doutor Artur Valente por me ter dado a oportunidade de integrar o seu grupo de trabalho, por todo o conhecimento científico que me foi passado durante o período de realização deste projeto, pela oportunidade de ter participado no congresso RICI8 com a realização de um poster, bem como das atividades "extra-curriculares" que permitiram uma boa integração no grupo de trabalho.

Gostaria também de agradecer aos Professores Doutores Alberto Canelas e Dina Murtinho pela disponibilidade e coorientação.

A todas as pessoas do RAIZ, responsáveis do projeto Inpactus, que sempre se mostraram disponíveis para o esclarecimento de qualquer dúvida, por me terem incentivado a fazer um bom trabalho e a ser crítica em relação ao mesmo, o meu sincero agradecimento.

Agradeço também ao Alan, que me ajudou não só no início, mas durante todo o processo de desenvolvimento desta tese.

Aos meus colegas de laboratório, Ana, Carmine, Gianluca, Joana, Jussara, Nacho, Roberto, agradeço por todos os momentos de partilha de ideias, por todas as horas de almoço, jantares e momentos que partilhámos juntos. À Ana e ao Roberto fica um agradecimento especial pela paciência e por todo o conhecimento que me transmitiram em relação ao projeto e à área do papel em particular. Aos restantes, obrigada por me aturarem no dia-a-dia de laboratório e por toda a ajuda e disponibilidade.

Aos meus colegas de curso, em especial aos que me acompanharam durante o ano de tese: Elisa, Mel, Patrícia e Ulisses. Obrigada por todas as horas de almoço, jantares e saídas em que partilhámos medos e receios, mas acima de tudo pela troca mútua de incentivos para que saíssemos vitoriosos desta fase da nossa vida.

À minha amiga principal, Catarina Páscoa, obrigada por todo o apoio e por toda a paciência que tens comigo sempre, mas em especial durante o período de tese.

Por último, mas não menos importante, agradeço à minha família por todo o apoio e incentivo durante toda a minha vida académica.

Funding

This work was carried out under the Project inpactus – innovative products and technologies from eucalyptus, Project N. ° 21874 funded by Portugal 2020 through European Regional Development Fund (ERDF) in the frame of COMPETE 2020 n°246/AXIS II/2017.

Table of Contents

Agradecimentos i
Funding iii
Table of Contents v
Index of Figures vii
Index of Tables xiii
Abstract xv
Resumo xvii
Abbreviation List xix
1. INTRODUCTION 1
1.1 Luminescence Processes 2
1.2 Rare Earth Elements 4
1.3 Luminescent Lanthanide Materials in Security Tagging 6
1.4 Nanophosphors 7
1.5 Lanthanide Polymer Complexes 12
1.6 Paper industry 14
2. EXPERIMENTAL PART 19
2.1 Materials and Reagents 19
2.2 General methods 20
2.3 Synthesis 20
2.4 Paper analysis 22
3. RESULTS AND DISCUSSION 27
3.1 Synthesis of luminescent lanthanide polymer complexes 27
3.2 Paper analysis 46
4. CONCLUSION 71
5. FUTURE PERSPECTIVES 75
6. REFERENCES 79

7. SUPPLEMENTARY INFORMATION 83
7.1 Pure lanthanide solutions 83
7.2 Lanthanide polymer complexes 83
7.3 Reaction of Lanthanide polymer complexes solutions with metals 84
7.4 Influence of the anion on the emission of Lanthanide polymer complex solutions 88
7.5 Detection limit of copper and nickel solutions 90
7.6 Costs Information 110

Index of Figures

Figure 1. Representation of a Jablonski Diagram (adapted from reference 41)..... 3
Figure 2. Extract of Periodic Table elements: the Lanthanides..... 4
Figure 3. Possible applications for Lanthanide Luminescent Materials..... 6
Figure 4. Schematic representation of an Excited State Absorption (ESA) mechanism. Green lines represent absorption and red lines emission. (Adapted from reference 17). 8
Figure 5. Schematic representation of an Energy Transfer Upconversion (ETU) mechanism. Green lines represent absorption, red lines emission and dashed lines energy transfer. (Adapted from reference 17)..... 8
Figure 6. Schematic representation of a Cooperative Sensitization mechanism. Green lines represent absorption, red lines emission and dashed lines energy transfer. (Adapted from reference 16). 9
Figure 7. Schematic representation of a Cooperative Luminescence mechanism. Green lines represent absorption, red lines emission and dashed lines energy transfer. (Adapted from reference 5)..... 10
Figure 8. Schematic representation of a Cross Relaxation Upconversion (CRU) mechanism. Green lines represent absorption, red lines emission and dashed lines energy transfer. (Adapted from reference 16)..... 10
Figure 9. Schematic representation of a Photon Avalanche (PA) mechanism. Green lines represent absorption, red lines emission and dashed lines energy transfer. (Adapted from reference 16). 11
Figure 10. Schematic representation of a Downconversion (DC) mechanism. Green lines represent absorption, red lines emission and dashed lines energy transfer. (Adapted from reference 5)..... 11
Figure 11. Schematic representation of the antenna effect between the ligand and the lanthanide ion. (Adapted from reference 26). 12
Figure 12. Chemical structure of the commonly used low molecular organic ligands. . 13
Figure 13. Emission spectrum of an aqueous solution of $EuCl_3.6H_2O$ (0.05 M) (λexc = 344 nm). 28
Figure 14. Emission spectrum of an aqueous solution of $EuCl_3.6H_2O$ (0.05 M) and a EuPSANapPhen (EtOH:H_2O) solution (λexc = 344 nm). 29

Figure 15. Emission spectrum of an aqueous solution of $TbCl_3.6H_2O$ (0.05 M) (λexc = 344 nm). 30
Figure 16. Emission spectrum of a TbPSANapPhen (EtOH:H_2O) solution and an aqueous solution of $TbCl_3.6H_2O$ (0.05 M) (λ exc = 344 nm). 30
Figure 17. Appearance of EuPSANapPhen (a) and TbPSANapPhen (b) aqueous solutions after reaction with different metal ions. 31
Figure 18. Emission spectra of solutions of EuPSANapPhen (EtOH:H_2O) in the presence of different metal ions (λexc = 344 nm) 32
Figure 19. Emission spectra of solutions of EuPSANapPhen (EtOH:H_2O) in the presence of Cu and Ni (λexc = 344 nm). 33
Figure 20. Quenching efficiency (%) of EuPSANapPhen-metal solutions (616 nm). 34
Figure 21. Photographs of EuPSANapPhen aqueous solutions in the presence of metal ions, under UV excitation at 366 nm. 34
Figure 22. Emission spectra of solutions of TbPSANapPhen (EtOH:H_2O) in the presence of several metal ions (λexc = 344 nm). 35
Figure 23. Emission spectra of solutions of TbPSANapPhen (EtOH:H_2O) in the presence of Cu and Ni, (λexc = 344 nm). 35
Figure 24. Photographs of TbPSANapPhen aqueous solutions in the presence of metal ions, under UV excitation at 366 nm. 36
Figure 25. Quenching efficiency (%) of TbPSANapPhen-metal solutions (543 nm) 37
Figure 26. Emission spectra of solutions of EuPSANapPhen (EtOH:H_2O) in the presence of different sodium salts (λexc = 344 nm). 38
Figure 27. Quenching efficiency (%) of EuPSANapPhen-sodium salts (616 nm) 39
Figure 28. Emission spectra of solutions of TbPSANapPhen (EtOH:H_2O) in the presence of different sodium salts (λexc = 344 nm). 40
Figure 29. Quenching efficiency (%) of TbPSANapPhen-sodium salts (543 nm). 41
Figure 30. Emission spectra of EuPSANapPhen solutions (EtOH:H_2O) in the presence of $Cu(NO_3)_2$ in the concentrations from 0.02 mM to 2 mM (λexc = 344 nm) 42
Figure 31. Dependence of the emission intensity of EuPSANapPhen ($^5D_0 \rightarrow ^7F_2$ transition) / Cu(II) mixed solutions on the Cu(II) concentration. 43
Figure 32. Stern-Volmer plot of EuPSANapPhen-Cu $^5D_0 \rightarrow ^7F_2$ transition (616 nm), vs Cu concentration. 44
Figure 33. Stamps used for the incorporation of EuPSANapPhen and TbPSANapPhen in paper sheets via the stamping method. 46

Figure 34. Photographs of the three types of paper sheets (filter, base and office) stamped with EuPSANapPhen, at eyesight. 47
Figure 35. Photographs of the three types of paper sheets (filter, base and office) stamped with EuPSANapPhen, under UV radiation (λ = 254 nm). 48
Figure 36. Photographs of the three types of paper sheets (filter, base and office) stamped with TbPSANapPhen, at eyesight. 50
Figure 37. Photographs of the three types of paper sheets (filter, base and office) stamped with TbPSANapPhen, under UV radiation (λ = 254 nm) 51
Figure 38. Photographs of the three types of paper sheets (filter, base and office) immersed in EuPSANapPhen, at eyesight. 52
Figure 39. Photographs of the three types of paper sheets (filter, base and office) immersed in EuPSANapPhen, under UV radiation (λ = 254 nm). 53
Figure 40. Photographs of the three types of paper sheets (filter, base and office) immersed in TbPSANapPhen, at eyesight. 53
Figure 41. Photographs of the three types of paper sheets (filter, base and office) immersed in TbPSANapPhen, under UV radiation (λ = 254 nm) 54
Figure 42. Photographs of the three types of paper sheets (filter, base and office) coated with EuPSANapPhen, at eyesight. 55
Figure 43. Photographs of the three types of paper sheets (filter, base and office) coated with EuPSANapPhen, under UV radiation (λ = 254 nm). 55
Figure 44. Photographs of the three types of paper sheets (filter, base and office) coated with TbPSANapPhen, at eyesight. 56
Figure 45. Photographs of the three types of paper sheets (filter, base and office) coated with TbPSANapPhen, under UV radiation (λ = 254 nm) 57
Figure 46. Photographs of the three types of paper sheets (filter, base and office) stamped with EuPSANapPhen after reaction to Cu and Ni ions, at eyesight. 59
Figure 47. Photographs of the three types of paper sheets (filter, base and office) stamped with EuPSANapPhen after reaction to Cu and Ni ions, under UV radiation (λ = 254 nm). 60
Figure 48. Photographs of the three types of paper sheets (filter, base and office) stamped with TbPSANapPhen after reaction to Cu and Ni ions, at eyesight 61
Figure 49. Photographs of the three types of paper sheets (filter, base and office) stamped with TbPSANapPhen after reaction to Cu and Ni ions, under UV radiation (λ = 254 nm). 61

Figure 50. Photographs of the three types of paper sheets (filter, base and office) immersed in EuPSANapPhen after reaction to Cu and Ni ions, at eyesight. 62
Figure 51. Photographs of the three types of paper sheets (filter, base and office) immersed in EuPSANapPhen after reaction to Cu and Ni ions, under UV radiation (λ = 254 nm). 63
Figure 52. Photographs of the three types of paper sheets (filter, base and office) immersed in TbPSANapPhen after reaction to Cu and Ni ions, at eyesight..... 63
Figure 53. Photographs of the three types of paper sheets (filter, base and office) immersed in TbPSANapPhen after reaction to Cu and Ni ions, under UV radiation (λ = 254 nm). 64
Figure 54. Photographs of the three types of paper sheets (filter, base and office) coated with EuPSANapPhen after reaction to Cu and Ni ions, at eyesight. 65
Figure 55. Photographs of the three types of paper sheets (filter, base and office) coated with EuPSANapPhen after reaction to Cu and Ni ions, under UV radiation (λ = 254 nm). 65
Figure 56. Photographs of the three types of paper sheets (filter, base and office) coated with TbPSANapPhen after reaction to Cu and Ni ions, at eyesight..... 66
Figure 57. Photographs of the three types of paper sheets (filter, base and office) coated with TbPSANapPhen after reaction to Cu and Ni ions, under UV radiation (λ = 254 nm). 66

Figure S 1. Excitation spectrum of an aqueous solution of $TbCl_3.6H_2O$ (λ_{em} = 543 nm). 83
Figure S 2. Excitation spectrum of an aqueous solution of $EuCl_3.6H_2O$ (λem = 616 nm). 83
Figure S 3. Excitation spectrum of the EuPSANapPhen (EtOH:H_2O) solution (λ_{em} = 616 nm). 83
Figure S 4. Excitation spectrum of the TbPSANapPhen (EtOH:H_2O) solution (λem = 543 nm). 83
Figure S 5. Emission spectra of EuPSANapPhen-metals (Ag, Ca, Cr, Cu, K, Mg, Na and Ni, respectively) (EtOH:H_2O) solutions (λ*exc* = 344 nm). 84
Figure S 6. Excitation spectra of EuPSANapPhen-metals (Ag, Ca, Cr, Cu, K, Mg, Na and Ni, respectively) (EtOH:H_2O) solutions (λem = 616 nm). 85
Figure S 7. Emission spectra of TbPSANapPhen-metals (Ag, Ca, Cr, Cu, K, Mg, Na and Ni, respectively) (EtOH:H_2O) solutions (λexc = 344 nm)..... 86

Figure S 8. Excitation spectra of TbPSANapPhen-metals (Ag, Ca, Cr, Cu, K, Mg, Na and Ni, respectively) (EtOH:H_2O) solutions (λem = 543 nm). 87
Figure S 9. Emission spectra of EuPSANapPhen-sodium salts (NaBr, NaCl, NaF, NaI, $NaNO_2$, $NaNO_3$, NaOAc, NaOH, and Na_2SO_4, respectively) (EtOH:H_2O) solutions (λexc = 344 nm) 88
Figure S 10. Excitation spectra of EuPSANapPhen-sodium salts (NaBr, NaCl, NaF, NaI, $NaNO_2$, $NaNO_3$, NaOAc, NaOH, and Na_2SO_4, respectively) (EtOH:H_2O) solutions (λem = 616 nm). 89
Figure S 11. Emission spectra of TbPSANapPhen-sodium salts (NaBr, NaCl, NaF, NaI, $NaNO_2$, $NaNO_3$, NaOAc, NaOH, and Na_2SO_4, respectively) (EtOH:H_2O) solutions (λexc = 344 nm) 90
Figure S 12. Excitation spectra of TbPSANapPhen-sodium salts (NaBr, NaCl, NaF, NaI, $NaNO_2$, $NaNO_3$, NaOAc, NaOH, and Na_2SO_4, respectively) (EtOH:H_2O) solutions (λem = 543 nm). 91
Figure S 13. Emission spectra of EuPSANapPhen-Cu (EtOH:H_2O) in a range of concentrations between 0.02 and 0.2 mM, (λ_{exc} = 344 nm). 92
Figure S 14. Emission spectra of EuPSANapPhen-Cu (EtOH:H_2O) in a range of concentrations between 0.4 and 2.0 mM (λexc = 344 nm). 93
Figure S 15. Excitation spectra of EuPSANapPhen-Cu (EtOH:H_2O) in a range of concentrations between 0.02 and 0.2 mM (λem = 616 nm). 94
Figure S 16. Excitation spectra of EuPSANapPhen-Cu (EtOH:H_2O) in a range of concentrations between 0.4 and 2.0 mM (λem = 616 nm) 95
Figure S 17. Emission spectra of EuPSANapPhen-Ni (EtOH:H_2O) in a range of concentrations between 0.02 and 0.2 mM (λexc = 344 nm) 96
Figure S 18. Emission spectra of EuPSANapPhen-Ni (EtOH:H_2O) in a range of concentrations between 0.4 and 2.0 mM (λexc = 344 nm). 97
Figure S 19. Emission spectra of EuPSANapPhen solutions (EtOH:H_2O) in the presence of $Ni(NO_3)_2.6H_2O$ in the concentrations from 0.02 mM to 2 mM (λexc = 344 nm) 98
Figure S 20. Stern-Volmer plot of EuPSANapPhen-Cu $^5D_0 \rightarrow {}^7F_2$ transition (616 nm), ranging Ni(II) concentration. 98
Figure S 21. Dependence of the emission intensity of EuPSANapPhen ($^5D_0 \rightarrow {}^7F_2$ transition) / Ni(II) mixed solutions on the Ni(II) concentration. 98
Figure S 22. Excitation spectra of EuPSANapPhen-Ni (EtOH:H_2O) in a range of concentrations between 0.02 and 0.2 mM (λem = 616 nm). 99

Figure S 23. Excitation spectra of EuPSANapPhen-Ni (EtOH:H_2O) in a range of concentrations between 0.4 and 2.0 mM (λem = 616 nm). 100
Figure S 24. Emission spectra of TbPSANapPhen-Cu (EtOH:H_2O) in a range of concentrations between 0.02 and 0.2 mM (λexc = 344 nm)..... 101
Figure S 25. Emission spectra of TbPSANapPhen-Cu (EtOH:H_2O) in a range of concentrations between 0.4 and 2.0 mM (λexc = 344 nm)..... 102
Figure S 26. Excitation spectra of TbPSANapPhen-Cu (EtOH:H_2O) in a range of concentrations between 0.02 and 0.2 mM (λem = 543 nm). 103
Figure S 27. Stern-Volmer plot of TbPSANapPhen-Cu $^5D_4 \rightarrow ^7F_5$ transition (543 nm), ranging Cu concentration. 104
Figure S 28. Dependence of the emission intensity of TbPSANapPhen ($^5D_4 \rightarrow ^7F_5$ transition) / Cu(II) mixed solutions on the Cu(II) concentration. 104
Figure S 29. Emission spectra of TbPSANapPhen solutions (EtOH:H_2O) in the presence of $Cu(NO_3)_2$ in the concentrations from 0.02 mM to 2 mM (λexc = 344 nm). 104
Figure S 30. Emission spectra of TbPSANapPhen-Ni (EtOH:H_2O) in a range of concentrations between 0.02 and 0.2 mM (λexc = 344 nm)..... 105
Figure S 31. Emission spectra of TbPSANapPhen-Ni (EtOH:H_2O) in a range of concentrations between 0.4 and 2.0 mM (λexc = 344 nm)..... 106
Figure S 32.Excitation spectra of TbPSANapPhen-Ni (EtOH:H_2O) in a range of concentrations between 0.02 and 0.2 mM, (λem = 543 nm). 107
Figure S 33. Excitation spectra of TbPSANapPhen-Ni (EtOH:H_2O) in a range of concentrations between 0.4 and 2.0 mM (λem = 543 nm). 108
Figure S 35. Dependence of the emission intensity of TbPSANapPhen ($^5D_4 \rightarrow ^7F_5$ transition) / Ni(II) mixed solutions on the Ni(II) concentration. 109
Figure S 34. Emission spectra of TbPSANapPhen solutions (EtOH:H_2O) in the presence of $Ni(NO_3)_2.6H_2O$ in the concentrations from 0.02 mM to 2 mM (λexc = 344 nm). 109
Figure S 36. Stern-Volmer plot of TbPSANapPhen-Cu $^5D_4 \rightarrow ^7F_5$ transition (543 nm), ranging Ni concentration. 109

Index of Tables

Table 1. Stern-Volmer constants, standard errors, respective detection limits and determination coefficients (r^2) of both metal ions (Cu(II) and Ni(II)) for the EuPSANapPhen and TbPSANapPhen systems. 45
Table 2. Quantification limits of both metal ions (Cu(II) and Ni(II)) for the EuPSANapPhen and TbPSANapPhen systems. 45
Table 3. Parameters used to calculate pick-up values from coating of filter (F), base (B) and office (O) paper sheets with EuPSANapPhen. 58

Table S 1. Prices of all the reagents used in this master thesis. 110
Table S 2. Specific costs for the production of a 50 mL EuPSANapPhen solution. 110
Table S 3. Specific costs for the production of a 50 mL TbPSANapPhen solution..... 110

Abstract

In this master's thesis, a complex to be used in security paper was developed. For the development of such type of paper, two main guarantees of security need to be present: a) the incorporation of a luminescent compound into the paper; and b) its reaction to a substance that would be responsive to it and prove its authentication. So, to have that security paper, firstly two lanthanide polyelectrolyte-based complexes, composed by europium and terbium salts, two low molecular weight organic ligands (1-naphthoic acid and 1,10-phenanthroline) and the poly(sodium acrylate) polymer (PSA) were synthesized: EuPSANapPhen and TbPSANapPhen. Their luminescent properties were studied by carrying out fluorescence analysis. Having known and studied their luminescent characteristics and confirmed the lanthanide enhancement of emission intensity expected by the use of the ligands and the polymer, the further step was to evaluate the effect of the interaction between the lanthanide complexes and metal ion solutions. All the tests were done by fluorometric analysis. Eight nitrate metal solutions were used: $Mg(NO_3)_2.6H_2O$, $Cu(NO_3)_2.xH_2O$, $Cr(NO_3).9H_2O$, $Ni(NO_3)_2.6H_2O$, $AgNO_3$, $Ca(NO_3)_2.4H_2O$, KNO_3 and $NaNO_3$. Quenching efficiency of EuPSANapPhen-metal solutions and TbPSANapPhen-metal solutions was calculated, being Cu and Ni the most effective metal ions for both lanthanide systems, by leading to an almost 100% emission quenching. The counterion effect was also tested, using nine sodium salts (NaBr, NaCl, NaF, NaI, $NaNO_2$, $NaNO_3$, NaOAc, NaOH and anhydrous Na_2SO_4). It was proved that the counterion had no significant effect on the intensity of emission for both lanthanide systems. The detection limit of both metal quenchers was determined by using the Stern-Volmer equation. For this step, the concentrations range for Cu and Ni was 0.02 to 2 mM. LOD for Cu was 0.219 mM (13.9 ppm) and 0.175 (11.1 ppm) and LOD for Ni was 0.085 mM (4.99 ppm) and 0.223 mM (13.1 ppm) for Eu and Tb systems, respectively. The quantification limit was also determined for both metal ions in both lanthanide systems. LOQ for Cu was 0.663 mM (42.1 ppm) and 0.531 mM (33.7 ppm) and LOQ for Ni was 0.257 mM (15.1 ppm) and 0.675 mM (39.6 ppm) for Eu and Tb systems, respectively. In so doing, the first and second guarantees of security had been proved in solution. Thereafter, paper tests were performed. For that purpose, three different grades of paper were used (Navigator office 80 g/m^2 paper, Navigator base paper and

Macherey-Nagel filter paper (type 713)). Moreover, three different methods of lanthanide polymer complexes' incorporation were also tested, namely stamping, submersion in solution and coating. To compare and analyse the paper results, photographs were taken at eyesight and under UV excitation (λ = 254 nm), using a Canon EOS 750D camera. The quenching effect provoked by the metal ions was tested using a wet brush with $Cu(NO_3)_2.xH_2O$ and $Ni(NO_3)_2.6H_2O$ (0.1 mM). It was possible to conclude that this effect was immediate upon contact of the bristles with the paper sheet that incorporated the lanthanide polymer complex. EuPSANapPhen revealed better visual results than TbPSANapPhen, since its emission intensity was higher, so it was easier to observe the quenching effect. The method of incorporation that resulted better consisted on the submersion of paper sheets in EuPSANapPhen and TbPSANapPhen solutions. Stamping of paper sheets with the lanthanide solutions was not efficient, in particular due to reproducibility issues. Moreover, the coating process was appropriate; however, it does not allow an easy visualization of the quenching effect. Finally, filter paper proved to be the best type of paper for the visualization and guarantee of authentication that was pretended in this project. Base and office paper could also allow the visualization, but with more difficulty, due to the optical agents present on their composition, that would hinder, in some way, the lanthanide emission.

KEYWORDS: *Lanthanide ions, rare-earths, luminescence, polymers, security tags, security paper, anti-counterfeiting*

Resumo

No decorrer desta tese de Mestrado foi desenvolvido um complexo para ser usado em papel de segurança. Para a criação deste tipo de papel, duas principais garantias de segurança têm que estar presentes: a) a incorporação de um composto luminescente no papel; b) a reação do mesmo com uma substância que reaja e permita a sua autenticação. Assim, para obter o tal papel de segurança, foram sintetizados primeiramente dois complexos à base de polieletrólitos e lantanídeos, compostos por sais de európio e térbio, dois ligandos orgânicos de baixo peso molecular (ácido 1-naftóico e 1,10-fenantrolina) e o polímero poli-(acrilato de sódio) (PSA): EuPSANapPhen e TbPSANapPhen. As suas propriedades luminescentes foram estudadas recorrendo a análises fluorimétricas. Tendo estudado as suas características de luminescência e confirmado o aumento da intensidade de emissão do lantanídeo, espectável devido ao uso dos ligandos e do polímero, o passo seguinte foi o estudo do efeito da interação entre os lantanídeos e soluções de iões metálicos. Todos os testes foram realizados através de análises fluorimétricas. Foram usadas oito soluções de nitratos metálicos para o estudo do efeito do ião metálico ($Mg(NO_3)_2.6H_2O$, $Cu(NO_3)_2.xH_2O$, $Cr(NO_3).9H_2O$, $Ni(NO_3)_2.6H_2O$, $AgNO_3$, $Ca(NO_3)_2.4H_2O$, KNO_3 e $NaNO_3$). A eficiência de quenching das soluções EuPSANapPhen-metal e TbPSANapPhen-metal foi calculada, comprovando-se que o Cu e o Ni são os metais mais eficientes no quenching da luminescência de ambos os sistemas, provocando um quenching de cerca de 100%. Também foi testado o efeito do contraião, usando para tal nove soluções de sais de sódio (NaBr, NaCl, NaF, NaI, $NaNO_2$, $NaNO_3$, NaOAc, NaOH e Na_2SO_4 anidro). Provou-se que o contraião não tem um efeito significativo na emissão de ambos os sistemas. O limite de deteção dos dois iões metálicos foi determinado, usando a equação de Stern-Volmer. Para este passo, foi utilizada uma gama de concentrações metálicas de 0,02 a 2 mM. O LOD determinado para o Cu foi 0,219 mM (13,9 ppm) e 0,175 mM (11,1 ppm) e o LOD para o Ni foi 0,085 mM (4,99 ppm) e 0,223 mM (13,1 ppm) para os sistemas de Eu e Tb, respetivamente. O limite de quantificação foi também determinado para os dois iões metálicos em ambos os sistemas. O LOQ determinado para o Cu foi 0,663 mM (42,1 ppm) e 0,531 mM (33,7 ppm) e o LOQ para o Ni foi 0,257 mM (15,1 ppm) e 0,675 mM (39,6 ppm) para os

sistemas de Eu e Tb, respetivamente. Com estes resultados, a primeira e segunda garantias de segurança terão sido comprovadas em solução. Seguidamente, foram realizados testes no papel. Para tal, três tipos diferentes de papel foram utilizados (papel *office* 80g/m^2 Navigator, papel base Navigator e papel de filtro Macherey-Nagel – tipo 713). Para além disso, três métodos distintos de incorporação dos compostos no papel foram também testados, nomeadamente solução carimbada no papel, papel submerso na solução e papel revestido com a solução). Para a comparação e análise dos resultados dos testes em papel, foram registadas fotografias à vista desarmada e debaixo de excitação no UV (λ = 254 nm), usando uma câmera Canon EOS 750D. O efeito de quenching provocado pelos iões metálicos foi testado usando um pincel molhado com soluções de $Cu(NO_3)_2.xH_2O$ e $Ni(NO_3)_2.6H_2O$ (0.1 mM). Foi possível concluir que este efeito era imediato após o contacto do pincel com a folha de papel onde estava incorporado o composto luminescente. O EuPSANapPhen revelou resultados visualmente melhores que o TbPSANapPhen, uma vez que a sua intensidade de emissão era significativamente mais elevada, facilitando assim a observação do efeito de quenching. O método de incorporação que apresentou melhores resultados foi a submersão das folhas de papel em EuPSANapPhen e TbPSANapPhen. A carimbagem das folhas de papel com as soluções de lantanídeo não se revelou eficiente, em particular, devido a dificuldades na reprodutividade do procedimento. Ademais, o revestimento do papel foi eficaz, embora não tenha permitido uma visualização fácil do efeito de quenching. Finalmente, o papel de filtro provou ser o tipo de papel que permite uma melhor visualização e garantia de autenticação, como era pretendido neste projeto. O papel base e o papel *office* também permitiram essa visualização, porém com maior dificuldade, devido à simultânea emissão dos agentes óticos também presentes na constituição desse tipo de papel, que bloqueava de certo modo a emissão do lantanídeo.

***PALAVRAS-CHAVE**: iões lantanídeos, terras-raras, polímeros, etiquetas de segurança, papel de segurança, anti-contrafação*

Abbreviation List

CDs	Carbon Dots
CL	Cooperative Luminescence
CNFs	Cellulose nanofibrils
CNs	Cellulose nanoparticles
CRU	Cross Relaxation Upconversion
CS	Cooperative Sensitization
CTU	Cooperative Transfer Upconversion
DC	Downconversion
ESA	Excited State Absorption
ETU	Energy Transfer Upconversion
EuPSANapPhen	Europium polymer complex
IC	Intersystem crossing
IUPAC	International Union of Pure and Applied Chemistry
K_{sv}	Stern - Volmer constant
LEDs	Light Emitting Diodes
LOD	Limit of Detection
LOQ	Limit of Quantification
MOFs	Metal Organic Frameworks
Nap	1-Naphtoic Acid
NIR	Near-Infrared
PA	Photon Avalanche
PCC	Precipitated calcium carbonate
Phen	1,10-Phenanthroline
PSA	Poly-(sodium acrylate)
QDs	Quantum Dots
REEs	Rare Earth Elements
RFID	Radiation Frequency Identification
S-V	Stern-Volmer
TbPSANapPhen	Terbium polymer complex
UC	Upconversion

UPNPs	Upconversion Nanophosphors
UV-Vis	Ultraviolet - Visible

CHAPTER I

INTRODUCTION

1. INTRODUCTION

Nowadays, counterfeiting has become a major global problem, causing adversities in different areas of common society life. Companies, governments, countries, industries and even general citizens can be affected by the act of counterfeiters that operate against their rights. Since a few years ago, counterfeiting has been increasing drastically, causing security issues that can go from affecting a single company, to a big national security problem. Different types of counterfeiting have been arising lately, including counterfeiting of valuable branded products, pieces of art, documents (e.g. passports), merchandising, pharmaceuticals and, most importantly, national currencies[1].

Counterfeiting of documents is illegal because it goes against copyrights, as counterfeiting of art and merchandise does too. On the topic of counterfeit drugs and pharmaceuticals, society can be in the presence of a public health security problem, since the use of illegal medicines can affect human health. Also, counterfeiting of national currencies is a problem that most governments have been trying to overcome, since it can cause a serious economic crisis, by the possibility of a decrease in the value of the money[2].

To overcome the current issue of counterfeiting, different anti-counterfeiting technologies have been and continue to be created, with the main purpose of producing objects and things that can easily be authenticated and difficult to falsify. However, because of the existence of high quality and sophisticated technologies, counterfeiters are also favoured and can make use of those for maleficent purposes[1]. So, to act against counterfeiters, governments and companies have been spending big amounts of money hoping to develop new and updated industries that can guarantee the security of their nations and clients. The efforts that are being made are also being paid off, despite the fact that nowadays the market of clandestine and counterfeited goods still involves billions of euros[3].

Recently, some of the anti-counterfeiting technologies that have been used by nations involve goods like watermarks, holograms, markers, spectroscopic analysis and electronic tracking using Radiation Frequency Identification (RFID). Nevertheless, those techniques, despite being inexpensive and easy to perform, are not easy to authenticate without being narrowly examined, which makes them time-consuming. Hence, different

materials, such as luminescent nanomaterials based on rare earth metals, have been used as an interesting alternative. These photo-responsive materials have extremely good optical, physical and chemical properties that are great for the purposes of anti-counterfeiting. Several optical materials have been used, namely quantum dots (QDs), carbon dots (CDs) and Metal Organic Frameworks (MOFs), and nowadays the current interest is on the usage of lanthanides compounds, since they possess and exhibit optimum optical properties[1–4].

1.1 Luminescence Processes

To explore the topic about luminescent materials, it is necessary to first clarify the concept of luminescence. Since the beginning of the 17th century, those materials that shine in the dark after exposure to light started being called by *phosphors*, a word that derived from the Greek and which means carrier of light[5]. Nowadays, a clearer and more accurate meaning of the word exists, and phosphors go by substances that features the property of luminescence. In 1888, the word luminescence was used for the first time, coming from the Latin *lumen*, that means light[6]. Currently, luminescence is described as the phenomenon of natural and spontaneous radiation emission from an electronic or vibrational excited species that is not at thermal equilibrium with its environment. Luminescence processes can be classified into Fluorescence and Phosphorescence depending on the duration of the emission after the excitation. Namely, fluorescence is a process characterized by the fact that emission rapidly disappears after the excitation, and in phosphorescence the emission prolongs in time. These different types of luminescence can also be distinguished by the changing in spin multiplicity, where in fluorescence remains the same and in phosphorescence it changes from triplet to singlet[5]. Depending on the source of excitation, luminescence can also be designated as bioluminescence (produced by animals and plants), chemiluminescence (result of a chemical reaction), crystalloluminescence (created during crystallization of solutions), electroluminescence (result of an electric discharge), radioluminescence (bombardment of ionizing particles), and thermoluminescence (emission upon heating of substances)[6]. Jablonski described a diagram where all the energy transfer mechanisms (vibrational and electronic) are explicitly represented (Figure 1). Usually, the first transition described corresponds to the absorption, that is, to the energy transferred when an electron is excited from a lower (normally at ground state) to a higher energy level. This energy transition occurs rapidly (~10^{-15} s). After the excitation of an electron, its energy can be dissipated in different ways, described in the same figure. If the

vibrational levels are almost overlapped with the electronic ones, then what occurs is a so-called internal conversion, a non-radiative process. In internal conversion, an electron goes from a vibrational level of the excited state to another vibrational state but with lower energy. When the energy coming from the photon to the electron is transferred to different vibrational modes in the shape of kinetic energy, it is a vibrational relaxation, also a non-radiative process. This process is also quick (10^{-14} to 10^{11} s), which makes it very probable to occur right after the absorption. As it refers to a vibrational process, the electron should not change its electronic level.

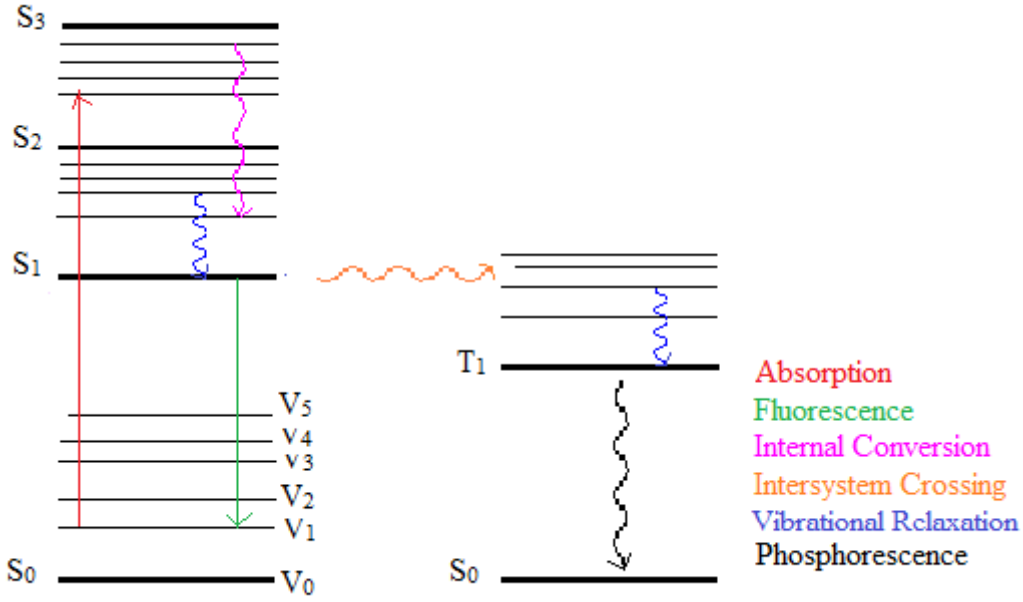

Figure 1. Representation of a Jablonski Diagram (adapted from reference 41).

Another way of energy transfer consists of fluorescence, that is a radiative slow process (10^{-9} to 10^{-7} s), where a photon is emitted. Because fluorescence is a process that requires spending more time, it is not the most common path for the dissipation of the energy, especially if it comes from energy levels above the first excited state. This process always occurs with the electron maintaining its spin multiplicity, that is, occurs between only singlet (paired electrons) or triplet (unpaired electrons) states. Differently, in the case of intersystem crossing (IC) (non-radiative process), the energy transfer changes the spin multiplicity of the electron from singlet excited state to triplet excited state. This process is the slowest one (many orders of magnitude slower than fluorescence). Based only on electronic rules this transition should not be allowed, but adding vibrational criteria, it turns slightly permitted. Because of that, this process gives origin to phosphorescence (radiative process), a slow and prohibited transition from triplet excited state to the ground state[7,8]. The difference between radiative and non-

radiative processes is that the former involves the emission of light and the latter are not associated with that, and so, are usually very much faster.

1.2 Rare Earth Elements

Materials that have lanthanides in their compositions have been chosen to be used for different anti-counterfeiting technologies, because they exhibit ideal optical properties for that. Lanthanides are a group of the Periodic Table of elements. They can also be called Rare Earth Metals or Intern Transition elements.

Rare Earth Elements (REEs), according to International Union of Pure and Applied Chemistry (IUPAC) consist in a group of elements that include all 15 lanthanides (lanthanum - La, cerium - Ce, praseodymium - Pr, neodymium - Nd, promethium - Pm, samarium - Sm, europium - Eu, gadolinium - Gd, terbium - Tb, dysprosium - Dy, holmium - Ho, erbium - Er, thulium - Tm, ytterbium - Yb and lutetium - Lu) (Figure 2), scandium (Sc) and yttrium (Y). They exist since the origin of the Earth, but it was only in the 18th century that the first element classified as Rare Earth was discovered (Arrhenius, in 1787, found a black mineral first called Ytterbite and later Gadolinite)[9]. The name "earth" was attributed because at that time oxidic materials were called earths and those elements presented the same characteristics. Also, at that time, the definition of "rare" meant something that was strange and surprising, so that is why the materials were classified as rare. Nowadays, the used nomenclature remains the same, even though those elements are actually abundant in Earth's crust, so this Rare Earth name becomes ambiguous.

Figure 2. Extract of Periodic Table elements: the Lanthanides.

In 1787, Arrhenius discovered a dark mineral that was a mixture of various rare earths, and it was only in 1803 that cerium (Ce) was successfully isolated for the first time. Since then, the rest of the lanthanides continued to be discovered by mineral extractions[9,10]. The detailed history of the discovery of Rare Earths is very complex and intricate because they present many similarities, so it was very common to first mistakenly classify a mixture of elements as a single one. Because of that, it took over 150 years to the discovery and identification of all 17 Rare Earth elements.

Despite this, it is common to refer to all REE's as if they were completely identical, although they present significant differences in their properties (i.e. melting point, vapor pressure[10] and magnetism). The physical and optical properties of this class of chemical

elements are ruled by their electronic configuration. All lanthanides present the same $6s^2$ configuration, with differences in the 4f orbitals filling, so their outer shell is full, and the electrons occupy the 4f orbital. Therefore, the exterior aspect remains the same for all lanthanides and as internal orbitals do not affect much their chemistry, it is why all Rare Earths look so similar[9].

Generally, lanthanide ions are trivalent, but some can also present different oxidation states. The specific differences that distinguish lanthanides are mainly related to 4f orbitals' properties. As an example, the melting points of this class of elements rapidly enhances by increasing the atomic number. Europium and ytterbium are exceptions to the rule, because they can be divalent. Also, magnetic properties of lanthanides depend on the number of unpaired electrons present on the 4f orbital, that is, as less unpaired electrons, less magnetic the lanthanide is[10]. 4f orbitals are usually characterized by a lower energy and are sufficiently blinded by the environment, which turns them less participative in metal-ligand bond. There is also a special quality of lanthanides electronic configuration called lanthanide contraction, which means that with the increase of the atomic number, the ionic radius shortens. That occurs because for each additional proton in the core, the corresponding electron will occupy the 4f orbital, which is too diffuse to blind the core as efficiently as an interior shell[6,11]. Also, as the 4f subshell is closer to the core than the outer occupied $5s^25p^6$ orbitals, the slight shielding of the nuclear charge of 4f electrons will cause the diminishment of the ionic radii through the series[12].

Therefore, Rare Earths can show very different physical characteristics and behaviours, which justify their wide range of its applications. Nowadays, the daily routine of society cannot escape to the presence of lanthanide based materials, since they are applied in a very vast variety of mundane objects, such as cell phones, computers and televisions (optical displays), cars (electronic parts make use of lanthanides, and also hybrids have them in their batteries), illumination (LEDs are nowadays an environment friendly choice that make use of lanthanides), magnets, lighter flints, etc[13]. The percentage of Rare Earths used in these applications is very low, but that does not make them less important, contrariwise, it turns them into more efficient and less heavy devices, both important properties for the consumer. As so, although REEs show many similarities, the fact that they can be applied in such different areas of industry, proves one more time that it is not correct to assume them as a single element[9,10]. To conclude, this class of elements has been chosen as ideal for security purposes, mainly because they are highly stable and soluble, have high intensity sharp band emissions, can be easily mass produced and can be excited in a large range of wavelengths (from UV to NIR)[1,2].

1.3 Luminescent Lanthanide Materials in Security Tagging

Among all materials used as security elements for anti-counterfeiting techniques, luminescent nanomaterials proved to be the most efficient ones, due to their ideal optical properties. Also, lanthanide luminescent materials have become the largest commercially application of Rare Earths.

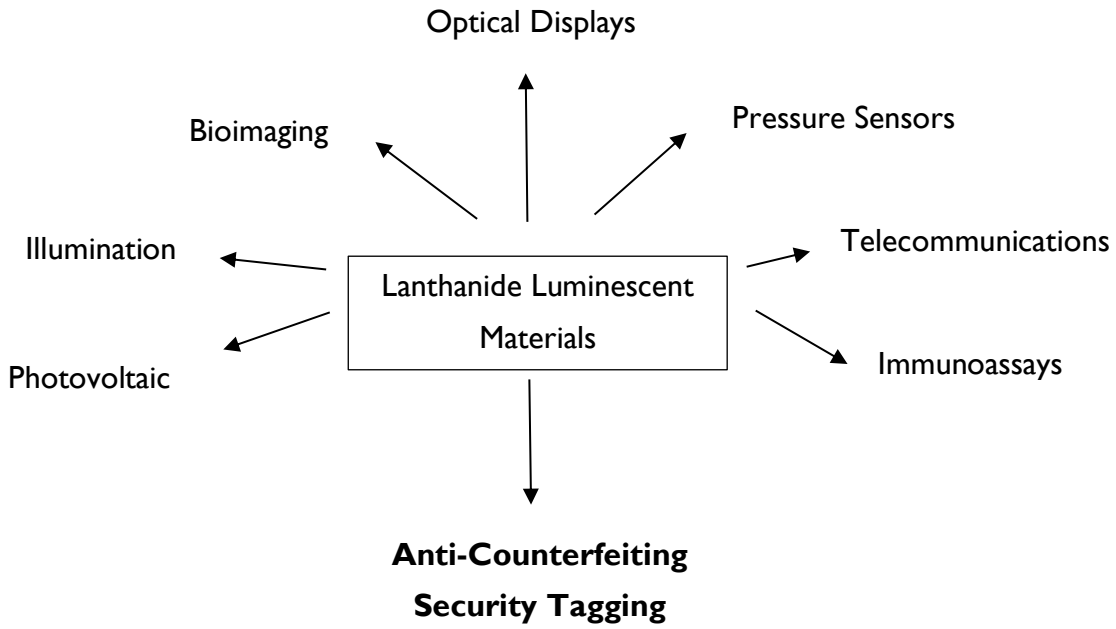

Figure 3. Possible applications for Lanthanide Luminescent Materials.

As previously described, lanthanide-based materials have a wide range of applications (Figure 3). Among them, the most important for governments and countries, for national security issues, is the use of luminescent compounds for the development of security elements. This industry branch can also benefit with the use of these elements to prevent data robbery and to improve their security against counterfeiting. Nowadays, luminescent security tags that emit light under UV excitation are the most common security elements to safeguard important documents, objects and currencies. Hence, a taggant can be described as a material that can be dispersed in a matrix in ppm concentrations without provoking changes in its properties, allowing that way an unmistakable identification of a product, and understate the risk of counterfeiting[14].

Generally, most lanthanides exhibit the property of luminescence and for security purposes it is useful their exceptional excitation in UV-Vis and emission in Vis-NIR. These good optical characteristics derive mostly from electronic rearranges between 4f orbitals (f→f transitions), that have long lifetimes. This, adding to their minimum bias to photobleaching, turns lanthanide based on materials optimum and unique security probes[15]. Using one or more luminescent lanthanide trivalent ions doped on a host

lattice is also an advantage in security over the use of different materials that does not belong to the same class of elements, because lanthanides present high emission due to the previously described f→f transitions, are highly stable both thermally and chemically and produce a broad emission spectrum since they have an exclusive spectral fingerprint[5].

Since the discovery of the property of luminescence, that several anti-counterfeiting techniques using luminescent materials have been described, that include designing luminescent papers or stickers with the purpose of easy authentication of documents and branded products; using luminescent pigments for security inks to create security bar codes, images or patterns; and incorporating luminescent pigments (nanotaggants) during paper manufacture[1].

1.4 Nanophosphors

The grouping of various lanthanides and a phosphor material can turn possible the design of recognition codes, that can be embed in microparticles to be used for anticounterfeiting. Thus, nanophosphors, nanomaterials based on luminescent lanthanides, become relevant. Nanophosphors can be divided in two main categories based on their luminescence mechanism: upconversion and downconversion luminescence.

Fundamentally, upconversion (UC) luminescence consists in the photoexcitation of a luminescent ion or molecule from its ground state to an intermediate excited state, through a non-linear process. This photoexcitation is then followed by a second excitation either by photon absorption or by energy transfer, which promotes it to a higher energy level. That is, generally, in upconversion mechanisms, two or more photons are absorbed and converted in higher energy ones[5]. This type of luminescence mechanism occurs mainly in molecules or ions that present energy enough in their intermediate excited state with long enough lifetimes to permit the gathering of excited electrons. In upconversion luminescence, the difference in energy between the excited and the absorbed photon is called the Anti-Stokes shift. As previously described, lanthanide materials are particularly suitable for this type of luminescence, due to their exceptional photophysical properties (long lifetimes, high photostability, fixed energy levels, …). In upconversion processes, it is common to use an inorganic host lattice doped with lanthanide trivalent ions (e.g. Er^{3+}, Tm^{3+} or Yb^{3+}) that are able to emit light when they are excited. Upconversion luminescence can also make use of only one (single ion method) or more lanthanides (multiple ion method)[5]. When two or more

lanthanide trivalent ions (Ln^{3+}) are used, there is always an activator ion, which is the one that emits the output photon; and a sensitizer ion, which is the first to be excited. Within upconversion luminescence processes, there are five main mechanisms, namely Excited State Absorption, Energy Transfer Upconversion, Cooperative Transfer Upconversion, Cross Relaxation Upconversion, and Photon Avalanche[16]. Excited State Absorption (ESA), described in Figure 4, occurs when an ion previously excited is then promoted to a higher energy level by consecutive absorption of a second photon, that is, when a fundamental state lanthanide ion photon is transferred firstly to the first excited state (E2), and then another photon promotes the excited ion to an even higher excited state (E3). The upconversion occurs when photons go back from excited state (E3) to the ground state (E1). So, essentially, ESA is a consecutive absorption of two photons. ESA phenomenon occurs mostly when the concentration of doping is low, because the opposite favours the happening of non-radiative cross relaxations, which diminish significantly the intensity of emission. Thulium (III), erbium (III) and neodymium (III) are highly efficient lanthanides used in excited state absorption mechanisms[5,17–19].

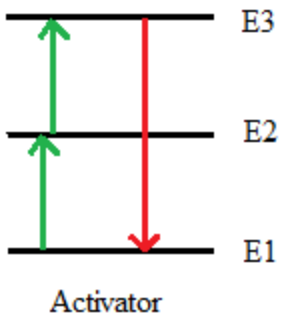

Figure 4. Schematic representation of an Excited State Absorption (ESA) mechanism. Green lines represent absorption and red lines emission. (Adapted from reference 17).

Between all upconversion mechanisms, Energy Transfer Upconversion (ETU) (Figure 5) is by far the most efficient one. In this one, both activator and sensitizer ions are impregnated in the upconversion unit.

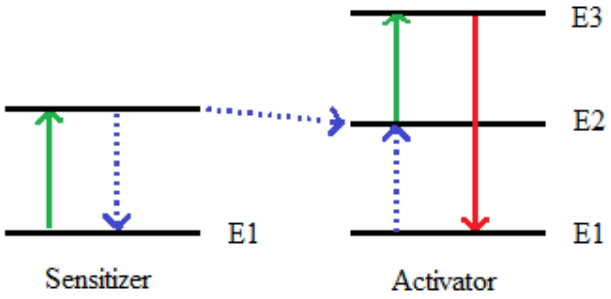

Figure 5. Schematic representation of an Energy Transfer Upconversion (ETU) mechanism. Green lines represent absorption, red lines emission and dashed lines energy transfer. (Adapted from reference 17).

After excitation of photons with low energies, the sensitizer and the activator can be guided to their excited states and therefore, the sensitizer donates non-radiatively its energy to the activator, through a dipole-dipole interaction. Most upconversion nanophosphors (UPNPs) reach efficient upconversion emissions by ETUs processes, so that is why this is the most efficient upconversion mechanism. When compared to ESA, ETU is beneficial because a single pump source is required. For that, lanthanide trivalent ions with multiple excited states are advantageous and their concentration must be high enough so that ion-ion interactions can prompt the energy transfer[18,19]

Cooperative Transfer Upconversion (CTU) can be divided in Cooperative Sensitization (CS) (Figure 6) and Cooperative Luminescence (CL) (Figure 7) and both mechanisms involve cooperative effects, i.e., more than one luminescent center participates in the luminescence process. In cooperative luminescence, there are two excited ions, and each one absorbs one photon and cooperate in the emission. Therefore, the coupling between two ions favours the transition when simultaneously they leave unoccupied their excited states, to cooperatively emit one photon. This mainly occurs in spectral regions where neither the sensitizer nor the activator presents absorption or emission, or in cases where the energy transfer upconversion cannot occur, i.e. when the concentration of the ions is low.

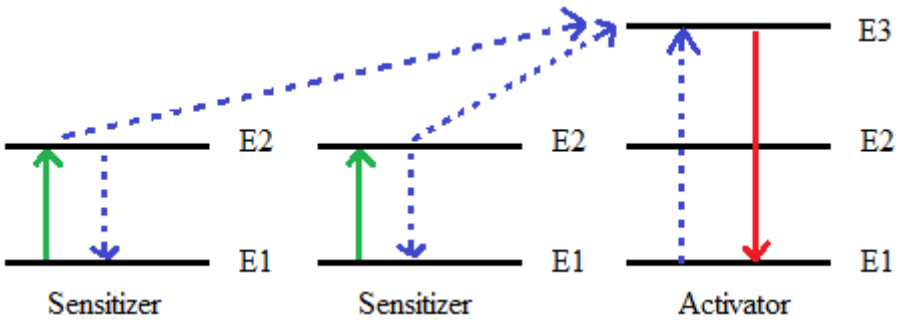

Figure 6. Schematic representation of a Cooperative Sensitization mechanism. Green lines represent absorption, red lines emission and dashed lines energy transfer. (Adapted from reference 16).

On the other hand, cooperative sensitization is when a single photon excites two ions simultaneously. That is, when each excited ion (both sensitizer and activator) absorbs one photon to create respective excited states and together transfer the energy to another ion that turns into its excited state. This upconversion mechanism is relatively inefficient, since in CTU lacks the existence of real intermediate states[17–19].

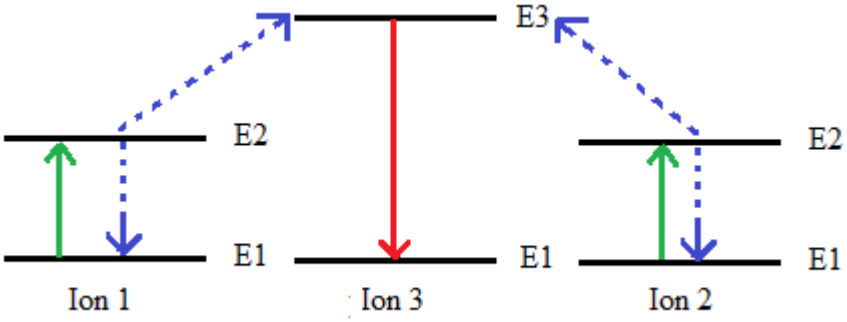

Figure 7. Schematic representation of a Cooperative Luminescence mechanism. Green lines represent absorption, red lines emission and dashed lines energy transfer. (Adapted from reference 5).

In Cross Relaxation Upconversion (CRU) (Figure 8), the sensitizer and the activator are similar in their natures. In their excited states, both ions can absorb photons and then an energy transfer process promotes the activator to its excited state, while the sensitizer goes back to the ground state[5,18].

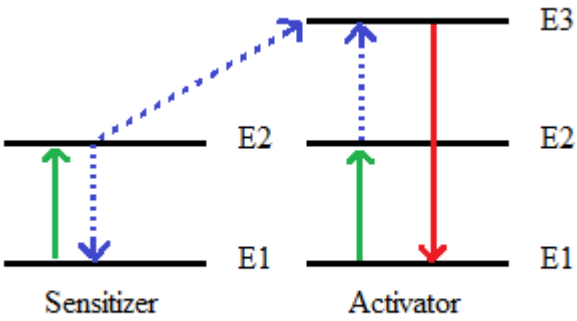

Figure 8. Schematic representation of a Cross Relaxation Upconversion (CRU) mechanism. Green lines represent absorption, red lines emission and dashed lines energy transfer. (Adapted from reference 16).

Lastly, Photon Avalanche (PA) (Figure 9) is an upconversion mechanism that involves a threshold excitation value. In this situation, the luminescent centers can go through an excited state absorption process to occupy a higher excited state if some electrons are promoted to the intermediate state.

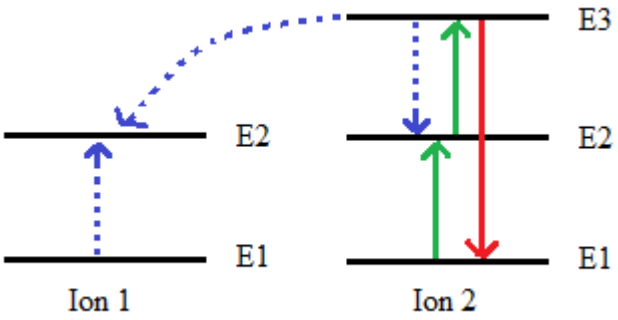

Figure 9. Schematic representation of a Photon Avalanche (PA) mechanism. Green lines represent absorption, red lines emission and dashed lines energy transfer. (Adapted from reference 16).

Therefore, cross relaxation occurs between the super-excited ion and the neighbouring fundamental state ion, which allows the occupation of the intermediate states of both ions. So, photon avalanche is a looping process (ESA and CRU) that offers feedback and the intermediate states become highly populated above the threshold excitation value because of the repetition of this process. Above the threshold value, luminescence intensity enhances many orders of magnitude. Besides that, PA is the less efficient upconversion mechanism and generally occurs in systems where the doping concentration is high enough to promote the occurrence of many cross relaxations. It is easy to recognise the happening of photon avalanche processes since they show long lifetimes (seconds)[5,19].

In Downconversion (DC) luminescence processes (Figure 10), the mechanism is the opposite as in upconversion ones, as mainly downconversion refers to the translation of a high energy photon (UV) into two lower ones (Vis)[20–22].

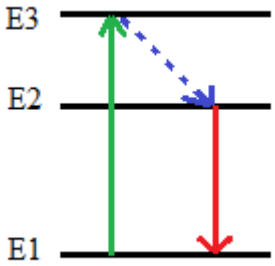

Figure 10. Schematic representation of a Downconversion (DC) mechanism. Green lines represent absorption, red lines emission and dashed lines energy transfer. (Adapted from reference 5).

DC obeys to Stokes law, so the energy difference between the emitted photon and the absorbed one is called the Stokes shift. As previously described, rare earth doped materials based on lanthanides are also good candidates to be used in these types of luminescence conversions.

Generally, DC materials consist in an inorganic host matrix doped by trivalent lanthanide ions, so-called activators. The inorganic host matrix has the function of sensitizing the luminescence, so it is the sensitizer (absorbs photons and transfers them to the activator ion) and it is also the host crystal which maintains the Ln's ions together. Over time, there have been described in literature various host inorganic matrices, such as oxy-sulfide, oxides, fluorides, vanadates and phosphates. Although downconversion mechanisms are expected for the majority of trivalent lanthanide ions, the main activators commonly used are europium (Eu^{3+}), terbium (Tb^{3+}), samarium (Sm^{3+}) and dysprosium (Dy^{3+}), due to the fact that they show abundant emission peaks in all visible region, under UV excitation. Usually, activators are soaked into the matrices in low concentrations (below 5%), to reduce the luminescence quenching and to not adulterate the crystalline structure of the host material. The efficiency of the energy transfer between the sensitizer and the activator reveals to be high which results in great emission efficiency. This fact can even be more efficient if the activator can be doped with another lanthanide ion, becoming the sensitizer, but for that the optical properties of the sensitizer and the emitter must be similar[5,23].

1.5 Lanthanide Polymer Complexes

Lanthanide compounds are commonly known for their great luminescent optical properties, sharp emission bands and long lifetimes. However, lanthanides when used alone exhibit low luminescence intensity due to the limitations of f→f transitions, and, to conquer that disadvantage, lanthanide complexes that present chromophores on their composition started being developed recently. Also, as lanthanides display low molar absorption coefficients ($\varepsilon < 10$ $Lmol^{-1}cm^{-1}$), new techniques are being developed to improve their spectroscopic properties[24].

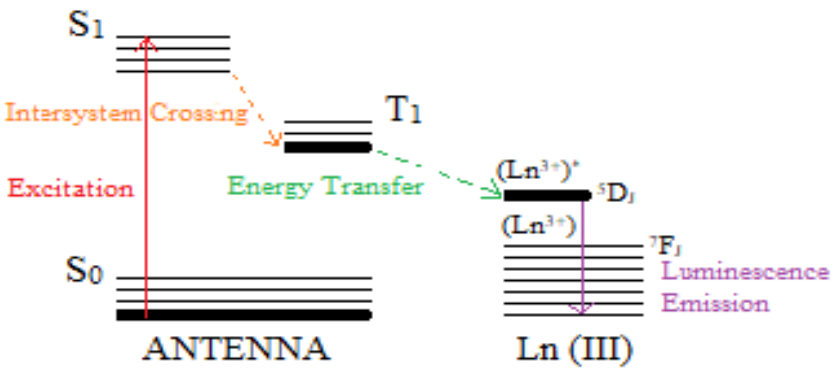

Figure 11. Schematic representation of the antenna effect between the ligand and the lanthanide ion. (Adapted from reference 26).

With the purpose of enhancing emission intensity of lanthanides, strongly light absorbing sensitizing chromophores, so called antennas, are incorporated in lanthanide complexes[12]. One of the common techniques used to upgrade luminescent properties of lanthanides involves their complexation with low molecular weight organic ligands. The latter are chosen since they can absorb the energy and transfer it to the lanthanide ions. Generally, Ln's are most easily coordinated with organic ligands that possess nitrogen (N) and oxygen (O) atoms in their chemical composition[25]. This energy transfer mechanism is called the antenna effect (Figure 11) and it can be explained mainly by the energy transfer from organic ligands to lanthanides. Specifically, low molecular weight organic ligands are used to obtain even better luminescent compounds, because the energy transfer will occur through the excitation of their $\pi \rightarrow \pi^*$ characteristic bands, which have high molar absorption coefficients (ε >10000 $Lmol^{-1}cm^{-1}$). The singlet excited state (S_1) of the ligand will be irradiated and will rapidly change via intersystem crossing to a triplet excited state (T_1) with higher lifetime, due to the lanthanide effect. So, to have an efficient energy sensitization, the energy transfer between the T_1 state and the Ln would also have to be efficient[24,26].

Therefore, the antennas have the function of absorbing electromagnetic radiation and transfer it to the triplet excited state of the lanthanide ion, generating an excited Ln state, where then the energy is successfully emitted as luminescence or deactivated non-radiatively[12]. The most commonly organic ligands used as antennas known in literature are 1,10-phenantroline, pyridine and aromatic carboxylic acids (Figure 12)[25].

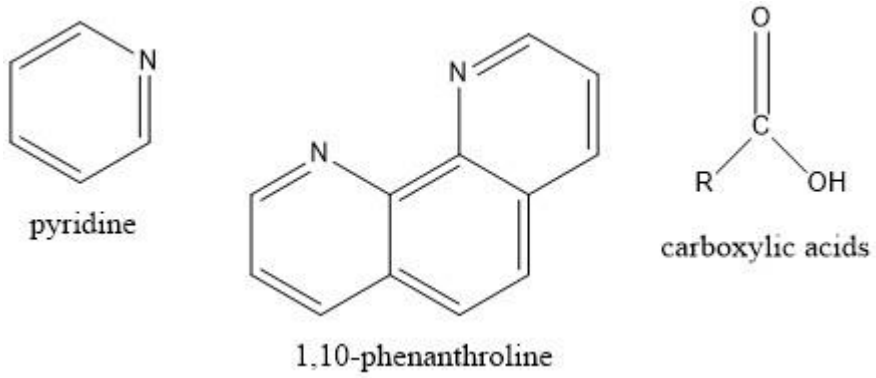

Figure 12. Chemical structure of the commonly used low molecular organic ligands.

However, despite actually enhancing the luminescent properties of lanthanides, what happens then with lanthanide complexes based on low molecular weight organic ligands is that they are normally doped in matrices, which comes with some disadvantages, namely low chemical stability, incompatibility with the matrix, long preparation protocol

or weak mechanic properties. So, incorporating lanthanide complexes in the polymer through interactions between rare earth elements and polymer functional groups can be extremely useful for the synthesis of new compounds that will present advantages both from the lanthanide (intrinsic luminescence) and from the polymer (toughness and high chemical stability)[27,28]. That way, a new class of complexes is formed: the lanthanide polymer complexes or also named polymer rare-earth complexes.

In this class of compounds, the chromophores are covalently bonded to the polymeric backbone. This can be achieved by two different pathways. The first one is when low molecular rare-earth complexes that contain a polymerizable double bond as a monomer are (co)polymerized to synthesize polymer rare-earth complexes. The second one and most commonly applied is when a direct reaction occurs between the Ln's ions and the functional groups of polymeric chains[27,29]. To improve luminescent properties of lanthanides, more than one type of ligands can be used at the same time and they can act both as antennas and diminish emission losses through non-radiative ways. The polymeric chains will also help in avoiding energy losses, by hydration of water molecules that are partially removed in the presence of the polymer[28].

1.6 Paper industry

The purpose of this master's thesis was to develop a security paper and, for that, having previously explained the details about the security features (namely the use of REEs and/or polymers), it is also necessary to understand paper manufacture, its composition and optical properties.

Paper possesses various good properties, such as recycling, biodegradability, accessibility, and flexibility and offers a lot of possibilities to change its surface and internal properties to obtain specific types of paper[30]. Paper has also been described as "hydrogen-bond-dominated solid", "a random network of natural cellulosic fibers", a "complex compound with an average composition of 89% of fiber, 8% filler and 3% paper chemicals[31]". As so, the major component of paper is cellulose fibers. Cellulose is essential on the structure of plants' cell wall, is naturally formed during the cellular plant development process via Van der Walls forces and hydrogen bonds. It is also the most abundant renewable organic polymer on the biosphere[32].

Paper substrates can be derived from several natural fibers, namely hardwoods (short fibers with high density), softwoods (long fibers with low density), and non-wood materials (e.g. bamboo, straw, and grasses)[30]. Moreover, all kinds of cellulose nanomaterials can be named cellulose nanoparticles (CN's) and between them, the most

used in papermaking industry has been the cellulose nanofibrils (CNFs). CNFs have been and continue to be used with the purpose of improving some paper qualities such as mechanical strength, gas and water impermeability and fire resistance[32].

Nowadays, writing and office papers represent a big amount of the total production of paper in Europe. This specific type of paper needs to present excellent optical properties, in order to have great printing features[33]. For that, papermaking industry devotes significant research on the study of paper composition and mainly on how to change its characteristics (brightness, opacity, thickness, smoothness, etc) to produce several types of paper, according to the user's needs.

The production of paper involves 5 major steps: pulping, bleaching, refining, sheet formation and surface treatment (coating). Pulping requires the isolation of the cellulose fibers from the raw material that is not going to be used. In this step of the papermaking process, the fibers are recovered from the wood, through a selective extraction protocol. There are four different wood pulp types, namely mechanical pulp, sulfite pulp, sulfate or Kraft pulp, and soda pulp. Generally, mechanical pulp is all the wood, except the bark and the parts that are lost during transportation and storage. The non-cellulosic components are usually dissolved during the treatment, so chemical pulps are mainly pure cellulose. The pulping process needs high pressure and temperatures between 120 and 130°C[30,31]. The cell wall of wood has three main polymeric materials in its constitution, namely cellulose (42-45%), hemicellulose (27-30%) and lignin (20-28%). For the creation of a quality printing white paper, the majority of lignin present must be removed, which occurs on the second step of the papermaking process, the bleaching, and involves a series of stages, where the pulp becomes whiter at each stage[34,35]. The third step is the refining, a process which involves swelling, cutting and fibrillation. In this step, the cell walls are fibrillated to give origin to microfibrils, a process that enhances the surface area and the number of contact points between the neighbouring fibers[30]. With refining, the bonding between the fibers is also enhanced. Afterwards, mineral fillers and other additives are added to the refined pulp, prior to the sheet formation. The main advantage of the addition of mineral fillers is that they will improve the optical and printing properties of the paper, but other than that, they are also advantageous, since they lower the cost of production because they are cheaper than the fibers. Fillers are added to occupy the gaps between fibers and they will affect the structure and the appearance of the paper, enhancing its brightness, opacity, thickness, smoothness and other properties[30,35,36]. For writing and office papers, the main mineral filler that is commonly applied is the precipitated calcium carbonate (PCC). PCC is a synthetic mineral filler, that by being used, reduces the need of forestry resources, minimizing the

paper costs. Moreover, PCC is used mainly for the improvement of the optical and printing capacities[33,36]. The fourth main step of the papermaking process is the sheet formation, which occurs at the wet-end. This process involves the flow of a very diluted water solution that contains the refined fibers through a very thin wet, which allows the water to go through, leaving the fibers together. The water is removed by gravity, suction and vacuum processes. As so, sheet formation is a process that requires filtration and thickening operations[30,34,35]. The final main step of the papermaking process is the surface treatment, or coating. This treatment can alter the printing capacities of the paper, because it consists on the application of "surface chemicals" (such as starch), that will improve the interaction between the printing inks and the paper surface. Moreover, surface treatment can also improve smoothness (by minimizing the porosity) and it will improve the fiber-fiber interaction. The "surface chemicals" are the last ones to be added during the papermaking process and they should only affect surface properties. Depending on which type of chemical is used, the same paper sheet can be converted in different types of paper[31,35]. The typical printing paper usually undergoes a "light" coating process. "Heavy" coatings are generally used for special papers when improvements of certain paper properties are wanted, such as high smoothness and high gloss or when alternative printing processes are also desired. Having known that, coating can be quantified and controlled through thickness gains. However, in industrial terms, it is more useful to measure the weight gain per square meter, or "pick-up".

As a matter of conclusion, for this master's thesis project, the main important step of the papermaking process should be the coating/surface treatment, since the security aspects, that is, the incorporation of lanthanide compounds into the paper structure, will mainly be studied with sheets already formed. So, for the development of a security paper, three methods of incorporation of great optical and luminescent compounds will be tested and further discussed (stamping, immersion and coating with lanthanide complexes), using three different types of paper sheets (filter, base and office paper). The pick-up values for the coating with lanthanide complexes will also be measured.

CHAPTER 2

EXPERIMENTAL PART

2. EXPERIMENTAL PART

2.1 Materials and Reagents

All the reagents and solvents were purchased from commercial suppliers and used as received. Europium(III) chloride hexahydrate (99,99%), terbium(III) chloride hexahydrate (99.9%), poly-(sodium acrylate) - PSA, and 1,10-phenantroline (>99%) were purchased from Aldrich. Chromium(III) chloride and 1-naphtoic acid (>98%) were obtained from Riedel-de Haen and TGI, respectively. The following nitrate salts were used: magnesium nitrate hexahydrate (Merck), copper nitrate hydrate (Alfa Aesar), nickel nitrate hexahydrate (Riedel-de-Haen), silver nitrate (ABSOLVE), calcium nitrate tetrahydrate (Riedel-de-Haen), potassium nitrate (Merck), sodium nitrate (Riedel-de-Haen) and chromium nitrate nonahydrate (Sigma-Aldrich). Several sodium salts were used: sodium bromide (José M. Vaz Pereira, S.A.), sodium chloride (Merck), sodium acetate (ABSOLVE), sodium fluoride (Riedel-de-Haen), sodium nitrate (Riedel-de-Haen), sodium nitrite (Riedel-de-Haen), sodium iodide (Merck), anhydrous sodium sulfate (José M. Vaz Pereira, S.A.) and sodium hydroxide (ABSOLVE). Ethanol and milli Q ultrapure water were used as solvents.

Navigator office 80 g/m^2 paper, Navigator base paper and Macherey-Nagel filter paper (type 713) were used for paper tests.

2.2 General methods

The Fluorescence spectra were recorded on a Fluoromax-4 spectrofluorometer, in a right-angle configuration. For the coating of paper, it was used a RK Printcoat Instruments K Lox Proofer and a Mathis laboratory coater model SVA-IR-B. Photographic results were recorded using a Canon EOS 750D camera.

2.3 Synthesis

2.3.1 Synthesis of luminescent lanthanide polymer complexes

An aqueous solution of poly-(sodium acrylate) - PSA (5.2668 g, 2.51×10^{-3} mol; 0.05 M) was prepared in a 50 mL flask. Then, a 1-naphthoic acid (70:30, EtOH: H_2O) (0.1735 g; 1.0×10^{-3} mol) solution was prepared in a 20 mL flask. At the same time, solutions of 1,10-phenantroline (70:30 v/v, EtOH: H_2O) (0.05 M), $EuCl_3.6H_2O$ (0.05 M, H_2O) and $TbCl_3.6H_2O$ (0.05 M, H_2O) were also prepared. Fluorescence analysis were performed, using solutions containing all components at 0.0125 M concentration (the order of addition was first, PSA, followed by Eu/Tb, then Phen and lastly Nap). Emission spectra were recorded with excitation at λ = 344 nm for both ions, and the emission was recorded in the range 300 to 800 nm. Excitation spectra were recorded with emission at λ = 616 nm and λ = 543 nm, for Eu and Tb, respectively. Excitation and emission slits of 0.5 nm were used.

2.3.1.1 Interaction of the functionalized polymer with metal ion solutions

The solutions prepared in the previous section (2.3.1) were also used in for the interaction assessment between the functionalized polymer and metal ions. Aqueous stock solutions (10 mM) of the following salts were prepared: $Mg(NO_3)_2.6H_2O$, $Cu(NO_3)_2.xH_2O$, $Cr(NO_3).9H_2O$, $Ni(NO_3)_2.6H_2O$, $AgNO_3$, $Ca(NO_3)_2.4H_2O$, KNO_3 and $NaNO_3$. To carry out the fluorescence analysis, a mix solution containing metal ion salts and the polymer, ligand, lanthanide or complex were prepared, in such a way that the final concentrations were obtained: 0.0125 M for Nap, Phen, Eu/Tb and PSA and 0.002 M for metal ions. Emission spectra were recorded in the same conditions. Quenching efficiency was calculated by using the following equation:

$$\text{Quenching efficiency (\%)} = \frac{(I0-I)}{I0} \times 100 \qquad \text{(Equation 1)},$$

where I_0 is the maximum luminescence intensity without the addition of any metal, and *I* is the maximum intensity of luminescence after contact with metal).

2.3.1.2 Effect of the type of anion on the luminescence response of complexes

For the evaluation of the anion effect on the luminescence quenching of lanthanide-based complexes, the solutions previously described in section 2.3.1 were used. A solution of 1,10-phenanthroline (3.6041 g; 0.02 mol) was prepared in a 50 mL flask. The cation chosen for this study was sodium and, consequently, several sodium salts solutions (NaBr, NaCl, NaF, NaI, $NaNO_2$, $NaNO_3$, NaOAc, NaOH and anhydrous Na_2SO_4) at 10 mM concentration were prepared. Fluorescence analysis were performed, where all the solutions described were mixed to the point where final concentration of Nap, Phen, Eu/Tb and PSA was 0.0125 M and of anion was 0.002M. Emission spectra were recorded in the same conditions as previously described. Quenching efficiency (Equation 1) was computed on the basis of the obtained fluorescence data.

2.3.1.3 Detection and quantification limits of metal ions

For finding the detection limit of the metal ions, it was chosen copper and nickel as the metal ions, since they were the ones that showed higher quenching efficiency. A stock aqueous solution of $Cu(NO_3)_2$ (10 mM) was initially prepared in a 50 mL flask. Then, solutions of Eu/Tb + PSA + Nap + Phen + the appropriate volume of $Cu(NO_3)_2$ were prepared, in a range of copper and nickel concentrations varying from 0.02 mM to 2 mM; the concentration of the other components was kept constant and equal to 0.0125M . The same procedure was applied to the aqueous solution of $Ni(NO_3)_2.6H_2O$ (10 mM). Fluorescence analysis were performed in the same conditions as previously described. Stern-Volmer (Equation 2) method was used to obtain the detection limit (LOD) (Equation 3). The quantification limit was determined by applying Equation 4.

$I_0/I = 1 + K_{SV}[Q]$ (Equation 2),

where I_0 and I are the luminescence intensities of the compound before and after the incorporation of the metal cation respectively, K_{SV} is the Stern-Volmer (S-V) constant and [Q] is the quencher (Cu or Ni) concentration.

$LOD = 3.3\sigma / k$ (Equation 3),

$LOQ = 10\sigma / k$ (Equation 4),

where σ is the standard error and $k = K_{SV}$ is the slope (i.e. the S-V constant).

2.4 Paper analysis

Navigator office 80 g/m^2 paper, Navigator base paper and Macherey-Nagel filter paper (type 713) were used for luminescence tests and interaction with metal solutions, with the main purpose of the development of a functionalized security paper.

2.4.1 Incorporation of luminescent lanthanide polymer complexes in paper

Different types of inclusion of the luminescent lanthanide polymer complexes (EuPSANapPhen and TbPSANapPhen) were tested, namely paper stamped with polymer solution and paper immersed for a second in the lanthanide luminescent polymer solution.

For the stamping process, stamps of letters EU and TB were used. 50 mL of luminescent solution were dropped on a Tupperware, the stamps were dipped in the solution and then marked on the respective paper sheet.

For the immersion of the paper into the lanthanide solution, 50 mL of each lanthanide polymer complex solution were dropped on a Tupperware, where then the sheets were left for a very small period of time (seconds), just until the sheet was completely covered with solution. Thereafter, the paper sheets were left drying overnight at room temperature.

Photographic results of both incorporation processes at eyesight were obtained and later compared to those attained in a dark room under UV excitation at λ = 254 nm.

2.4.2 Lanthanide polymer complexes as a paper coating

EuPSANapPhen and TbPSANapPhen solutions were submitted to a freeze-drying process and the obtained powder was added to starch suspension used for coating of several paper sheets (filter, base and office paper).

The starch suspension was prepared following a reported protocol (RAIZ- Instituto de Investigação da Floresta e Papel). The starch is dispersed in cold water and then the dispersion is heated to 80°C under vigorous stirring. 0.45 µL of enzyme suspension (α-amylase) is added per gram of starch used and the dispersion is maintained at 80°C for 5 minutes. After that, 0.17 mL of zinc sulfate per gram of starch is added, to deactivate the enzyme. Then, the dispersion is heated to 90°C-100°C and cooked at that temperature for 15 min. The dispersion is cooled to 50°C and is finally ready to use. Lanthanide polymer complexes were added at this point and left under stirring until the use in the coating process.

The coating with EuPSANapPhen was done making use of a RK Printcoat Instruments K Lox Proofer and the coating with TbPSANapPhen making use of a Mathis laboratory coater model SVA-IR-B.

Pick-up is defined as the grammage gain of the paper sheet, that depends mainly on the roughness of the roller, the distance between the application roll and the doctor roll, the relative velocity of the application roll over the sheet, the viscosity and temperature of the coating suspension, and the properties of the paper sheet. In this case, rolling pins were set so that a low pick-up value was achieved.

Pick-up values were calculated after the coating process.

2.4.3 Effect of metal ion solutions on the functionalized paper

Copper and nickel nitrate solutions were used to test the response of the stamped, soaked and coated paper (with EuPSANapPhen and TbPSANapPhen) to the presence of metal ions. The results were obtained photographically, with a Canon EOS 750D camera at eyesight and under conditions with UV excitation (λ = 254 nm).

CHAPTER 3

RESULTS AND DISCUSSION

3. RESULTS AND DISCUSSION

Functionalized luminescent polymer complexes based on poly-(sodium acrylate) using lanthanides (europium and terbium) were prepared: EuPSANapPhen and TbPSANapPhen. Their interaction with metal ions and the influence of the anion were evaluated using fluorometric techniques. Quenching efficiencies and detection limits of the metal ions were assessed.

Incorporation of the prepared luminescent polymer complexes in Navigator office 80g/m^2 paper, Navigator base paper and Macherey-Nagel filter papers (type 713) was carried out through different methods. The response behaviour of complex-containing paper to the presence of copper and nickel-based solutions was also tested as a proof of concept.

3.1 Synthesis of luminescent lanthanide polymer complexes

Regarding the synthesis of a lanthanide complex, it is known from literature[24,26] that lanthanide ions when used alone, in aqueous solution, do not present intense luminescence properties ($\varepsilon < 10$ $Lmol^{-1}cm^{-1}$), so the use of low molecular weight organic ligands is recommended, as explained previously in the Introduction. It is also advantageous to incorporate polymeric chains in lanthanide complexes to improve their possible applications, becoming owners of advantages both of lanthanides (great optical properties) and of polymers (good chemical stability). So, in this project, 1,10-phenanthroline and 1-naphtoic acid were the chosen organic ligands, used as *antennas* and PSA was the polymer used for the preparation of luminescent lanthanide polymer complexes.

The synthesised lanthanide polymer complexes (EuPSANapPhen and TbPSANapPhen) are colourless to the eyesight, but present intense fluorescence (red and green, respectively) when under UV radiation.

Figure 13 shows an emission spectrum of an aqueous solution of $EuCl_3.6H_2O$. Upon excitation at 344 nm, the compound shows few strong distinguished emission peaks at 555 nm, 590 nm, 616 nm, 650 nm and 698 nm that can be attributed to the characteristic transitions of Eu^{3+} ions ($^5D_0 \rightarrow {}^7F_J$, J=1-5). The most intense peak, localized at 590 nm, is the responsible for the characteristic red emission of europium caused by

the $^5D_0 \rightarrow ^7F_2$ electronic transition. In Figure 14, the emission spectrum of the prepared lanthanide polymer complex (EuPSANapPhen) can be observed – for the sake of comparison the spectrum for the aqueous solution of $EuCl_3.6H_2O$ is duplicated. Characteristic peaks of europium transitions $^5D_0 \rightarrow ^7F_J$, J=0-5 are also presented at 578, 590, 616, 650, 687 and 698 nm, respectively[37,38]. In Figure S1 of the Supporting Information, the excitation spectrum of the same $EuCl_3.6H_2O$ aqueous solution can be observed.

When comparing the intensity of the peaks of the emission spectra of the europium solution (Figure 13) and that of the polymer complex (EuPSANapPhen, Figure 14), it is obvious that the antenna effect of the low molecular weight organic ligands 1,10-phenantroline and 1-naphtoic acid can be observed, since the luminescence intensity suffers a visible enhancement.

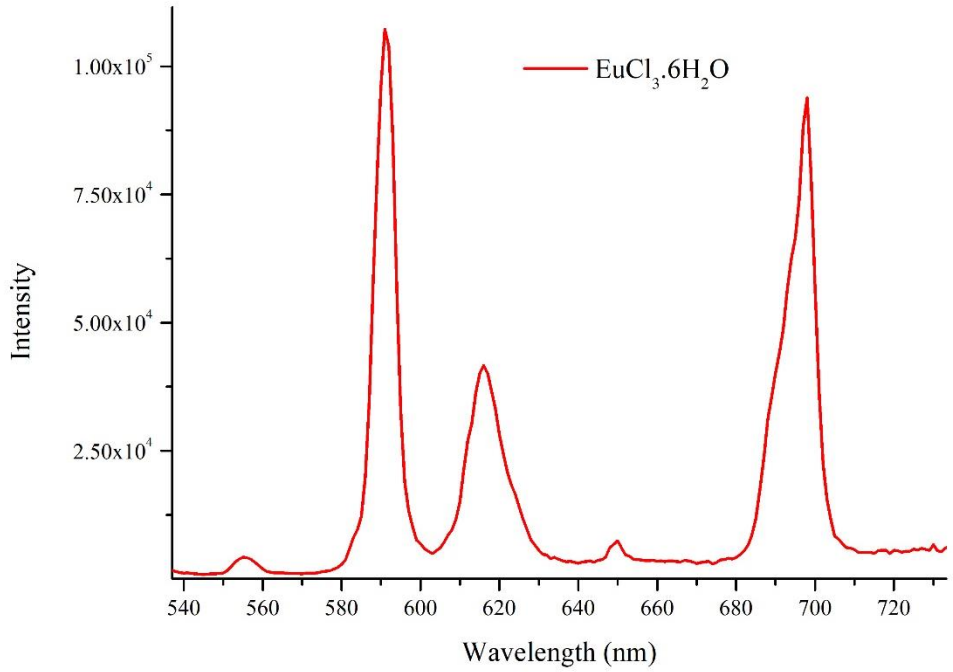

Figure 13. Emission spectrum of an aqueous solution of $EuCl_3.6H_2O$ (0.05 M) (λexc = 344 nm).

This detail can be assigned to the fact that coordination ability of the ligands is higher and so, Phen and Nap will occupy the position of the water molecules in the complex formed. Consequently, the quenching provoked by the vibration of the hydroxyl groups of water molecules will be avoided, enhancing that way the fluorescence intensity[37]. It can be concluded that the low molecular weight organic ligands are good sensitizers of luminescence emission. Moreover, the only visible peaks in the emission spectrum of EuPSANapPhen are those corresponding to the Eu^{3+} electronic transitions, which suggests that the energy transfer is successfully occurring between the PSA and the

europium trivalent ions. The mechanism of energy transfer can be explained as follows: first, the PSA is excited to the singlet state (S_1) by photon absorption in UV, which is then relaxed to the triplet state (T_1) via intersystem crossing. The energy is formerly transferred non-radiatively from the excited state of the polymer to the excited state of europium ions and lastly, lanthanide ions emit fluorescence on the visible region through the relaxation of multiple photons from the excited state to the fundamental state of Eu(III)[29]. In Figure S4 of Supporting Information, the excitation spectra of the EuPSANapPhen solution can be observed.

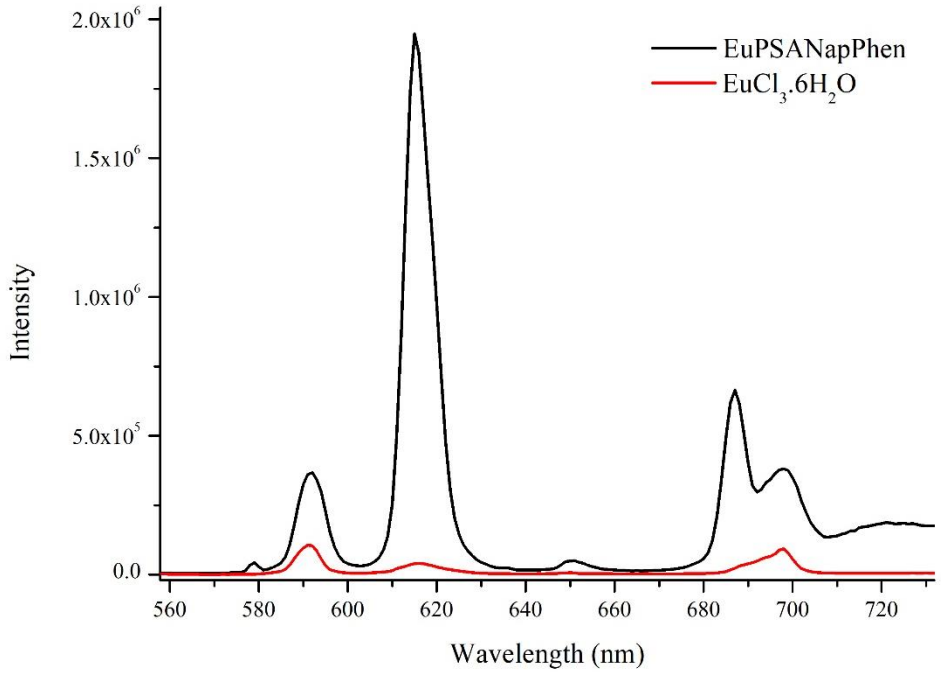

Figure 14. Emission spectrum of an aqueous solution of $EuCl_3.6H_2O$ (0.05 M) and a EuPSANapPhen ($EtOH:H_2O$) solution (λexc = 344 nm).

A similar procedure was applied to the prepared TbPSANapPhen complex. In Figure 15 the emission spectrum of $TbCl_3.6H_2O$ is depicted. Upon excitation at 344 nm, it can be observed strong emission characteristic peaks of terbium electronic transitions ($^5D_4 \rightarrow ^7F_J$, J=6-3)[19]. The most intense peak located at 543 nm is the responsible for the characteristic green emission of terbium compounds, caused by the $^5D_4 \rightarrow ^7F_5$ Tb transition. It is worth noticing that the same antenna effect of the organic ligands occurred when terbium is used, as it can be observed from Figure 16. In this figure, the emission spectrum of TbPSANapPhen is represented.

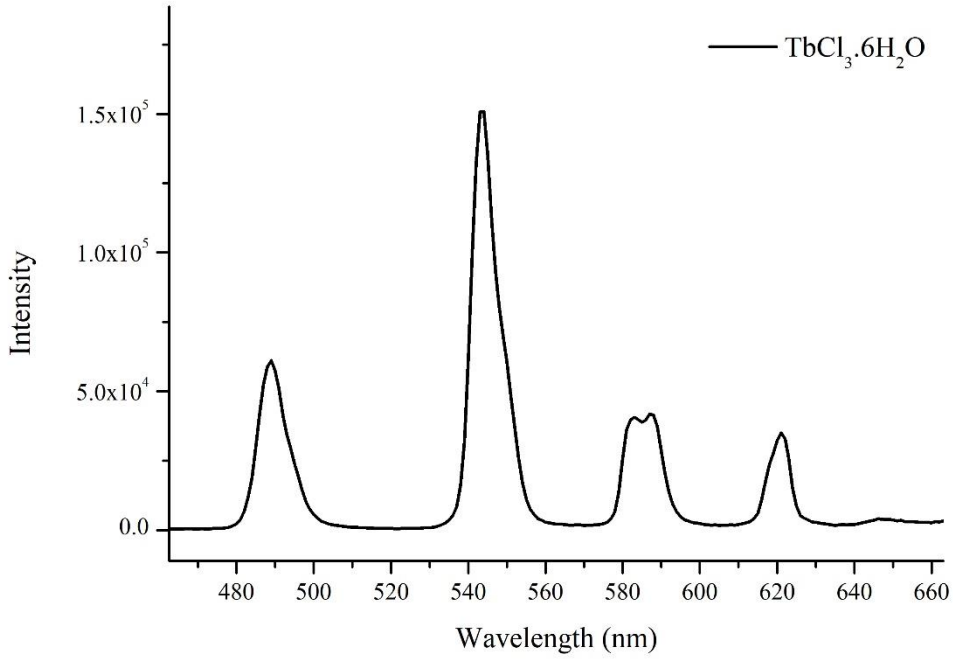

Figure 15. Emission spectrum of an aqueous solution of $TbCl_3.6H_2O$ (0.05 M) (λexc = 344 nm).

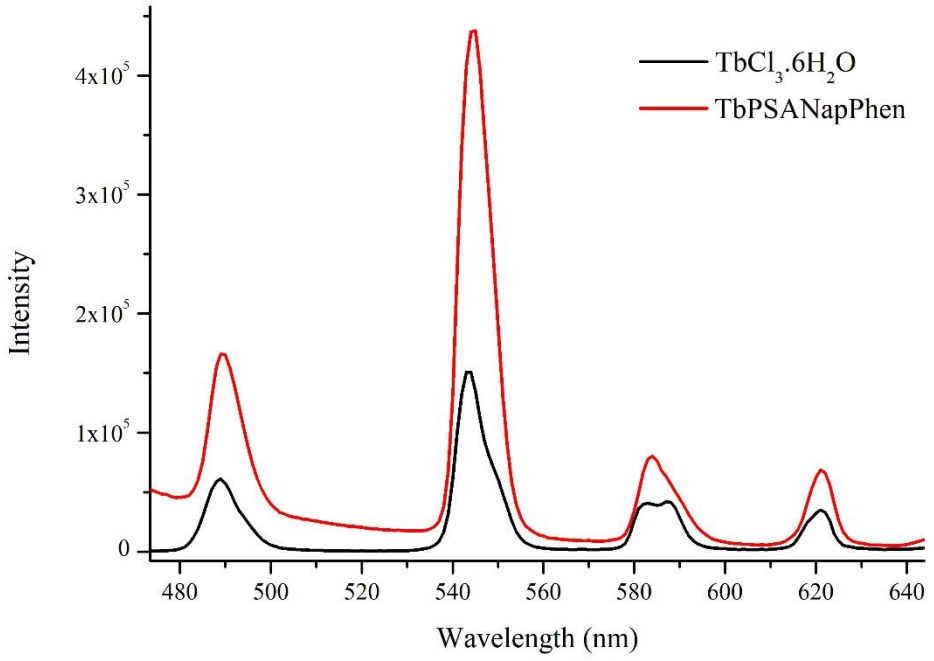

Figure 16. Emission spectrum of a TbPSANapPhen ($EtOH:H_2O$) solution and an aqueous solution of $TbCl_3.6H_2O$ (0.05 M) (λ exc = 344 nm).

Similarly to EuPSANapPhen, it can be seen (Figure 16) that an enhancement of luminescence intensity occurs upon complexation of Tb(III) with PSA, Nap and Phen, which is a result of the antenna effect of the organic ligands, as previously explained. The characteristic peaks of electronic transitions of terbium remain visible at 488, 544 (most intense, green colour), 583 and 621 nm. These are the only visible peaks in the emission spectrum of TbPSANapPhen compound, which allows to conclude that the energy transfer is also successfully occurring between the PSA and the terbium trivalent ions. For the terbium polymer complex, the mechanism of energy transfer occurs in an identical way to the above mentioned for EuPSANapPhen, where first there is an excitation by photon absorption, followed by relaxation via intersystem crossing and energy transfer from excited state of polymer to fundamental state of lanthanide, which ends with the emission of terbium ions by multiple relaxation of photons[29]. In Figure S2 and S3, the excitation spectra of $TbCl_3.6H_2O$ and TbPSANapPhen can be observed, respectively.

3.1.1 Interaction of the functionalized polymer with metal solutions

After the synthesis of two lanthanide luminescent polymer complexes, EuPSANapPhen and TbPSANapPhen, and having studied their fluorescence properties, the next step was to investigate their possible interaction mechanisms with different metal ions and what could result from it.

It shall be stated that the EuPSANapPhen and TbPSANapPhen solutions, just before the addition of the metal ion solutions, are transparent and colourless, suggesting the existence of a homogeneous solutions. However, upon the mixture with some salt solutions (Figure 17), some solutions presented a colourful aspect.

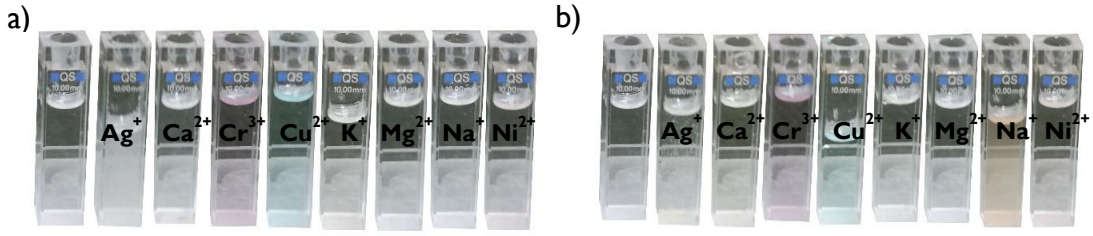

Figure 17. Appearance of EuPSANapPhen (a) and TbPSANapPhen (b) aqueous solutions after reaction with different metal ions.

Fluorometric results from each interaction of europium polymer complex with different metals can be seen in Figure 18. The characteristic europium transition peaks occurring at 578, 591, 616, 650, 687 and 698 nm, remain in the spectra regardless of the addition or not of a metal solution to the luminescent complex. Interpreting these results, it is possible to observe that, in a first approach, there is no significative difference on the intensity of the complex luminescence when metal ions are added, regarding the characteristic red emission peak (616 nm).

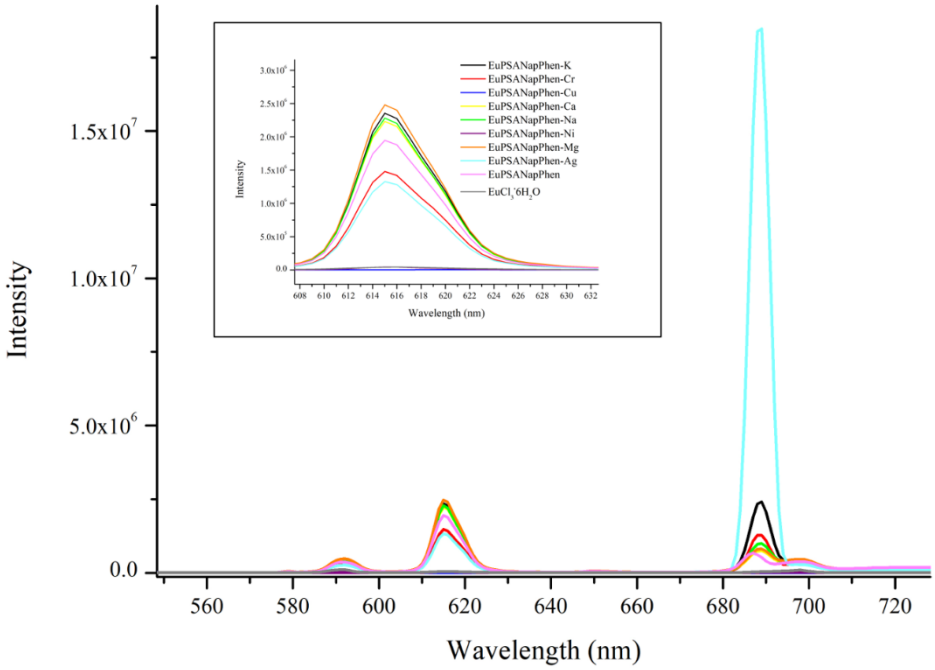

Figure 18. Emission spectra of solutions of EuPSANapPhen (EtOH:H_2O) in the presence of different metal ions (λexc = 344 nm).

However, when adding silver nitrate, represented in Figure 18 as light blue colour, it was possible to observe an intense enhancement of the peak located at 688 nm ($^5D_0 \rightarrow {}^7F_4$), which is coincident with the fact that at eyesight the EuPSANapPhen-Ag solution presented a different colourful appearance due to the formation of a precipitate (AgCl), which will reveal different optical properties, resulting in a different emission spectrum, mainly due to an increase in the turbidity. From the analysis of Figure 18, it can also be concluded that the presence of Cu and Ni does not lead to an increase in the intensity of emission of the $EuCl_3.6H_2O$ aqueous solution. To better evaluate the difference between the addition of different metal ions, a new graph containing just the europium polymer complex solution, the pure lanthanide solution and the solutions after the addition of copper and nickel was plotted (Figure 19). Also, in Figure S5 and S6 of

Supporting Information, emission and excitation spectra of the EuPSANapPhen solutions in the presence of different metal ions can be seen, respectively.

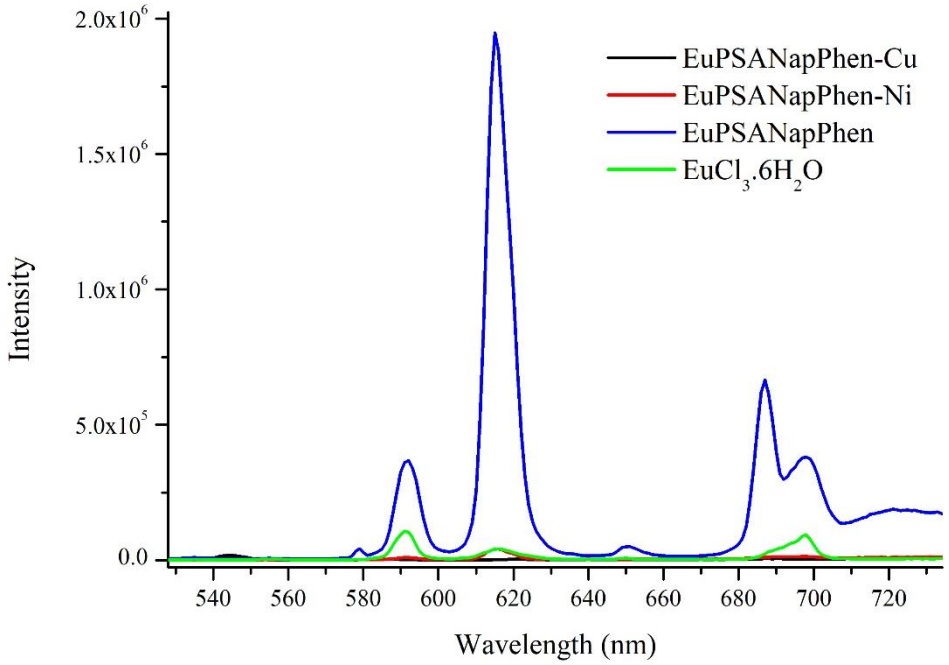

Figure 19. Emission spectra of solutions of EuPSANapPhen (EtOH:H_2O) in the presence of Cu and Ni (λexc = 344 nm).

From the discussion above, it seems out that Cu(II) and Ni(II) lead to a different luminescence response (i.e., quenching). As it can be seen in Figure 19, the intense characteristic peaks of europium transitions, located at 579, 591, 616, 650 and 687 nm in the EuPSANapPhen spectrum become almost indistinguishable in the presence of Cu and Ni ions (represented in black and red lines, respectively). This can be explained due to the higher ability of the metallic center to interact with the ligands, which involves an energy transfer mechanism. In this type of systems, the sensitization of the europium ion is blocked by the bonding of Cu/Ni ions with Phen and the excited state of the antenna suffers electronic transfer to the Cu/Ni[39]. The coordination sphere of Eu is nearly affected by the occurring of the bond between the ligand and the metal and that is why the changes in the emission spectrum are mainly in its intensity and not in its form. As so, most of metal ions did not trigger the intensity of emission, but copper and nickel ions revealed to be effective luminescence quenchers, which can be useful for further applications in security devices that will later be discussed in detail.

Quenching efficiency (%) of all metal ions was evaluated using Equation 1. The corresponding values for Q (Quenching Efficiency = Q), as computed at 616 nm for europium solutions, are shown in Figure 20.

From the analysis in Figure 20, it can be seen that Cu and Ni ions are almost efficient quenchers of europium luminescence emission, possessing a quenching efficiency of nearly 100%. Silver and chromium revealed to be also quenchers, even though not so efficiently as the previous transition metals (with 32 and 24% of quenching efficiency, respectively). Calcium, sodium, potassium and magnesium not only did not quench the luminescence intensity, but they induced an enhancement of emission.

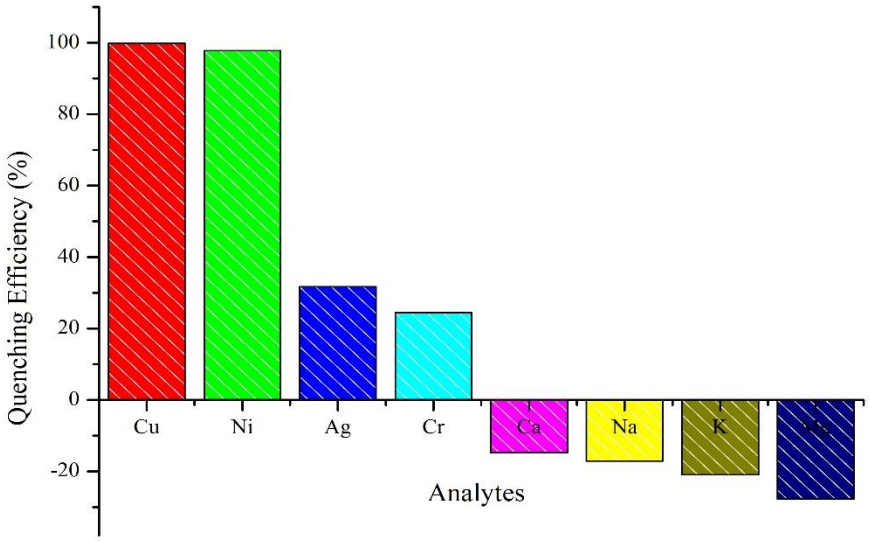

Figure 20. Quenching efficiency (%) of EuPSANapPhen-metal solutions (616 nm).

In the matter of visible appearance, all EuPSANapPhen solutions mixed with metal ions did not present luminescence at eyesight, but when submitted to UV excitation, visible red (Eu) colour was possible to be observed. In Figure 21 photographic results obtained under excitation at 366 nm can be observed. Once again, these results are in agreement with spectroscopic ones, since when Cu(II) and Ni(II) are added to the lanthanide polymer solution, they become colourless, in result of the quenching that occurs.

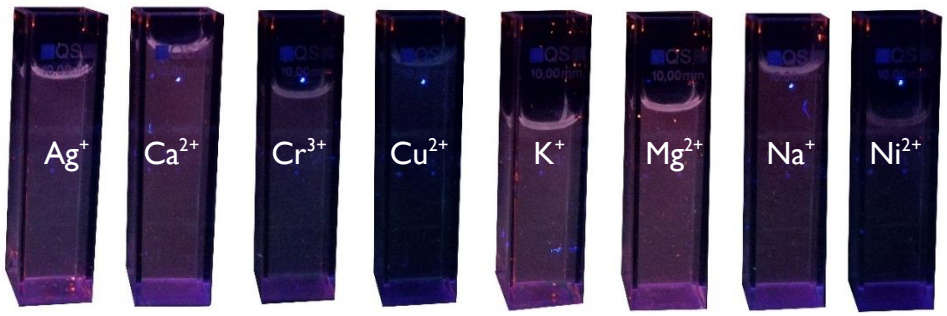

Figure 21. Photographs of EuPSANapPhen aqueous solutions in the presence of metal ions, under UV excitation at 366 nm.

The same procedure was applied to the terbium polymer complex, TbPSANapPhen and results of emission spectra of pure solutions and in the presence of different metal ions can be observed in Figure 22 and Figure 23. In Figure S7 and S8 of Supporting Information, the emission and excitation spectra of the corresponding solutions are shown, respectively.

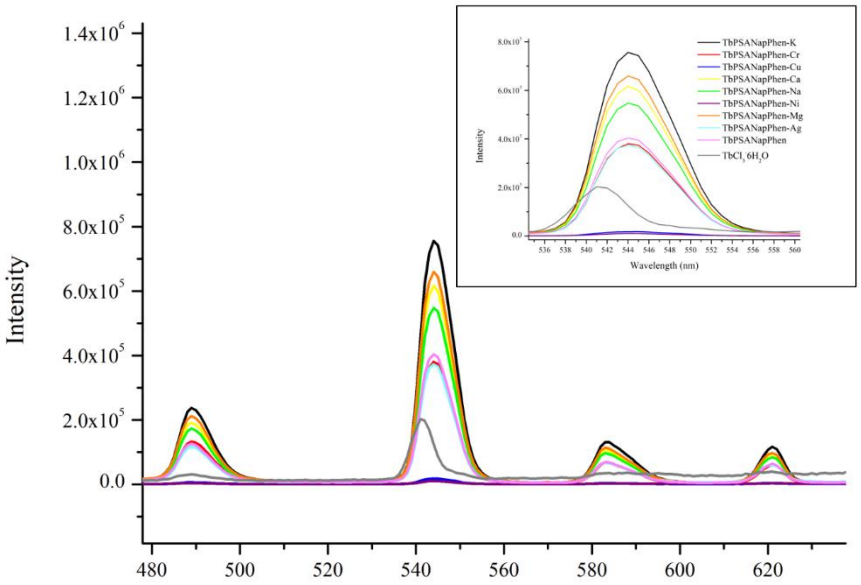

Figure 22. Emission spectra of solutions of TbPSANapPhen (EtOH:H_2O) in the presence of several metal ions (λexc = 344 nm).

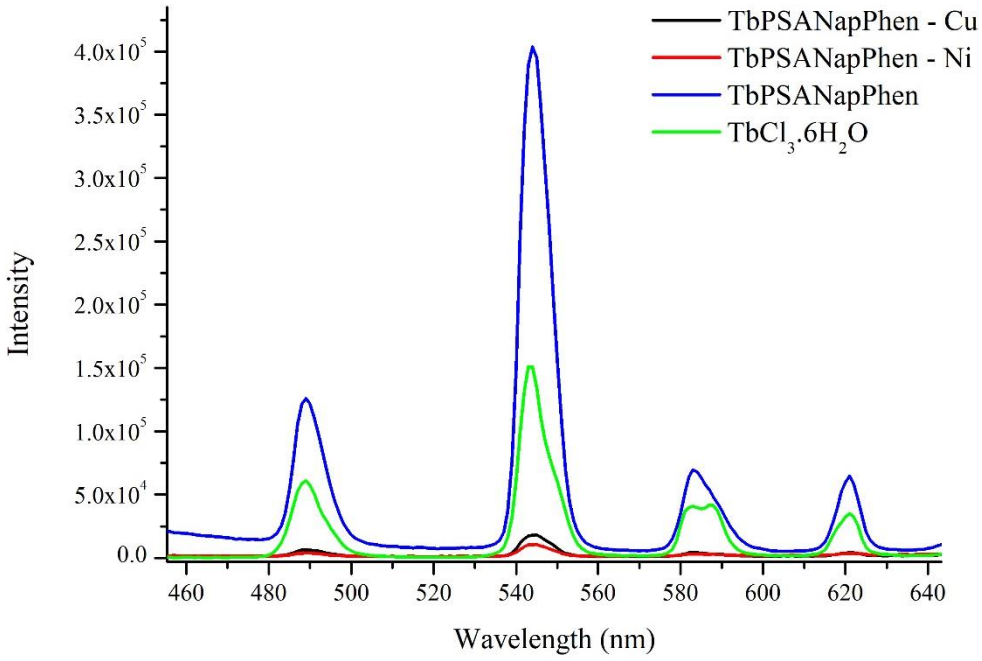

Figure 23. Emission spectra of solutions of TbPSANapPhen (EtOH:H_2O) in the presence of Cu and Ni, (λexc = 344 nm).

Once again, as equal to europium systems, copper and nickel salts revealed to be the most effective emission quenchers for terbium compounds. The quenching effect of these two metal ions induces an almost blur of the characteristic peaks of $^5D_4 \rightarrow ^7F_J$ terbium electronic transitions, occurring at 488, 544, 583 and 620 nm in the TbPSANapPhen spectrum and almost indistinguishable in the ones where the lanthanide polymer compound was in their presence. When comparing emission intensities (see the inset of Figure 22), some small differences could be observed between metal ions. This quenching fact is due to similar reasons as the quenching observed for the Eu system. That is, the bonding of the metal ion to the ligand Phen, which has great affinity towards Cu(II) and Ni(II), is blocking the sensitization of terbium because the excited state of the antenna undergoes electronic transfer to the Cu/Ni[39]. The differences that can be observed in the spectrum are mainly in the emission intensity and not in the general form, because the coordination sphere of terbium is not significatively altered with the bonding to the metal.

In the same way as it was for europium systems, Tb compounds were also photographed under UV excitation at 366 nm upon interaction with several metal ions, and the results obtained can be observed in Figure 24.

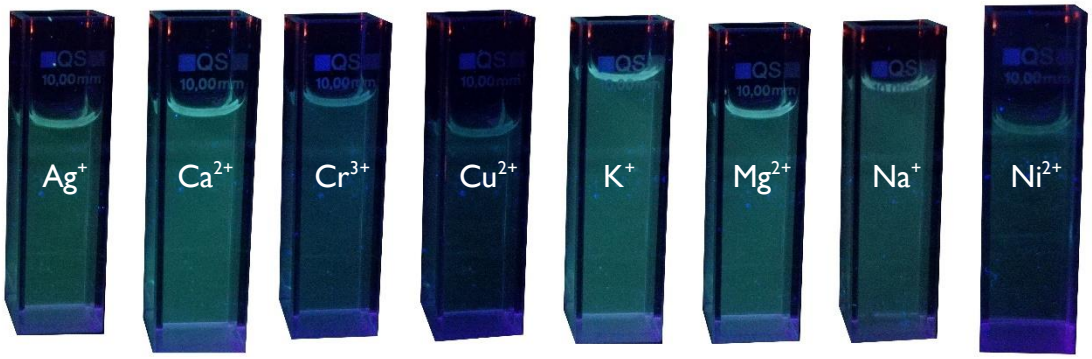

Figure 24. Photographs of TbPSANapPhen aqueous solutions in the presence of metal ions, under UV excitation at 366 nm.

Eu and Tb systems proved to be very similar both in terms of appearance at the eyesight and in terms of luminescence when in the presence of different metal ions. That is, they both suffered emission quenching after the addition of copper and nickel, turning colourless, which ensures the spectroscopic results that were obtained after fluorometric procedures.

Quenching efficiency of metal ions in terbium compounds was also calculated through the same equation, but in this case considering the intensity values at wavelength of 543 nm (maximum intensity). The obtained results are shown in Figure 25.

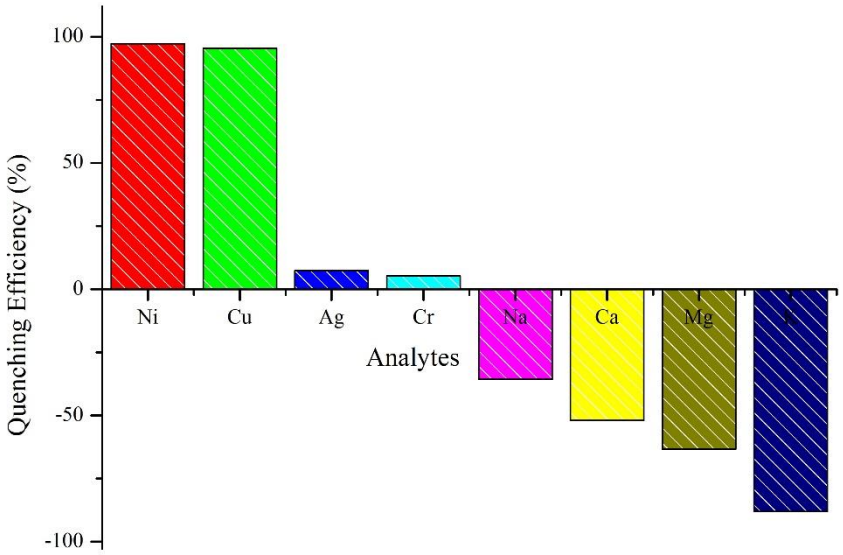

Figure 25. Quenching efficiency (%) of TbPSANapPhen-metal solutions (543 nm).

Anew, remarkably, copper and nickel ions showed almost total quenching efficiency (~100%), showing this time a slight (not much relevant) difference between the europium system, as nickel presented higher efficiency than copper. Despite that, the efficiency of the metal ions is almost identical when comparing Eu or Tb complexes, since in this case the other quenchers were also silver and chromium, even though with lower percentage of efficiency, and the other metal ions (Na, Ca, Mg and K) show some luminescence enhancement.

So, taking into account these results, corresponding to the effect of some metal ions in the luminescence emission of the lanthanide polymer complexes, copper and nickel salts were chosen for the study of the potential application of lanthanide-based complexes as paper security tags.

3.1.2 Influence of the anion in the intensity of luminescence of lanthanide-based complexes

In order to discover the effect of the counterion on the intensity of emission of the prepared lanthanide polymer complexes, different sodium salts were added to the solutions of EuPSANapPhen and TbPSANapPhen in the same concentration (0.002 M). Figure 26 shows emission spectra of EuPSANapPhen solutions in the presence of different sodium salts. Moreover, Figure S9 and S10 of the Supporting Information show the emission and excitation spectra of EuPSANapPhen solutions in the presence of sodium salts, respectively.

As aforementioned, sodium proved not to be a quencher of emission, so it was predictable to observe an enhancement of emission with the addition of sodium salts to the complex solutions. Characteristic peaks of europium electronic transitions continued to be observable on emission spectra of EuPSANapPhen-sodium salts solutions (Figure 26) at 579, 591, 615, 651, 690 and 698 nm ($^5D_0 \rightarrow {}^7F_J$, J=0-5).

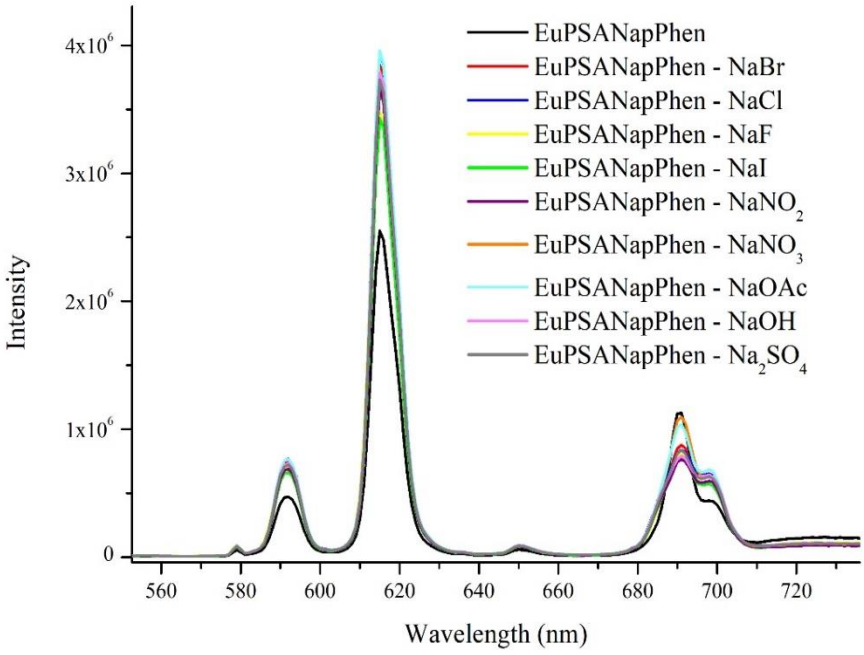

Figure 26. Emission spectra of solutions of EuPSANapPhen (EtOH:H_2O) in the presence of different sodium salts (λexc = 344 nm).

The predictable result of emission enhancement was effectively observed, since no significant changes of intensity could be detected. That is, the counterion in this case did not have any significant effect on the intensity of fluorescence emission, since all of sodium salts that were added to the lanthanide complex solution induced a similar enhancement of emission. Having the fluorometric results obtained, quenching efficiency

of the different sodium salts was also calculated via the abovementioned equation, considering intensity values at wavelength of 616 nm (maximum intensity) and the results can be observed in Figure 27.

As explicit in Figure 27, it can be concluded that the counterion utilized (Br^-, Cl^-, F^-, I^-, OAc^-, OH^-, NO_2^-, NO_3^-, or anhydrous SO_4^{2-}) to test its effect on the emission of europium complex systems was not relevant, since no particular changes occurred after the addition of different salts. That is, all sodium salts proved to enhance thereabout luminescence emission characteristic of europium.

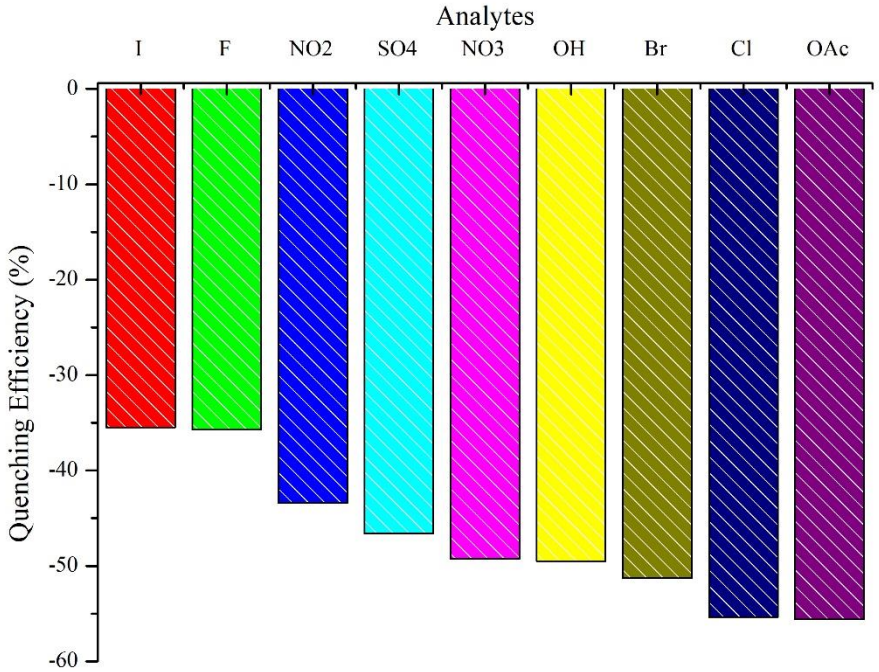

Figure 27. Quenching efficiency (%) of EuPSANapPhen-sodium salts (616 nm).

Moreover, it is also worth noticing that despite a negative value of the quenching efficiency may have no physical meaning, its negative algebraic result proves that the anions are efficient on the enhancement of the lanthanide complex emission.

The effect of different sodium salts on the luminescence behaviour of Tb-based polymer complexes was also evaluated. The results are shown in Figure 28. Moreover, in Figure S11 and S12 of the Supporting Information, emission and excitation spectra of TbPSANapPhen solutions in the presence of different sodium salts are reported, respectively.

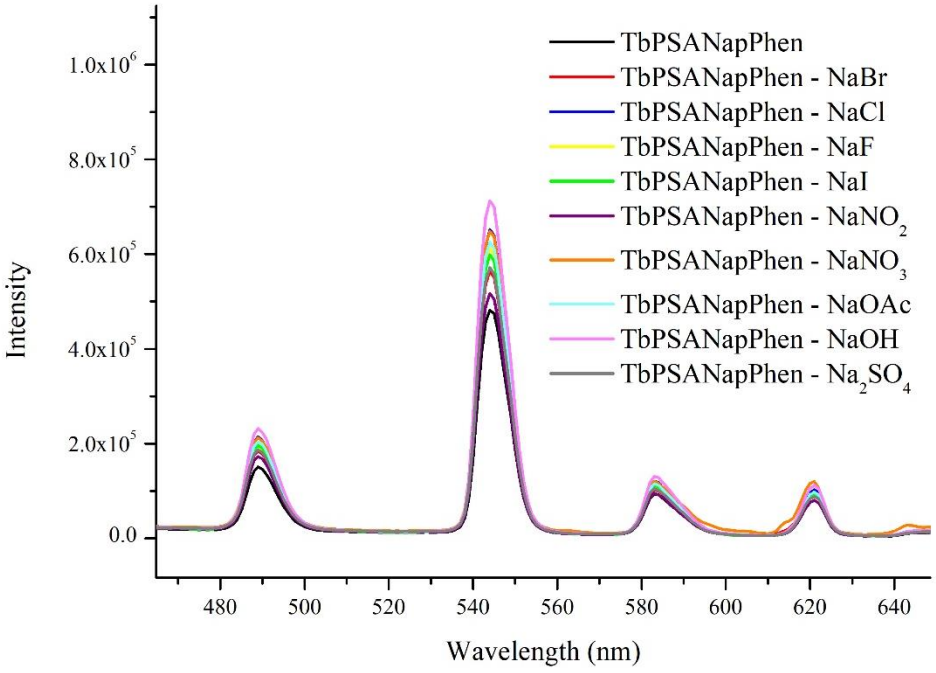

Figure 28. Emission spectra of solutions of TbPSANapPhen (EtOH:H_2O) in the presence of different sodium salts (λexc = 344 nm).

Analysing these results, it is possible to observe that the characteristic emission peaks of terbium electronic transitions ($^5D_4 \rightarrow {}^7F_J$, J=6-3) are still visibly distinguishable at 489, 544, 583 and 620 nm. Also, as expected because sodium caused enhancement of emission of TbPSANapPhen, no quenching occurred after the addition of different sodium salts.

Contrarily, addition of several sodium salts triggered the intensity of emission, although no significative changes could be observed for each salt. In other words, the effect of the salt counterion in terbium complexes was nearly irrelevant, as in europium complexes. Despite that conclusion, the quenching efficiency of the counterions for terbium systems was calculated mathematically considering the values at 543 nm (maximum intensity) with the results presented in Figure 29.

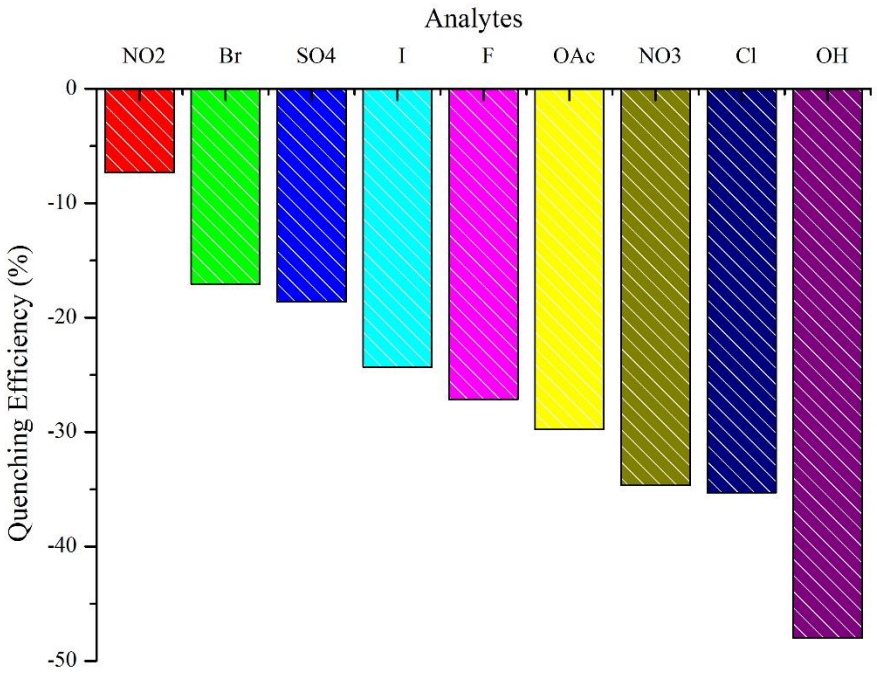

Figure 29. Quenching efficiency (%) of TbPSANapPhen-sodium salts (543 nm).

Remarkably, all different counterions of sodium salts enhance luminescence emission intensity in terbium compounds. Contrarily to what happened with Eu complexes where the efficiencies of quenching were nearly equal, in TbPSANapPhen solutions there were slight differences. However, those small differences were not considered relevant, since all sodium salts proved to enhance terbium emission. Therefore, it was possible to conclude that no difference between Eu and Tb systems in terms of the counterion effect was reflected. That is, in both cases, the presence of a different salt was not significantly related to the intensity of emission.

3.1.3 Detection limit of metal ions

Having chosen copper and nickel as the perfect candidates for further applications in paper analysis for security applications, since they showed optimal emission quenching properties, its detection limits were studied, with the main purpose of finding the perfect concentration that would later be applied on the surface of the functionalized paper. For that, solutions of EuPSANapPhen and TbPSANapPhen were mixed with $Cu(NO_3)_2$ and $Ni(NO_3)_2.6H_2O$ in a range of concentrations, varying from 0.02 mM to 2 mM. Fluorometric analysis were done and emission spectra were recorded with excitation fixed at 344 nm for both systems.

a. Detection limit of copper in EuPSANapPhen

In order to simplify the discussion, only the detailed procedure to find the detection limit of copper in the europium system will be detailed here. As the procedure is the same, not only the detection limit for nickel in europium system, but also for both metal ions in the terbium system will have their data shown in the Supporting Information section.

To analyse the sensitivity to Cu(II) of europium-based complex aqueous solution, its emission spectra were recorded. For that, a set of solutions with different molar ratios [Cu(II)]/[EuPSANapPhen], and keeping the [EuPSANapPhen] constant, were prepared and their emission spectra recorded. Figure 30 shows the emission spectra of the corresponding EuPSANapPhen-Cu systems.

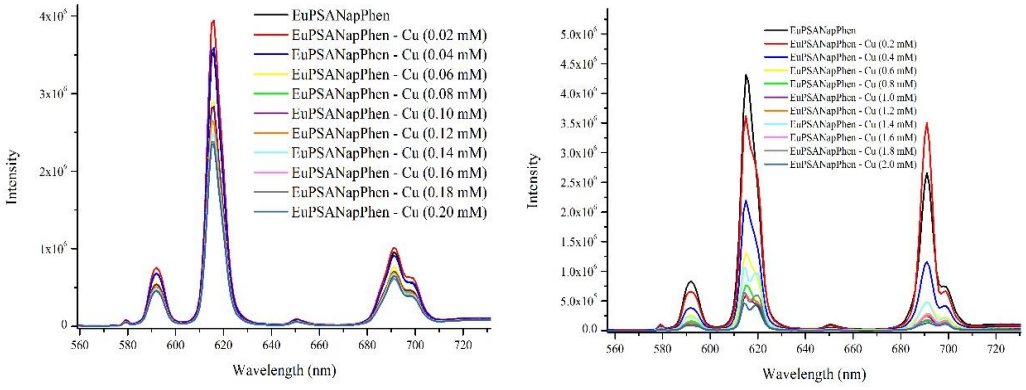

Figure 30. Emission spectra of EuPSANapPhen solutions (EtOH:H_2O) in the presence of $Cu(NO_3)_2$ in the concentrations from 0.02 mM to 2 mM (λexc = 344 nm).

Moreover, in Figure S13 and S14 of Supporting Information, emission spectra of EuPSANapPhen solutions in the presence of Cu(II) salts can be observed. The corresponding excitation spectra are shown in Figure S15 and S16.

Analysing the results shown in Figure 30, the quenching process upon addition of copper is explicit. That is, as the amount of Cu is enhanced, the intensity of luminescence emission decreases. For better understanding the spectroscopic results, a graphic representation of intensity at wavelength of 616 nm (most intense peak – $^5D_0 \rightarrow ^7F_2$ transition) versus copper concentration has been plotted (Figure 31).

Notably, there is an exponential decrease of intensity according to an enhancement of metal concentration. The non-linear shape of the curve could be explained by the occurrence of simultaneous static and dynamic quenching mechanisms.

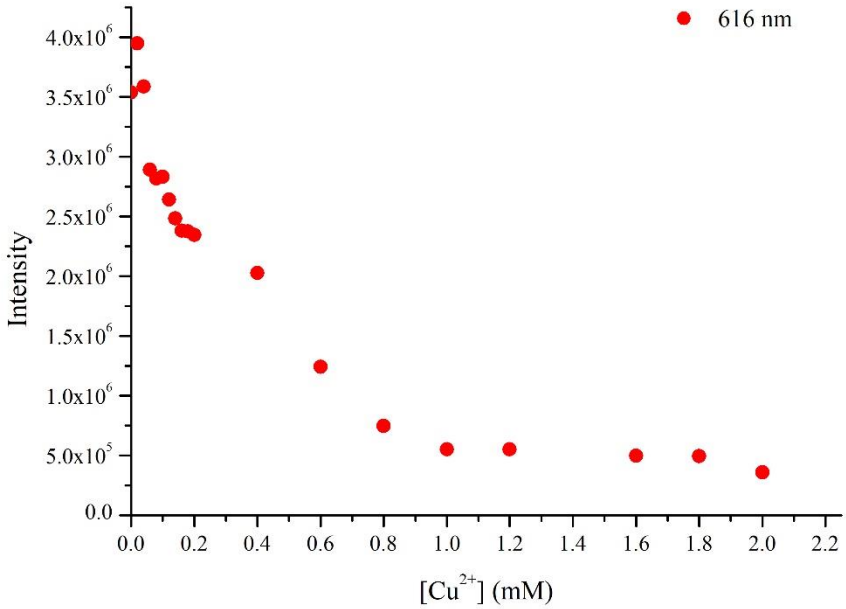

Figure 31. Dependence of the emission intensity of EuPSANapPhen ($^5D_0 \rightarrow ^7F_2$ transition) / Cu(II) mixed solutions on the Cu(II) concentration.

The quenching of fluorescence can be described, by using the Stern-Volmer Equation (2). In Figure 32 can be observed the S-V plot for the EuPSANapPhen-Cu ($^5D_0 \rightarrow ^7F_2$ transition at 616 nm) system.

From the analysis of Figure 32, it can be concluded that a straightline equation fits well (r^2=0.997) the experimental data of I_0/I as a function of $[Cu^{2+}]$, i.e., the dependence of I_0/I follows a good linear correlation. The obtained K_{SV} is equal to 2.76 mM^{-1}. Having known both the S-V constant and the standard error, it is possible to calculate the limit of detection for copper ions by europium-containing complexes, following Equation 3.

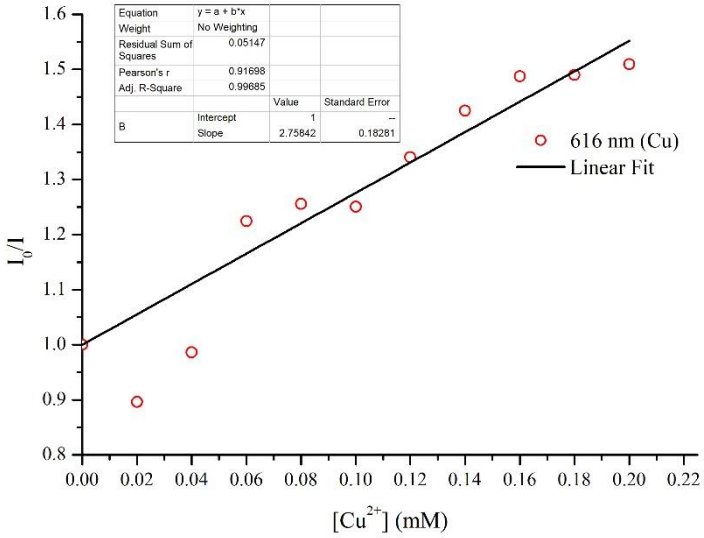

Figure 32. Stern-Volmer plot of EuPSANapPhen-Cu $^5D_0 \rightarrow {}^7F_2$ transition (616 nm), vs Cu concentration.

For EuPSANapPhen compounds, the limit of detection obtained was 0.219 mM (ca.13.9 ppm) and, therefore, it can be said that EuPSANapPhen shows great sensitivity to copper ions.

Regarding the values obtained for the S-V constant, it can be concluded that a certain type of quenching could be occuring. To be sure what type of quenching is, in fact, present, the experiment could be done at different temperatures. If the constant obtained would suffer an increasement with temperature, then it it would be dynamic quenching. On the other hand, if K_{sv} would decrease with the temperature, then it would be static quenching[40,41]. However, due to time constraints during this project, experiments varrying the temperature could not be done, so it was not possible to conclude which type of quenching was in fact occuring with the addition of the metal solution.

Table 1 shows the corresponding, S-V constants, standard errors, limits of detection for both metal ions (Cu(II) and Ni(II)) for both systems (Eu and Tb) and the determination coefficients (r^2).

Table 1. Stern-Volmer constants, standard errors, respective detection limits and determination coefficients (r^2) of both metal ions (Cu(II) and Ni(II)) for the EuPSANapPhen and TbPSANapPhen systems.

	K_{sv} (mM^{-1})	σ (mM^{-1})	LOD (mM)	LOD (ppm)	R^2
Eu-Cu	2.8	0.2	0.22	14	0.997
Eu-Ni	2.8	0.1	0.08	5	0.999
Tb-Cu	2.1	0.1	0.17	11	0.999
Tb-Ni	2.5	0.2	0.22	13	0.997

3.1.4 Limit of quantification for metal ions

The limit of quantification of both copper and nickel metal ions on both europium and terbium systems was also determined, taking into consideration the results obtained after the fluorometric analysis, previously described. The quantification limit was determined using Equation 4.

Table 2 shows the respective values obtained for the quantification limit of both EuPSANapPhen and TbPSANapPhen systems.

Table 2. Quantification limits of both metal ions (Cu(II) and Ni(II)) for the EuPSANapPhen and TbPSANapPhen systems.

	LOQ (mM)	LOQ (ppm)
Eu-Cu	0.66	42
Eu-Ni	0.26	15
Tb-Cu	0.53	34
Tb-Ni	0.67	40

The results present on both Table 1 and 2 reveal good results for a future application of the methodology developed in this project on the effluents study, using the europium and terbium polymer complexes as probes for both copper and nickel ions.

3.2 Paper analysis

After the synthesis of two luminescent lanthanide polymer complexes (EuPSANapPhen and TbPSANapPhen), and to pursuit the scope of this project, the complexes were incorporated in paper sheets aiming the development of a functionalized paper. That should be achieved without compromise the quality and the function of paper. On other words, the paper should be white at eyesight but luminescent under UV radiation, being the latter used for security applications. Different types of paper namely filter paper, base paper and office paper were tested. Moreover, different methods of incorporation of Eu and Tb-based compounds were also tested. Finally, their interactions with copper and nickel ion solutions, previously chosen due to their quenching effects on the emission of both europium and terbium complexes were also assessed.

3.2.1 Incorporation of luminescent lanthanide polymer complexes in paper

EuPSANapPhen and TbPSANapPhen solutions, prepared following the protocol previously described in section 2.3.1 were used in this stage of the project, with the purpose of incorporating compounds with optimum optical properties in paper sheets (filter, base and office paper). Two methods were tested: a) luminescent lanthanide polymer complex solutions stamped in paper, and b) paper submerged in luminescent lanthanide polymer complex solutions.

3.2.1.1 Luminescent lanthanide polymer complexes stamped in paper

To test the effectiveness of incorporation of EuPSANapPhen and TbPSANapPhen in the paper sheets via stamping of lanthanide polymer complex solutions, stamps of letters EU and TB (Figure 42) were used.

Figure 33. Stamps used for the incorporation of EuPSANapPhen and TbPSANapPhen in paper sheets via the stamping method.

After stamping the respective paper sheets with both EuPSANapPhen and TbPSANapPhen solutions, the sheets were left drying at room temperature for 24 hours. Photographic results at eyesight were obtained and later compared to those attained in a dark room under UV excitation at λ = 254 nm. In Figure 34 photographic results (visual inspection) obtained after stamping of paper sheets with the EuPSANapPhen solution are reported.

From the observation of the photos shown in this discussion, it is worth noticing that the images do not accurately represent what is seen by the eyes of the user. This fact reflects mainly in the results obtained under UV radiation, where frequently it was not possible to get a picture that revealed the actual colour being emitted by the respective lanthanide. However, despite that, it was possible to visualize the presence of the luminescent compound on the paper. Moreover, it is also necessary to elucidate the reader that technical printing conditions could result in printed images showing patterns of colours that are not visible when seeing the same picture in optical devices, nor in the actual paper sheet. So, with that being said, the results shown are the best that was possible to obtain under eyesight and UV radiation, upon stamping with the luminescent solutions, and the further discussion of the obtained results will try to be as clear as possible, in a way that the reader can visualize himself the actual results.

The purpose of this first used method is to obtain a sheet that would not show any visual differences for consumers, but when excited by using an UV-lamp it would reveal the characteristic lanthanide emission colour on the stamped region.

So, in Figure 34, it can be seen the visual inspection of the three different types of paper sheets stamped with EuPSANapPhen.

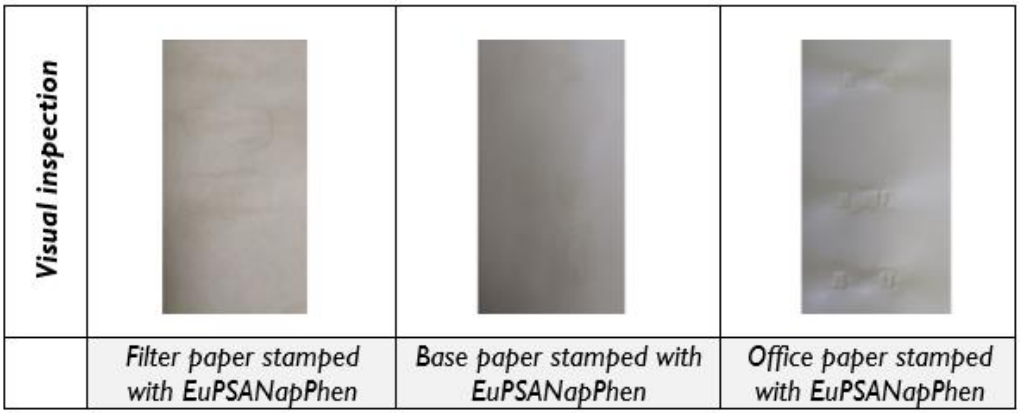

Figure 34. Photographs of the three types of paper sheets (filter, base and office) stamped with EuPSANapPhen, at eyesight.

Regarding these results, it was intended that no significant changes could be noted at eyesight in any type of paper, but when observing the pictures by using an optical device, on the office paper sheet, the site of the stamp can be recognized. Moreover, when observing the actual paper sheets at eyesight, it is possible to see, without being needed particular examination, the sites where the stamp was applied. This fact can be assigned to the strength/pressure that was applied during the stamping. In other words, it is not easy to always apply the same pressure on the paper sheet because the procedure is not an automatic one; consequently, the reproducibility of the method is not totally achieved. Another aspect that can be noticed on all types of paper, but mainly on filter paper stamped with EuPSANapPhen, is that the lanthanide polymer complex solution could not be fixed exactly on the spot of the stamp; contrarily, it would disperse a little sideways of the stamp. This can be occurring due to the fact that the volume of solution present on the stamp cannot be controlled and the solution viscosity is similar to that of water; thus, different applications lead to different dispersion degrees. This could be improved in the future by preparing a solution with higher viscosity.

With that in mind, it was possible to incorporate the lanthanide complex into all three types of paper, although this method of incorporation needs to be improved in the future, so that the visualization of the stamped regions at eyesight would not be experienced.

When observing the photographs resulting from the exposure of sample paper to UV radiation (λ = 254 nm) (Figure 35), it can be concluded that the lanthanide polymer complex is effectively incorporated into the paper. This fact is visually explicit, since when the complex is excited with a 254 nm wavelength radiation, the paper sheets that are white at visible light, show luminescence emission of the characteristic colour of the respective lanthanide (in this case, Eu(III) – emits a red colour).

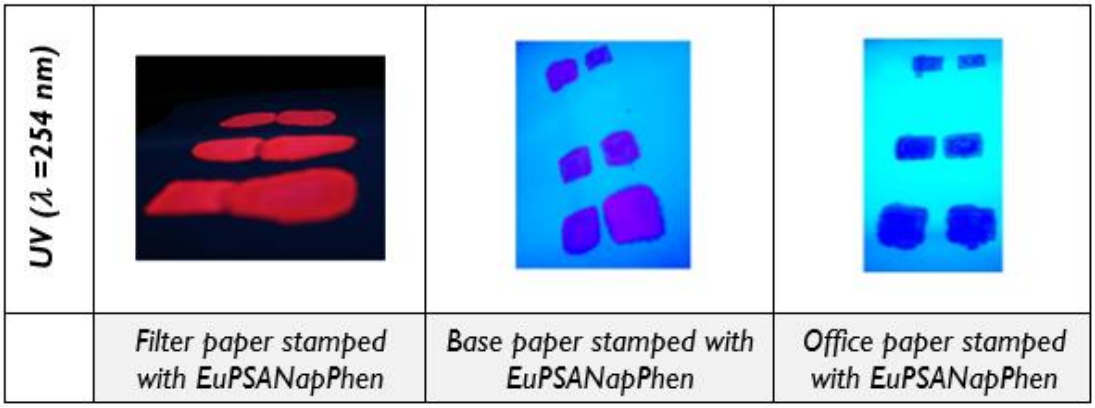

Figure 35. Photographs of the three types of paper sheets (filter, base and office) stamped with EuPSANapPhen, under UV radiation (λ = 254 nm).

Regarding the filter paper, the red colour emission can be easily seen. However, when analysing the UV results of the base paper and office paper stamped with EuPSANapPhen solution, it is not so easy to obtain a picture that can actually reflect the lanthanide emission radiation. Despite that, when observing the images by using an optical device, the result obtained for the base paper sheet permits the observation of a light pink colour, but the user can observe the characteristic red colour of europium. The blue colour that can also be observed in background, either in base or office paper, is caused by the optical agents that are incorporated onto the paper sheets during the manufacture processes, to improve the optical and printing paper properties. Moreover, this incorporation of optical agents may be one of the reasons behind the difficulty for obtaining the perfect image of the lanthanide emission (in base and office papers), since not only the lanthanide emits radiation when under UV excitation, but also because the optical agent emit a blue colour. The effect of paper fillers (e.g. $CaCO_3$) on this process cannot also be ruled out. However, despite the difficulties to obtain an accurate image of what was occurring, it can also be concluded looking at the base and office paper stamped with the lanthanide polymer complex solution, that these types of paper can receive the incorporation of a security element that will only emit radiation when excited via a UV source. When observing the photographic results of the office paper, it is seen a less strong red colour emission characteristic of europium. This detail is not only caused by the difficulties of getting a real picture, but in fact, office paper revealed a less intense emission, upon excitation. Thus, that could be related to the fact that office paper suffers a more intense coating process, with components that could react to the lanthanide polymer complex solution presented in this project, blocking in some way its luminescence emission. Nevertheless, the incorporation of EuPSANapPhen solution could be confirmed in all types of paper, being more easily recognized on filter paper, since it is the one which suffers less whitening and coating processes[35]. Another important aspect that can be noticed in all photographic results obtained either at eyesight or under UV radiation after stamping with EuPSANapPhen solution, is that it is not possible to recognize the "EU" pattern of the stamps. That is, the effect on all types of paper, provoked by the stamping with the lanthanide polymer complex solution, is seen but not with the ideal shape (EU) that was the first purpose. When observing the photographic results of the office paper sheet at visible light, it is slightly possible to observe the shape of the letters (probably due to more intense strength applied).

This can be easily seen by the user. However, the same paper sheet cannot permit the observation of the EU pattern of the stamp when submitted to UV radiation. Once

again, this fact could be attributed to the difficulties of reproducibility of the stamping process and applying the same strength/pressure.

So, in the future, the best stamping conditions (volume and pressure) should be determined, in order to improve the incorporation of complex solutions on the paper.

Figure 36 shows the photographic results for the stamping with TbPSANapPhen, at eyesight. The photos obtained after stamping filter, base and office paper with the terbium solution (TbPSANapPhen) present the same colour issues described before, so the reader must bear that in mind. Once again, the further discussion will try to clarify that in such a way that the reader can experience the same as the user.

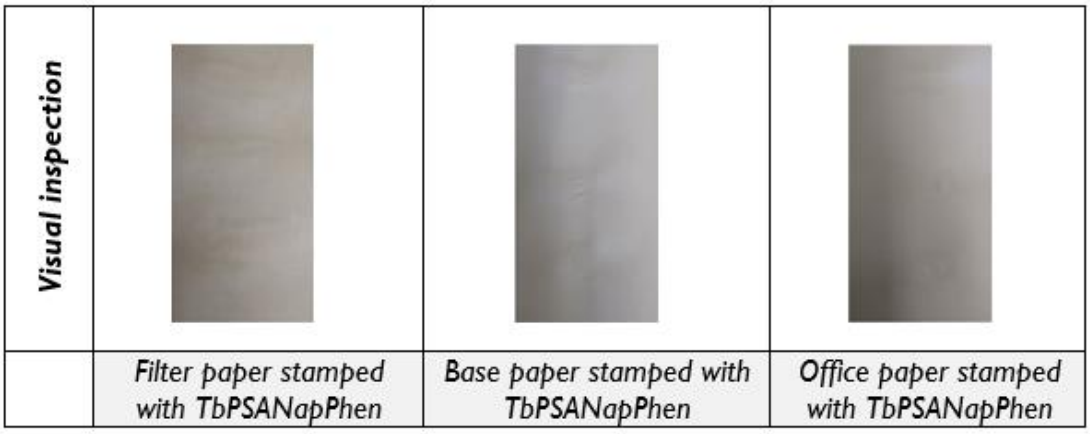

Figure 36. Photographs of the three types of paper sheets (filter, base and office) stamped with TbPSANapPhen, at eyesight.

After visual inspection (Figure 36) of the stamped filter, base and office papers, no significant differences between them can be observed. Moreover, it can be possible to admit that the purpose of getting a paper that did not present any visual changes was, in fact, achieved. However, when the user has these paper sheets on their hands, a similar aspect of the paper that had been stamped with EuPSANapPhen could also be observed. That is, when looking directly to the three different paper sheets after being stamped with TbPSANapPhen, the region of the sheet that had been stamped can be easily detected, with no need of a detailed examination. Another aspect worth noting is that when using the terbium solution, the same dispersion problem occurs, resulting in a stain section of the paper sheet. As previously explained, this fact is attributed to the difficulty of not being able to control the intensity of the strength and pressure applied while stamping nor being able to control the volume of solution that is applied with each stamp, due to it being manually done; moreover, the viscosity of the complex solution being similar to that of water solutions, can also be an explanation for that fact. Also, as equal to Eu systems, when the paper sheets were stamped with the TB stamps, the

pattern was not supposed to be noticed by visual inspection, only under UV radiation (Figure 37). However, in the perspective of the user, this pattern can be easily observed in base and office paper sheets stamped with TbPSANapPhen. So, for the incorporation of Tb complexes into paper, the same conclusion can be taken. That is, the confirmation of incorporation was achieved; however, the method still needs to be improved in the future.

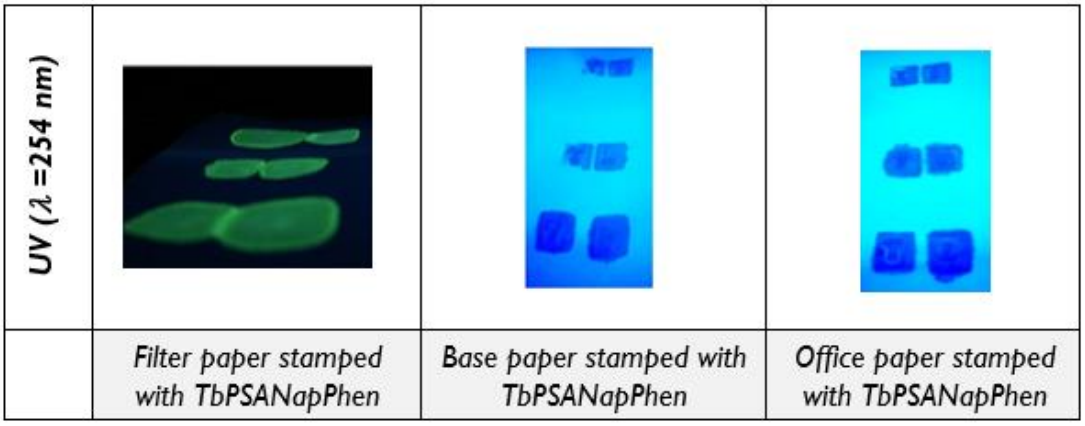

Figure 37. Photographs of the three types of paper sheets (filter, base and office) stamped with TbPSANapPhen, under UV radiation (λ = 254 nm).

Regarding the results obtained after excitation at 254 nm, the filter paper sheet stamped with TbPSANapPhen showed the characteristic green emission colour of terbium, confirming the incorporation of the lanthanide solution into paper. So, although the incorporation of the complex was succeeded, the method developed to impress letters (or signs) into paper must be improved. For both base and office papers submitted to UV radiation, the same issue related with the perfect image of what could be experienced by the user by visual inspection or by photography has occurred. Therefore, the images present in Figure 37 do not completely describe what can be seen, since it seems that no emission is occurring, but the user can actually observe green emission, despite less intense than in the filter paper. As to the Eu system, here the optical agents' effect is also noticeable in the base and office paper sheets. In this case, regarding the characteristic terbium emission, the intensity was lower than the one of europium, and with so, no much differences between the base and the office paper sheet can be observed.

3.2.1.2 Paper immersed in luminescent lanthanide polymer complex solutions

A second method for the incorporation of the lanthanide polymer complex solutions (EuPSANapPhen and TbPSANapPhen) on paper was tested. In this method, all three types of paper sheets (filter, base and office papers), were immersed for one second in the lanthanide solution.

In Figure 38, photographic results for visual inspection of paper sheets containing EuPSANapPhen can be observed.

Regarding all of the results shown in Figure 38, the reader must bear in mind that the images do not reflect with accuracy what can be observed by the user's eyes, as previously explained, and that printing techniques could lead to printed images with colour patterns that are not what the user experience.

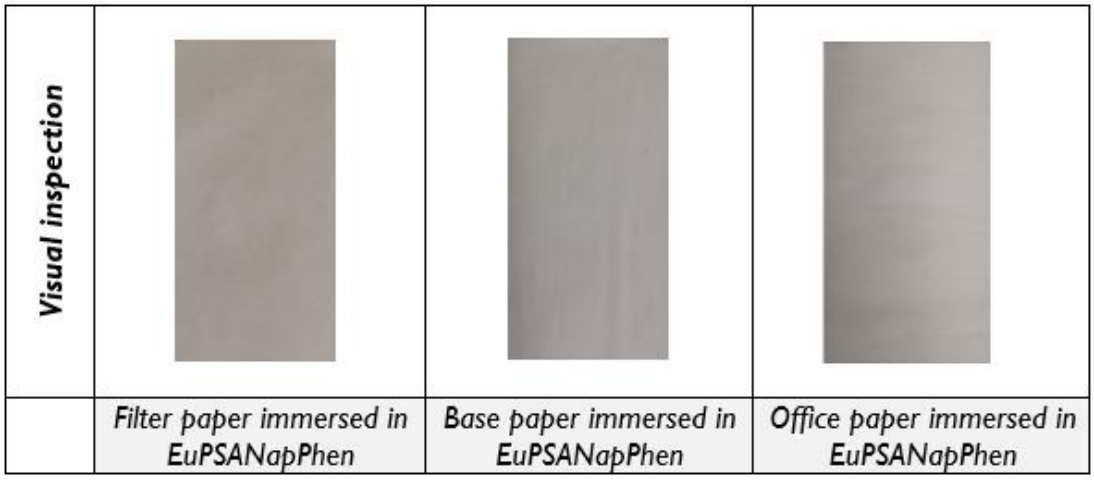

Figure 38. Photographs of the three types of paper sheets (filter, base and office) immersed in EuPSANapPhen, at eyesight.

Analysing these results by visual inspection either by the user's eye or by an optical device, no specific differences between paper types (filter, base or office) can be noticed, nor even differences between a sheet with and without incorporation of the lanthanide polymer complex. So, at first sight, it is very likely that the method of immersion of the paper sheet in EuPSANapPhen solution can be efficiently used for the incorporation of security elements. Thereafter, the incorporation of the luminescent solution into the paper was further confirmed by submitting the samples to UV radiation; the obtained photos are shown in Figure 39. Regarding the immersion of the three types of paper in the luminescent europium solution, it is evident that in the filter paper, the lanthanide was successfully incorporated, due to the characteristic red emission of the full paper sheet, observed under UV excitation at wavelength of 254 nm.

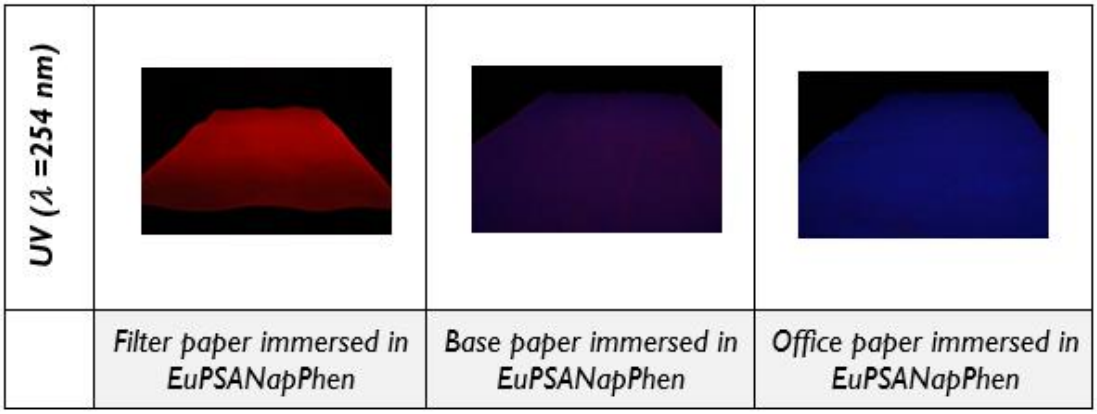

Figure 39. Photographs of the three types of paper sheets (filter, base and office) immersed in EuPSANapPhen, under UV radiation (λ = 254 nm).

By comparing filter paper with base and office paper sheets, the easiness of finding a perfect image that could reflect the actual colour decreases. Thus, with that being said, it is plausible to say that in the latter types of paper, the incorporation of the lanthanide polymer complex solution was also efficient, despite the fact that was not so easy to confirm. The pinkish and blueish colours of photographs of base and office paper sheets, respectively, can be assigned to the optical agents also incorporated on these types of paper's manufacture. So, it can be concluded that this method of incorporation can also be successfully applied.

This method was also tested with the terbium solution, TbPSANapPhen, and the photographic results can be observed in Figure 40.

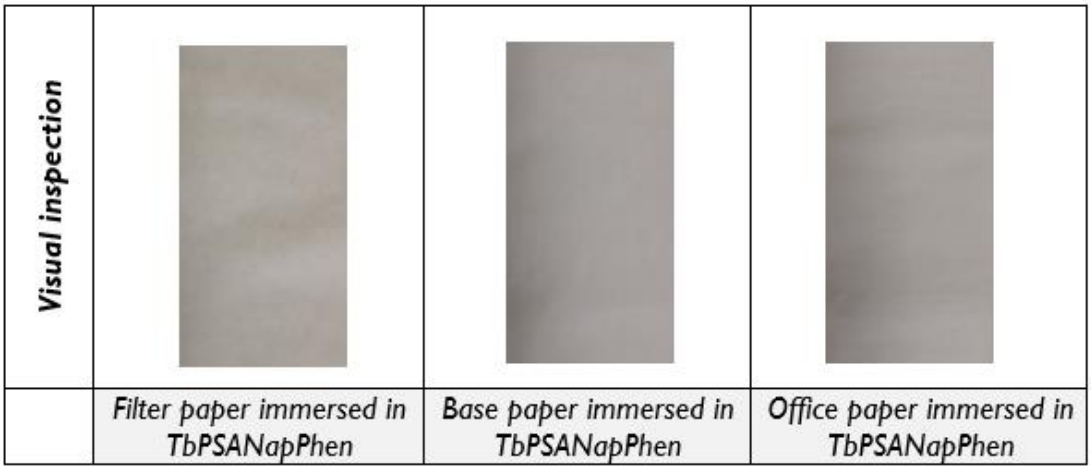

Figure 40. Photographs of the three types of paper sheets (filter, base and office) immersed in TbPSANapPhen, at eyesight.

Regarding the visual inspection by the user's eye, no particular differences between types of paper can be observed, as it was described for Eu. It is also worth to notice that the user cannot identify the complex into paper sheet without additional confirmation by UV lamp, a fact that turns this incorporation method a possible valid one. So, to confirm that hypothesis, the same paper sheets were submitted to 254 nm radiation and the photographic results are shown in Figure 41.

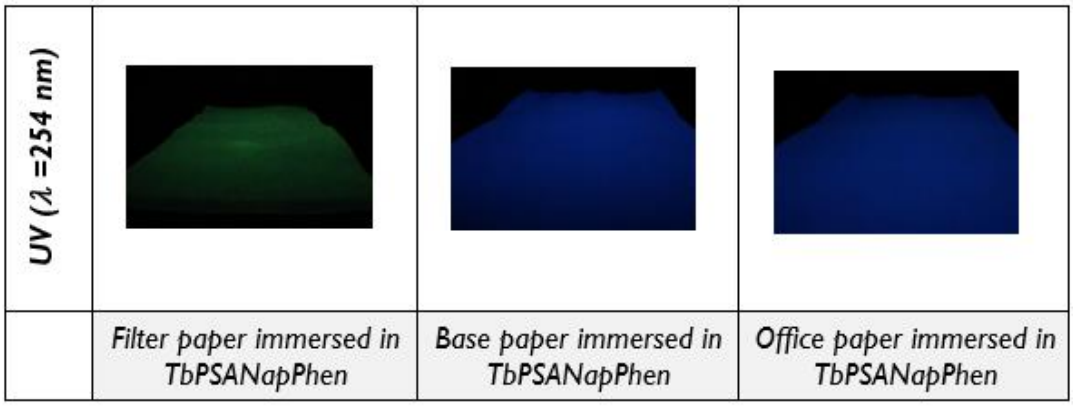

Figure 41. Photographs of the three types of paper sheets (filter, base and office) immersed in TbPSANapPhen, under UV radiation (λ = 254 nm).

Considering the results shown in Figure 41, filter paper was also the best type to prove the successful incorporation of TbPSANapPhen. That is, when under UV excitation, the filter paper sheet immersed in Tb(III)-containing solution, emits its characteristic green colour, that can be visualized with high intensity. Base and office papers also immersed in TbPSANapPhen showed a green emission, although with lower intensity then that observed by the user. Once again, that is associated with the optical agents also incorporated on the paper during its fabrication process. This can also justify the blue colour emitted by these sheets as seen by photos. Despite that, it can be concluded that the incorporation of TbPSANapPhen in all types of paper was also successfully achieved.

3.2.2 Coating of paper with lanthanide polymer complexes

For the preparation of a functionalized security paper, a different method of incorporation of the lanthanide polymer complex into the paper was tested. Namely, in this stage of the project, the same three types of paper sheets (filter, base and office) were submitted to a coating process with the respective lanthanide complex (EuPSANapPhen and TbPSANapPhen).

The photographic results at visual inspection of the paper sheets coated with EuPSANapPhen are shown in Figure 42.

For a better evaluation and discussion, the reader should be advised for the colour patterns and printing issues, in the same way as in prior subsections of the results discussion section.

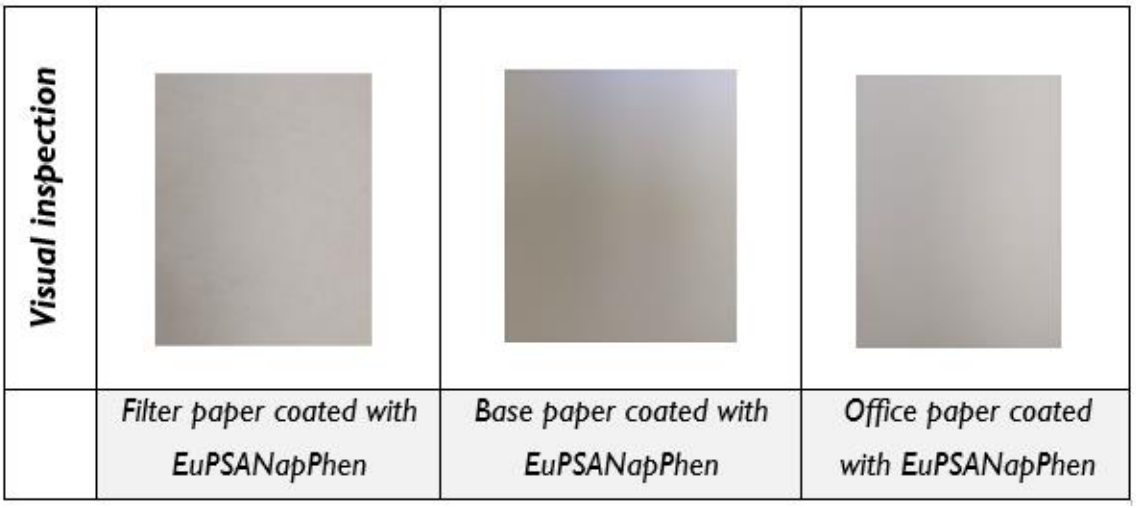

Figure 42. Photographs of the three types of paper sheets (filter, base and office) coated with EuPSANapPhen, at eyesight.

Analysing the results obtained at eyesight, represented in Figure 42, no significant differences independently of the paper sheet can be observed. Thus, the first conclusion can be that this method of lanthanide incorporation into the paper can also be used for practical purposes. However, taking just into account the visual inspection results, such hypothesis cannot be confirmed. So, photographic results of those paper sheets were taken under UV radiation of 254 nm (Figure 43).

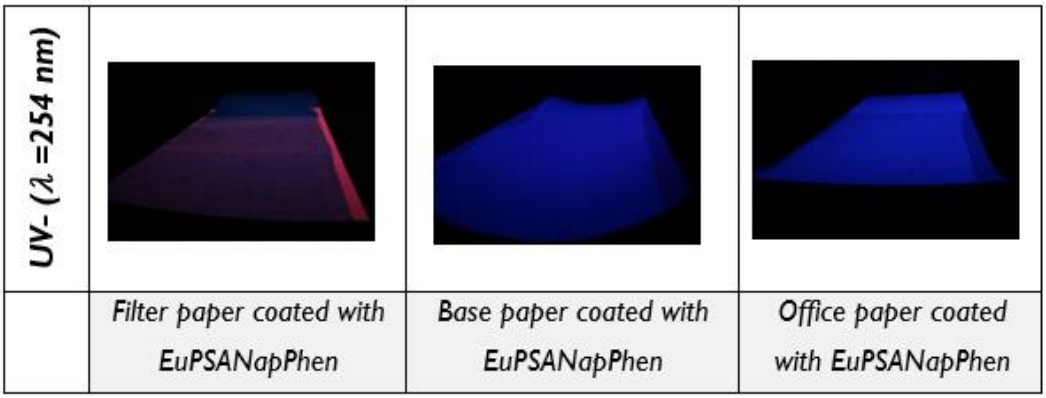

Figure 43. Photographs of the three types of paper sheets (filter, base and office) coated with EuPSANapPhen, under UV radiation (λ = 254 nm).

Observing the filter paper sheet coated with EuPSANapPhen, it is possible to conclude with certainty that the europium complex was incorporated in the paper, since its characteristic luminescence emission (red colour) can be observed. Another aspect that

is worth noting is that the coating process did not result in a homogeneously dispersed solution on top of the paper sheet, having a more concentrated region of lanthanide polymer complex on the periphery of the sheet, as seen by a more intense emission on that region. Moreover, the pinkish colour of the image of the filter paper coated with EuPSANapPhen does not do justice to the more intense red colour that can be observed by the user. Comparing the coating results to the ones obtained when the filter paper was immersed in the lanthanide polymer complex solution (Figure 39), the main difference is the dispersion effect. When the paper sheets suffer the coating process, is the dispersion is lower than when immersed, which also is reflected by a less intense colour emission of the coated filter paper sheet. Regarding the coating results of base and office paper, the presence of the optical agents previously mentioned did not allow an easy observation of the lanthanide emission. However, despite not being easy to understand by looking at the photographs on an optical device, the user could confirm the incorporation of the Eu polymer complex on both base and office paper, since it could be observed a light red colour emission. Moreover, it is also important to clarify the reader that the office paper sheet revealed a less intense lanthanide emission under UV excitation, but once again, that could be explained by the more intense coating process of this type of paper sheets. However, it was possible to conclude that this method of incorporation of the lanthanide polymer complex into the paper was also successfully achieved.

The same coating process was applied with the terbium polymer complex solution and the results obtained at eyesight are explicit in Figure 44.

Visual inspection			
	Filter paper coated with TbPSANapPhen	*Base paper coated with TbPSANapPhen*	*Office paper coated with TbPSANapPhen*

Figure 44. Photographs of the three types of paper sheets (filter, base and office) coated with TbPSANapPhen, at eyesight.

Analysing the visual inspection, no significant differences between types of paper can be noticed, nor can be possible to distinguish sheets that had not been coated from the

ones that suffered the coating with TbPSANapPhen. Thus, it could be expected that the first guarantee of security could have been achieved. However, that hypothesis needed to be confirmed with accuracy and, for that, photographic results were recorded exposing samples to UV radiation (Figure 45).

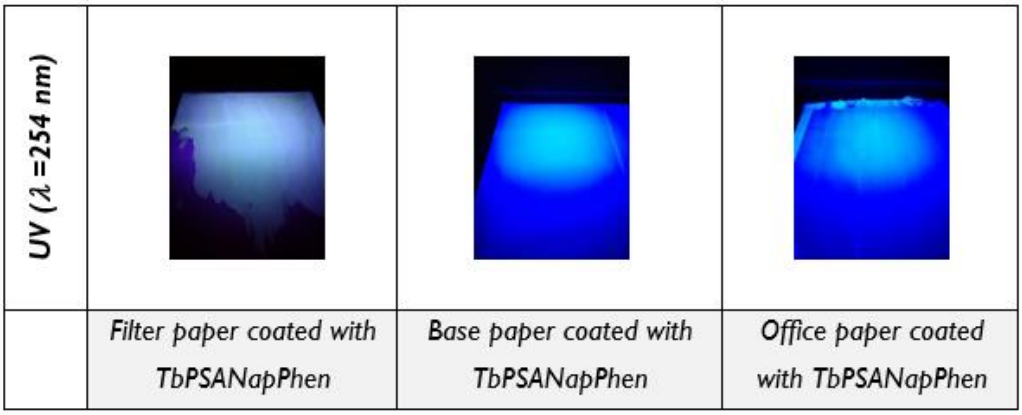

Figure 45. Photographs of the three types of paper sheets (filter, base and office) coated with TbPSANapPhen, under UV radiation (λ = 254 nm).

When observing the UV photographs, the first thing that can be concluded is that the incorporation of the terbium polymer complex did not result in a homogeneous dispersion, which is explicit on the filter paper sheet coated with TbPSANapPhen photograph. The coating with Eu did not also result in a homogeneous dispersion, however, when using Tb, what was achieved was an even worse dispersion. This can be attributed to the fact that the coating process had been done using a different equipment. There were also experimental difficulties on having a homogeneous solution when adding the terbium compound, so the less good coating result obtained could also be due to that fact. In this case, terbium green colour emission was lower than the corresponding europium red colour. However, despite being less easy to confirm, it is also possible to guarantee the authentication of the paper sheet. When analysing both base and office paper sheets coated with TbPSANapPhen, the conclusions can be made simultaneously. The blue colour on the background of the paper sheet's images is derived from the emission of the optical agents incorporated during paper manufacture. These optical agents are also blocking in some way the emission of the lanthanide, turning that way the confirmation of incorporation much difficult. In this case, the confirmation of terbium incorporation into the paper cannot be easily done by the user. Therefore, it can be concluded that Tb is less efficient for the purpose of creating a security paper, since it was less easy to confirm its presence on the paper sheets. Moreover, it can also be concluded that this method of incorporation was less efficient than when the paper sheets were immersed in EuPSANapPhen and TbPSANapPhen.

3.2.2.1 Paper pick-up values

Generally, a paper machine is set to a specific grammage, and, thus, both the sheet formation and the coating processes need to be controlled. The former should attain the desired grammage minus the coating pick-up, while the latter should attain said pick-up. After having submitted all three types of paper sheets, namely filter, base and office paper to the coating with EuPSANapPhen, the pick-up values were determined. To make these calculations, the coating process was done in quadruplicate and the reported value is an average of the four. For that, the length and width of the coated paper sheets were measured, as well as the weight. The weight prior to the coating was known and the weight after coating was measured. Thus, the pick-up value will correspond to the difference of weight obtained after and prior to the coating with the lanthanide polymer complexes. The obtained results are summarized in Table 3.

Table 3. Parameters used to calculate pick-up values from coating of filter (F), base (B) and office (O) paper sheets with EuPSANapPhen.

	Width (m)	**Length (m)**	**Area (m^2)**	**Weight (g)**	**Grammage prior (g/m^2)**	**Grammage after (g/m^2)**	**Pick-up**	**Average pick-up**
F1	0.108	0.127	0.0137	1.0159	72.7	74.1	1.4	1.1
F2	0.110	0.130	0.0143	1.0333		72.3	-0.4*	
F3	0.109	0.136	0.0148	1.0566		71.3	-1.4*	
F4	0.109	0.132	0.0144	1.0589		73.6	0.9	
B1	0.110	0.128	0.0141	1.0971	77.0	77.9	0.9	1.0
B2	0.109	0.127	0.0138	1.0825		78.2	1.2	
B3	0.105	0.128	0.0134	1.0452		77.8	0.8	
B4	0.110	0.125	0.0138	1.0652		77.5	0.5	
O1	0.113	0.134	0.0151	1.2445	81.4	82.1	0.8	0.8
O2	0.111	0.133	0.0148	1.2136		82.2	0.8	
O3	0.110	0.132	0.0145	1.1999		82.6	1.2*	
O4	0.111	0.138	0.0153	1.2577		82.1	0.7	

Note: values with a superscript * were left apart from the average pick-up calculations, since they do not have physical meaning and revealed to be *outliers*.

After the analysis of the results shown in Table 3, the effective incorporation of EuPSANapPhen in the different types of paper could be re-confirmed analytically. The pick-up values obtained are according to what was expected, since rolling pins that were used for the coating would permit a low pick-up (< 2 g/m^2).

3.2.3 Response of functionalized paper to metal solutions

After having confirmed the incorporation of the lanthanide polymer complex solutions (EuPSANapPhen and TbPSANapPhen) through the three different methods previously explained (stamped paper, immersed paper and coated paper), the first security guarantee was achieved. Therefore, to obtain a second guarantee of authentication of the paper, its response to copper and nickel solutions was tested. It is worth noting that copper and nickel were the chosen ions to test these interactions, since they were the ones that provoked almost total quenching of luminescence emission, characteristic of the lanthanides, as previously explained in section 3.1.1.

3.2.3.1 Stamped paper after addition of copper and nickel

In Figure 46, photographic results at eyesight of the EuPSANapPhen stamped paper sheets after interaction with copper and nickel ions can be observed. Regarding these results, the reader has also the need to be informed of the same colour and printing issues, as previously explained.

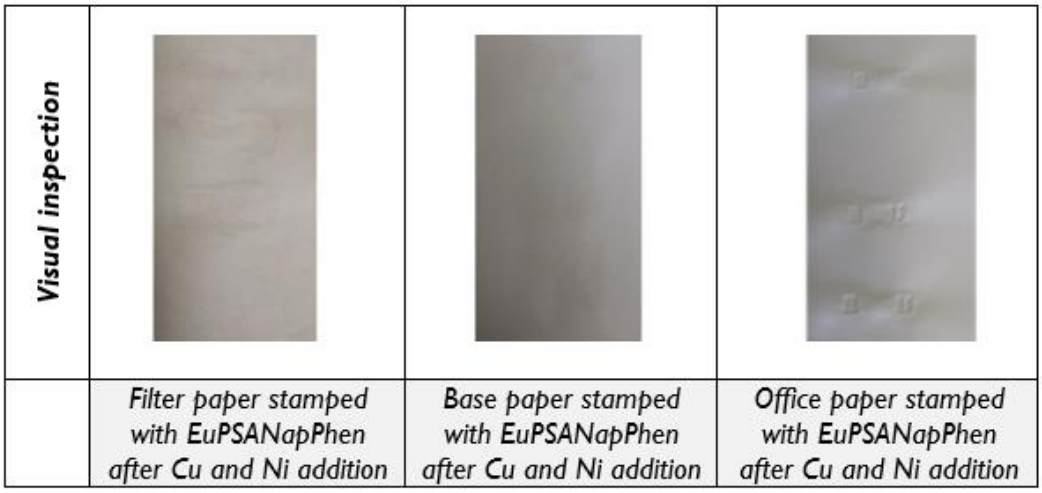

Figure 46. Photographs of the three types of paper sheets (filter, base and office) stamped with EuPSANapPhen after reaction to Cu and Ni ions, at eyesight.

Analysing all three types of paper sheets that had been previously stamped with EuPSANapPhen and that were now submitted to an interaction with copper and nickel solutions, by a visual inspection (Figure 46), no significant changes can be observed. That is, it is not possible to notice by visual inspection any differences between the paper sheet prior and after the interaction with copper and nickel. Moreover, by visual inspection, no differences between types of paper, filter, base or office, can also be noticed. To have that second guarantee of authentication of the product, the confirmation can only be done under an UV source, where the quenching effect

provoked by the metal ions would be noticed, causing the vanishing of the emission of the red europium characteristic colour.

Figure 47 shows the photographic results recorded under UV excitation at a wavelength of 254 nm of the paper sheets stamped with Eu and interacted with Cu and Ni.

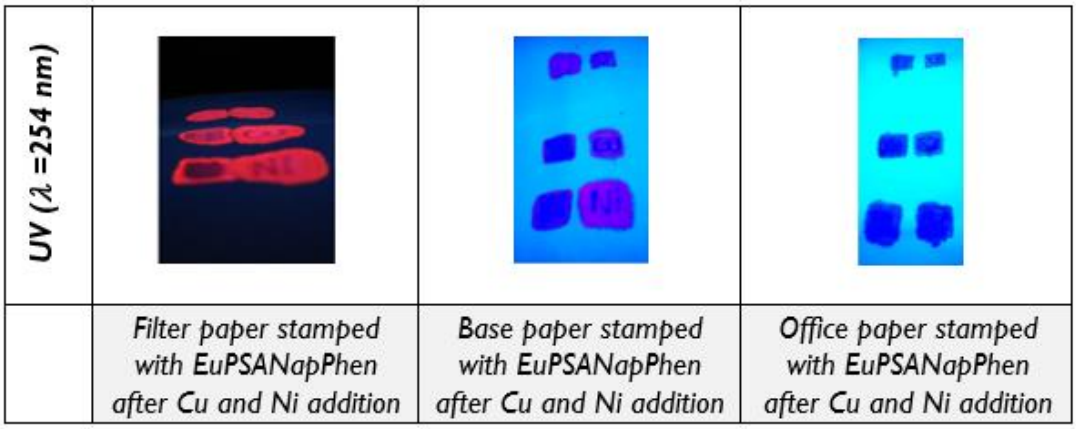

Figure 47. Photographs of the three types of paper sheets (filter, base and office) stamped with EuPSANapPhen after reaction to Cu and Ni ions, under UV radiation (λ = 254 nm).

Observing the user's procedure of the reaction of both metal ions, it can be noticed that the vanishing of colour was immediate and only on the sites where the wet brush is applied. Regarding the photographic results of the filter paper sheet, it can be said that the colour that is registered is almost the same as the one seen by the user. It is also very easy to notice where the metal solution was applied, since instead of appearing a vivid red colour, what is seen is a "shadow effect", where the colour vanishes completely. Looking to the results of the base paper sheet, the same effect can be noticed, despite the intensity of the colour being lower. However, in this stage of the security mechanism, the intensity of emission is not very much important, but instead the visual effect caused with the addition of the metal ion solutions. So, observing the photographic results of the base paper sheet, it is also noticeable the vanishing of the europium emission in the sites where the brush passes. The blue background that is reflected on the image is a result of the emission of the optical agents. This same blue emission can also be observed in the office paper sheet stamped with EuPSANapPhen and reacted with both copper and nickel solutions. With that being explicit, it is possible to say that the user can observe the "shadow effect" upon addition of Cu and Ni. So, it can be concluded that the second guarantee of security by interaction with copper and nickel solutions is easily done, with special visualization in filter paper sheets.

The paper sheets that had been previously stamped with TbPSANapPhen did also pass through the test of the presence of metal ions (Cu and Ni). Figure 48 shows photographic results taken after visual inspection of those paper sheets.

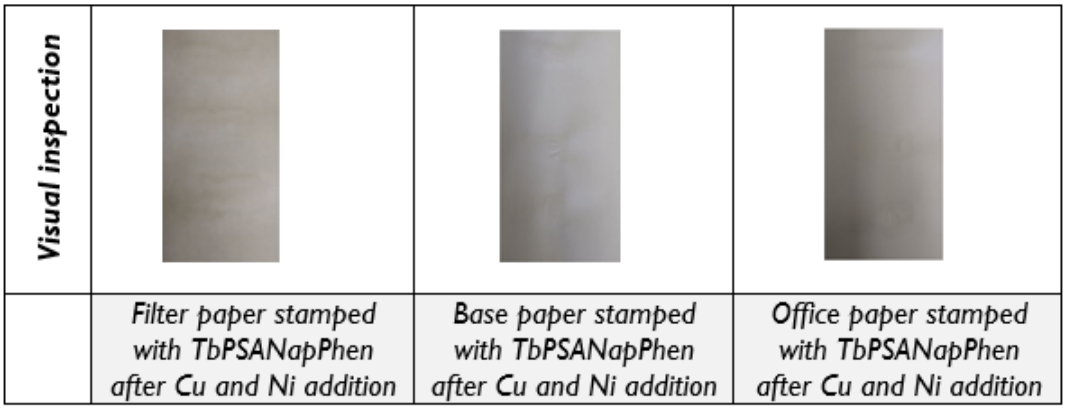

Figure 48. Photographs of the three types of paper sheets (filter, base and office) stamped with TbPSANapPhen after reaction to Cu and Ni ions, at eyesight.

Regarding what can be seen by the user, no significant differences between the type of paper sheet can be observed, neither can be differentiated a sheet without the presence of copper and nickel ions from a sheet with just the terbium compound incorporated. So, with just the visual inspection, the purpose of having a sheet that did not show any differences could be achieved.

However, the confirmation of such achievement can only be done under UV excitation at a wavelength of 254 nm. So, in Figure 49, UV photographic results of the filter, base and office paper sheets stamped with TbPSANapPhen and after interaction with copper and nickel solutions, can be observed. The response of the sample to the contact with the quencher was immediate, resulting in a "shadow effect" in the sites where the wet brush would pass.

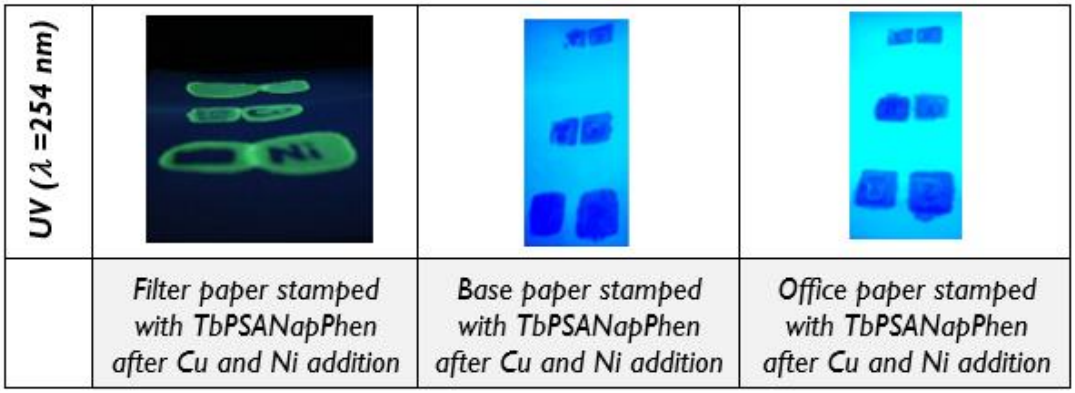

Figure 49. Photographs of the three types of paper sheets (filter, base and office) stamped with TbPSANapPhen after reaction to Cu and Ni ions, under UV radiation (λ = 254 nm).

According to the results obtained for base and office paper sheets stamped with Tb, the visualization of the green colour emission was more difficult. As this is explicit, there could be an emission competition between the lanthanide and the optical agents, making that way difficult the visualization of the terbium colour emission. Despite that, the visualization of the "shadow effect" caused by the presence of the metal ions, was achieved, but the user had difficulty to conclude that, especially in the office paper sheet. So, it can be concluded that the second guarantee of security and authentication of the product could also be achieved with the terbium polymer complex solution, despite being more difficult to prove than with the europium one.

3.2.3.2 Immersed paper after the interaction with copper and nickel

The response to Cu and Ni was also performed in all the paper sheets that had been previously immersed in the lanthanide polymer complex solutions. Figure 50 shows the photographic results recorded at eyesight. From now on, the reader should also be informed of the same aforementioned colour and printing issues.

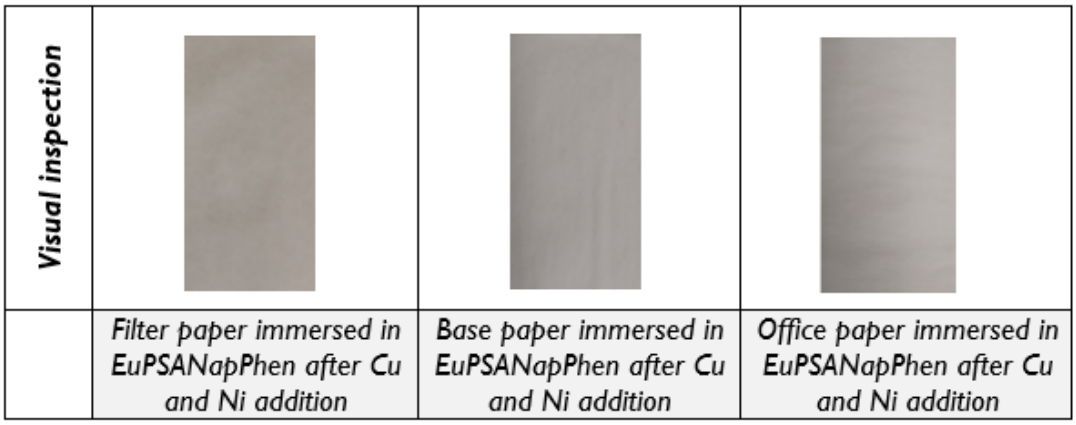

Figure 50. Photographs of the three types of paper sheets (filter, base and office) immersed in EuPSANapPhen after reaction to Cu and Ni ions, at eyesight.

Regarding the photographic results explicit in Figure 50, no significant changes between type of paper sheet (filter, base or office) can be noticed by the user. Moreover, it is also not possible to determine at eyesight which paper sheet had been in touch with the metal solutions. So, as equal to the results obtained for the stamped papers, at this point, it can be said, even without no actual confirmation, that the first and second security guarantees had been achieved. Thereafter, to have that second security confirmation, the paper sheets immersed in EuPSANapPhen and interacted with Cu and Ni, were submitted to UV radiation at 254 nm, and the photographic results are shown in Figure 51.

UV (λ =254 nm)	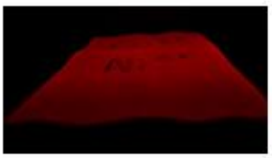		
	Filter paper immersed in EuPSANapPhen after Cu and Ni addition	*Base paper immersed in EuPSANapPhen after Cu and Ni addition*	*Office paper immersed in EuPSANapPhen after Cu and Ni addition*

Figure 51. Photographs of the three types of paper sheets (filter, base and office) immersed in EuPSANapPhen after reaction to Cu and Ni ions, under UV radiation (λ = 254 nm).

Analysing the filter paper, it was very noticeable that the europium characteristic red emission, suffered total quenching, after the contact with copper and nickel. It is also worth noting that the "shadow effect" resultant of the interaction with the metal ions is immediate and is only felt in the paper sheet regions were the wet brush is applied. When observing the base paper sheet results, the same effect can be noticed, even if the intensity of lanthanide emission is lower due to the presence of the optical agents. Regarding the office paper, the optical effect can also be observed by the user, after contact with Cu and Ni, but it is also worth noting that this type of paper, due to the more intense coating process during its manufacture, did not permit to observe the red europium emission colour under UV radiation. The response to copper and nickel ions can be noticed, because the emission is lower, but in this case, it cannot be said that this emission is from the lanthanide, because it could also be from the optical agents. So, it can be said that the second guarantee of authentication of the product could also be achieved, with more easiness of recognition on filter papers that had been immersed in EuPSANapPhen.

The paper sheets that had been previously immersed in TbPSANapPhen have also been subjected to the interaction with copper and nickel solutions and the corresponding photographic results can be observed in Figure 52.

Visual inspection			
	Filter paper immersed in TbPSANapPhen after Cu and Ni addition	*Base paper immersed in TbPSANapPhen after Cu and Ni addition*	*Office paper immersed in TbPSANapPhen after Cu and Ni addition*

Figure 52. Photographs of the three types of paper sheets (filter, base and office) immersed in TbPSANapPhen after reaction to Cu and Ni ions, at eyesight.

Photographic results of visual inspection do not show any particular difference between the ones obtained prior to the response to metal ions, nor do show differences between types of paper (filter, base and office).

So, it is probable that the second guarantee of authentication had been successfully achieved. However, with just the results seen by the eyesight of the user, that could not be confirmed. Thus, results obtained upon UV excitation at a wavelength of 254 nm were recorded and are present in Figure 53.

UV (λ =254 nm)			
			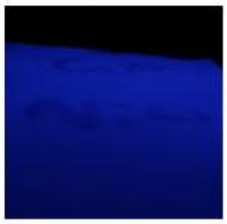
	Filter paper immersed in TbPSANapPhen after Cu and Ni addition	*Base paper immersed in TbPSANapPhen after Cu and Ni addition*	*Office paper immersed in TbPSANapPhen after Cu and Ni addition*

Figure 53. Photographs of the three types of paper sheets (filter, base and office) immersed in TbPSANapPhen after reaction to Cu and Ni ions, under UV radiation (λ = 254 nm).

The filter paper sheet shows the actual green colour observed. The high intensity of lanthanide emission, after interaction with copper and nickel, is completely blocked, resulting that way the "shadow effect", that is seen on the photographic result.

Here, the quenching of emission is also visualized immediately after the metal solution touches the paper sheet (no matter the type of paper). Regarding the results obtained for the base and office paper, the conclusions that can be taken are similar for both types of paper. Namely, the luminescence lanthanide emission is not easy to be seen, due to the competition between lanthanide and optical agents. However, despite not being easy to see the green emission, the "shadow effect" of the metal solutions can also be observed by the user and it is correctly represented on the photographic results. So, it can be concluded that the second guarantee of security could also be successfully achieved, being easier to observe on filter paper, but not invalidating its application on both base and office paper sheets.

3.2.3.3 Coated paper after the reaction to copper and nickel

All the paper sheets that had been submitted to a coating process, incorporating the lanthanide polymer complexes into them, also suffered the same interaction with the presence of copper and nickel ions. Photographic results at eyesight have been registered and can be observed in Figure 54.

Visual inspection			
	Filter paper coated with EuPSANapPhen after Cu and Ni addition	*Base paper coated with EuPSANapPhen after Cu and Ni addition*	*Office paper coated with EuPSANapPhen after Cu and Ni addition*

Figure 54. Photographs of the three types of paper sheets (filter, base and office) coated with EuPSANapPhen after reaction to Cu and Ni ions, at eyesight.

Regarding the results explicit in Figure 54, it is possible to admit that the second guarantee of authentication had been efficient. However, to confirm that hypothesis, photographic results under an UV lamp had to be recorded and are explicit in Figure 55.

UV (λ =254 nm)		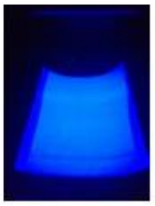	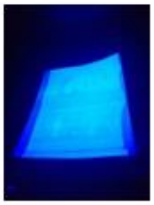
	Filter paper coated with EuPSANapPhen after Cu and Ni addition	*Base paper coated with EuPSANapPhen after Cu and Ni addition*	*Office paper coated with EuPSANapPhen after Cu and Ni addition*

Figure 55. Photographs of the three types of paper sheets (filter, base and office) coated with EuPSANapPhen after reaction to Cu and Ni ions, under UV radiation (λ = 254 nm).

Observing the filter paper, the "shadow effect" can be observed immediately, which is a prove that the second guarantee of security had been achieved. This effect can easily be seen since the emission of the europium red colour is blocked right away when the wet brush touches the paper sheet. Regarding the results obtained for the base and office paper sheets, the conclusions to be made are similar, since the user cannot differentiate

easily one type from another. This can be explained due to their similarities on paper composition. As that emission is not visible, the metal quenching effect cannot be also visible. However, this impossibility of visualization of the lanthanide emission can also be related to the fact of the coating not being uniformly dispersed on the paper sheet (base and office). Therefore, for the paper sheets coated with EuPSANapPhen, it cannot be said that the second guarantee of authenticity had been successfully achieved in all types of paper, because the response to copper and nickel ions could only be easily observed on the filter paper sheet.

The same coating procedure was also applied with TbPSANapPhen solutions and the photographic results at eyesight are explicit in Figure 56.

Visual inspection			
	Filter paper coated with TbPSANapPhen after Cu and Ni addition	*Base paper coated with TbPSANapPhen after Cu and Ni addition*	*Office paper coated with TbPSANapPhen after Cu and Ni addition*

Figure 56. Photographs of the three types of paper sheets (filter, base and office) coated with TbPSANapPhen after reaction to Cu and Ni ions, at eyesight.

Regarding to the results visualized at eyesight, no significant differences between type of paper can be noticed, nor it can be recognized a sheet interacted with metal ions from a non-interacted. With just this observation, at first sight it can be concluded that the second guarantee of security would have been achieved. However, to have that confirmation, photographic results had to be taken under UV excitation (Figure 57).

UV(λ =254 nm)		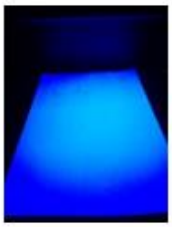	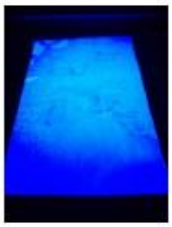
	Filter paper coated with TbPSANapPhen after Cu and Ni addition	*Base paper coated with TbPSANapPhen after Cu and Ni addition*	*Office paper coated with TbPSANapPhen after Cu and Ni addition*

Figure 57. Photographs of the three types of paper sheets (filter, base and office) coated with TbPSANapPhen after reaction to Cu and Ni ions, under UV radiation (λ = 254 nm).

Comparing the type of paper sheets, it is also possible to be concluded that filter paper is the type of paper that can best reflect the easier to observe results. The "shadow effect" previously explained can also be noticed immediately after the contact of the brush with metal solutions (copper and nickel) with the paper sheets. Once again, this effect is more easily noticed in filter paper, due to the optical properties of the base and office paper sheets. So, as it was not easy to observe the metal quenching effect on the paper sheets coated with TbPSANapPhen, it cannot be possible to conclude that the second guarantee of security had been successfully achieved.

CHAPTER 4

CONCLUSION

4. CONCLUSION

This master's thesis work has been carried out in the framework of project Inpactus, from RAIZ – Instituto de Investigação da Floresta e Papel. Its main purpose was the development of a security paper. To achieve that goal, two main requirements had to be met, namely the incorporation of a luminescent compound into the paper and its reaction with a substance that would guarantee its authentication. So, the first thing that was done was the synthesis of two lanthanide polymer complexes with ideal optical properties for security applications. Two low molecular organic ligands were chosen (1-naphthoic acid and 1,10-phenantroline) to act as antennas, enhancing the intensity emission of the lanthanides (Eu and Tb), and a polymer (PSA) was also chosen to benefit from its properties (i.e. chemical stability). Thus, EuPSANapPhen and TbPSANapPhen were successfully synthesized. Their luminescent properties were evaluated by fluorometric analysis and, after confirmation of their good potential for security applications, its reaction to the presence of metal ions was evaluated. The quenching efficiency of the several metals was calculated and it was concluded that, for both lanthanide systems, copper and nickel proved to be effective quenchers, provoking an almost total (~100%) blocking of lanthanide characteristic emission. Thereafter, the effect of the counterion was also tested, using several sodium salts. From that study, no significative counterion effect could be noticed. Pursuant to that, limits of detection and quantification of both quenchers (Cu and Ni) were determined following Stern-Volmer equation. LOD of Cu was 13.9 ppm and 11.1 ppm and of Ni was 4.99 ppm and 13.1 ppm for Eu and Tb systems, respectively, which proved that both systems are very sensitive to the presence of either copper or nickel ions. LOQ of Cu was 42.1 ppm and 33.7 ppm and of Ni was 15.1 ppm and 39.6 ppm, for europium and terbium systems, respectively. Having all of this explicit, the first and second guarantees of authentication were concluded in solution. So, the further step was to perform paper analysis. For that, three different types of paper had been studied, namely filter, base and office paper, and three different methods of incorporation of EuPSANapPhen and TbPSANapPhen had also been tested: stamping with lanthanide solution, immersion of paper sheets on the lanthanide solution, and coating of paper sheets with the lanthanide polymer complexes. To analyse and compare the paper tests, photographic results were recorded at eyesight and under

UV radiation. It was possible to conclude, looking at the UV results, that the incorporation of both lanthanide compounds had been successfully achieved for all of the different methods tested. The incorporation of europium allows an easier visualization of the incorporation of the lanthanide complexes into the paper, since its red luminescence emission is significantly higher than the characteristic green one of terbium. At eyesight, it is never easy to differentiate a sheet with no surface treatment from the tested ones, which is a good sign for the possible applications in security ranges. The quenching effect caused by the presence of Cu and Ni was also tested in paper sheets, by using a wet brush with $Cu(NO_3).xH_2O$ and $Ni(NO_3)_2.9H_2O$. It is possible to observe that the "shadow effect" occurs immediately upon the contact of the brush with the paper sheets that had been treated with the lanthanide polymer complexes. Also, between all three methods of incorporation, it is possible to conclude that the paper sheets that were submitted to a submersion in the lanthanide polymer complex solution, allow a better visualization of both the incorporation of Eu and Tb in the paper and also the quenching effect of Cu and Ni. The stamping procedure with EuPSANapPhen and TbPSANapPhen did not permit good results, due to difficulties of reproducibility of the process (volume of solution and pressure applied). Moreover, the coating process was effective, that is, it is possible to observe for both europium and terbium systems, the incorporation in the paper. However, when analysing the quenching effect, it is not so easy, since the dispersion of the lanthanide compounds on the paper sheets is not homogenous. Regarding the comparison of results from types of paper, it is possible to conclude that in every method of incorporation and also in both lanthanide systems, filter paper proved to be the one that allows for the better results. Base and office paper sheets, despite still allowing the observation of the expected effects, do not allow an easy process of authentication. This fact is attributed to the presence of optical agents on their composition, incorporated to improve the printing capacities, but that are blocking the lanthanide emission, turning not easy to identify their presence on the paper sheets.

Summing up, it is possible to conclude that the goal proposed on the start of this master's thesis had been successfully achieved, that is, it was possible to create a functionalized paper with possible security applications.

Nevertheless, there are still numerous aspects that can be studied and improved, in order to the method proposed in this thesis to be used in the papermaking industry.

CHAPTER 5

FUTURE PERSPECTIVES

5. FUTURE PERSPECTIVES

In this master's thesis, very good and promising results had been taken from the development of a security paper. However, to apply the method proposed here on the papermaking industry, many aspects need to be studied and improved.

A proposal of future studies from a chemical point of view can be to understand what quenching mechanism is occurring after the addition of metal ions to the lanthanide polymer complex solution. That could be done by performing fluorometric analysis under different temperatures or by doing some lifetime measurements.

On the other hand, as a practical point of view, more paper analysis could be done, namely the study of general aspects of paper, such as brightness, opacity, printing capacities, light scattering coefficient, colour/yellowness, smoothness, roughness, etc. Also, to try to obtain better results with the stamping procedure, an industrial mechanism where the volume of solution and the pressure applied while stamping would be controlled could be a possibility to consider in the future. Adding to that, it could also be interesting to test the same methodology, but instead using a solution with higher viscosity. Moreover, it could also be interesting to test the durability of the impregnation of the luminescent compound in the paper, that is, to evaluate the same paper sheets after a considerate time-lapse. Finally, another aspect worth testing would be the reaction of the paper to water, that is, to study its effect on both the impregnated lanthanide and the paper's properties, upon contact to an aqueous solution.

Regarding the second guarantee of security and authentication, an important aspect to improve in the future would be the method of metal reaction. A suggestion that could be done is to try to obtain a simpler and immediate object (i.e. a pen of Cu and/or Ni) that could be used to prove the immediate quenching effect on the incorporated EuPSANapPhen and TbPSANapPhen.

The methodology proposed here reveals also to be a good candidate for applications in Cu and Ni probes in effluents, so it is another aspect to be considered in the future.

CHAPTER 6

REFERENCES

6. REFERENCES

1 A. K. Gangwar, A. Gupta, G. Kedawat, P. Kumar, B. P. Singh, N. Singh, A. K. Srivastava, S. R. Dhakate and B. K. Gupta, *Chem. - A Eur. J.*, 2018, **24**, 9477–9484.

2 P. Kumar, J. Dwivedi and B. K. Gupta, *J. Mater. Chem. C*, 2014, **2**, 10468–10475.

3 X. Li and Y. Hu, *Carbohydr. Polym.*, 2019, **203**, 167–175.

4 G. Gong, S. Xie, Y. Song, H. Tan, J. Xu, C. Zhang and L. Xu, *J. Nanosci. Nanotechnol.*, 2018, **18**, 8207–8215.

5 P. Kumar, S. Singh and B. K. Gupta, *Nanoscale*, 2016, **8**, 14297–14340.

6 J.-C. G. Bünzli and G. R. Choppin, Elsevier, 1989, p. 432.

7 E. . Priestley and A. Haug, *J. Chem. Phys.*, 1968, **49**, 622–629.

8 H. H. Jaffe and A. L. Miller, *J. Chem. Educ.*, 1966, **43**, 469–473.

9 V. Zepf, Springer Theses, 2013, pp. 11–39.

10 V. K. Pecharsky and K. A. G. Jr., *Encycl. Br.*, 2019.

11 R. B. Heslop and K. Jones, *INORGANIC CHEMISTRY A Guide to Advanced Study*, Elsevier, 1976.

12 D. E. Barry, D. F. Caffrey and T. Gunnlaugsson, *Chem. Soc. Rev.*, 2016, **45**, 3244–3274.

13 I. Anastopoulos, A. Bhatnagar and E. C. Lima, *J. Mol. Liq.*, 2016, **221**, 954–962.

14 O. Guillou, C. Daiguebonne, G. Calvez and K. Bernot, *Acc. Chem. Res.*, 2016, **49**, 844–856.

15 J. C. G. Bünzli, *Eur. J. Inorg. Chem.*, 2017, **2017**, 5058–5063.

16 L. Sun, R. Wei, J. Feng and H. Zhang, *Coord. Chem. Rev.*, 2018, **364**, 10–32.

17 T. N. Nguyen, F. M. Ebrahim and K. C. Stylianou, *Coord. Chem. Rev.*, 2018, **377**, 259–306.

18 J. Zhou, Q. Liu, W. Feng, Y. Sun and F. Li, *Chem. Rev.*

19 H. Dong, L. D. Sun and C. H. Yan, *Chem. Soc. Rev.*, 2015, **44**, 1608–1634.

20 H. Wang, H. Xia, J. Hu, Y. Zhu and B. Chen, *Phys. B Condens. Matter*, 2019, **553**, 18–22.

21 R. S. Yadav and S. B. Rai, *Opt. Laser Technol.*, 2019, **111**, 169–175.

22 J. Hu, Y. Zhao, B. Chen, H. Xia, Y. Zhang and H. Ye, *J. Lumin.*, 2019, **205**, 500–507.

23 S. Gai, C. Li, P. Yang and J. Lin, *Chem. Rev.*, 2014, **114**, 2343–2389.

24 Y. Hasegawa, Y. Kitagawa and T. Nakanishi, *NPG Asia Mater.*, 2018, **10**, 52–70.

25 Z. J.-J. Wu Xiao-Hui, Ren Ning, *J. Chem. Thermodyn.*, 2019, **132**, 476–483.

26 M. C. He, L. M. Matosziuk and T. J. Meade, *Chem. Rev.*, 2014, **114**, 4496–4539.

27 Y. Wu, H. Hao, Q. Wu, Z. Gao and H. Xie, *Opt. Mater. (Amst).*, 2018, **80**, 65–70.

28 A. F. Y. Matsushita, A. A. C. C. Pais and A. J. M. Valente, *Colloids Surfaces A Physicochem. Eng. Asp.*, 2019, **569**, 93–101.

29 B. Gao, L. Zhang and Y. Li, *J. Photochem. Photobiol. A Chem.*, 2016, **324**, 23–32.

30 P. Samyn, A. Barhoum, T. Öhlund and A. Dufresne, *J. Mater. Sci.*, 2018, **53**, 146–184.

31 C. Hagiopol and J. W. Johnston, *Chemistry of Modern Papermaking*, CRC Press, 2012.

32 A. H. Tayeb, E. Amini, S. Ghasemi and M. Tajvidi, *Molecules*, 2018, **23**, 1–24.

33 A. F. Lourenço, R. S. Simões, A. P. Costa, J. A. F. Gamelas and P. J. Ferreira, *Nord. Pulp Pap. Res. J.*, 2016, **31**, 341–346.

34 A. R. García, Pablo de Olavide University, 2017.

35 Navigator Company, http://en.thenavigatorcompany.com/Pulp-and-Paper/Paper/How-Paper-is-Made, (accessed 20 June 2019).

36 M. A. Hubbe and R. A. Gill, *BioResources*, 2016, **11**, 2886–2963.

37 Y. Wu, H. Hao, Q. Wu, Z. Gao and H. Xie, *Opt. Mater. (Amst).*, 2018, **80**, 65–70.

38 C. Du, Y. Xu, L. Ma and W. Li, *J. Alloys Compd.*, 1998, **265**, 81–86.

39 de B. A. Dias, *Luminescence of Lanthanide Ions in Coordination Compounds and Nanomaterials*, John Wiley and Sons, Lda, 2014.

40 V. I. Tomin, *Opt. Spectrosc.*, 2008, **104**, 838–845.

41 Joseph R. Lakowicz, *Principles of fluorescence spectroscopy*, Springer US, 2006.

CHAPTER 7

SUPPLEMENTARY INFORMATION

7. SUPPLEMENTARY INFORMATION

7.1 Pure lanthanide solutions

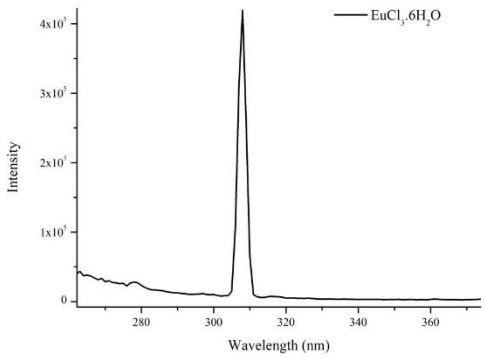

Figure S 1. Excitation spectrum of an aqueous solution of $EuCl_3.6H_2O$ (λem = 616 nm).

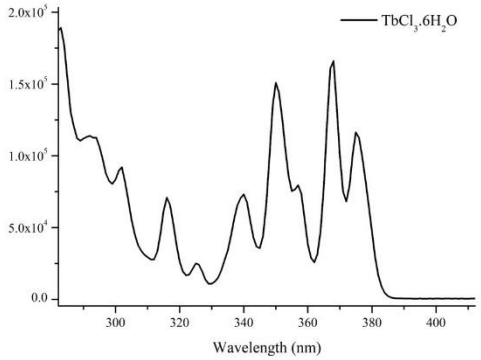

Figure S 2. Excitation spectrum of an aqueous solution of $TbCl_3.6H_2O$ (λ_{em} = 543 nm).

7.2 Lanthanide polymer complexes

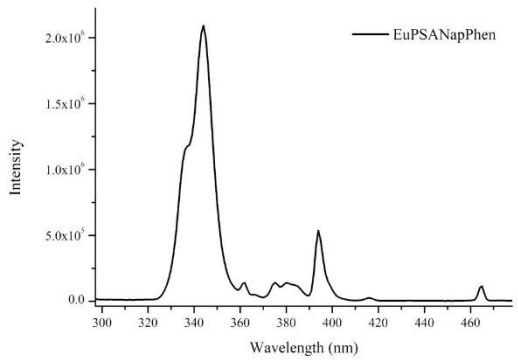

Figure S 3. Excitation spectrum of the EuPSANapPhen (EtOH:H_2O) solution (λ_{em} = 616 nm).

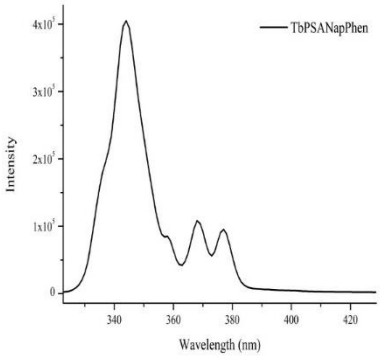

Figure S 4. Excitation spectrum of the TbPSANapPhen (EtOH:H_2O) solution (λem = 543 nm).

7.3 Reaction of Lanthanide polymer complexes solutions with metals

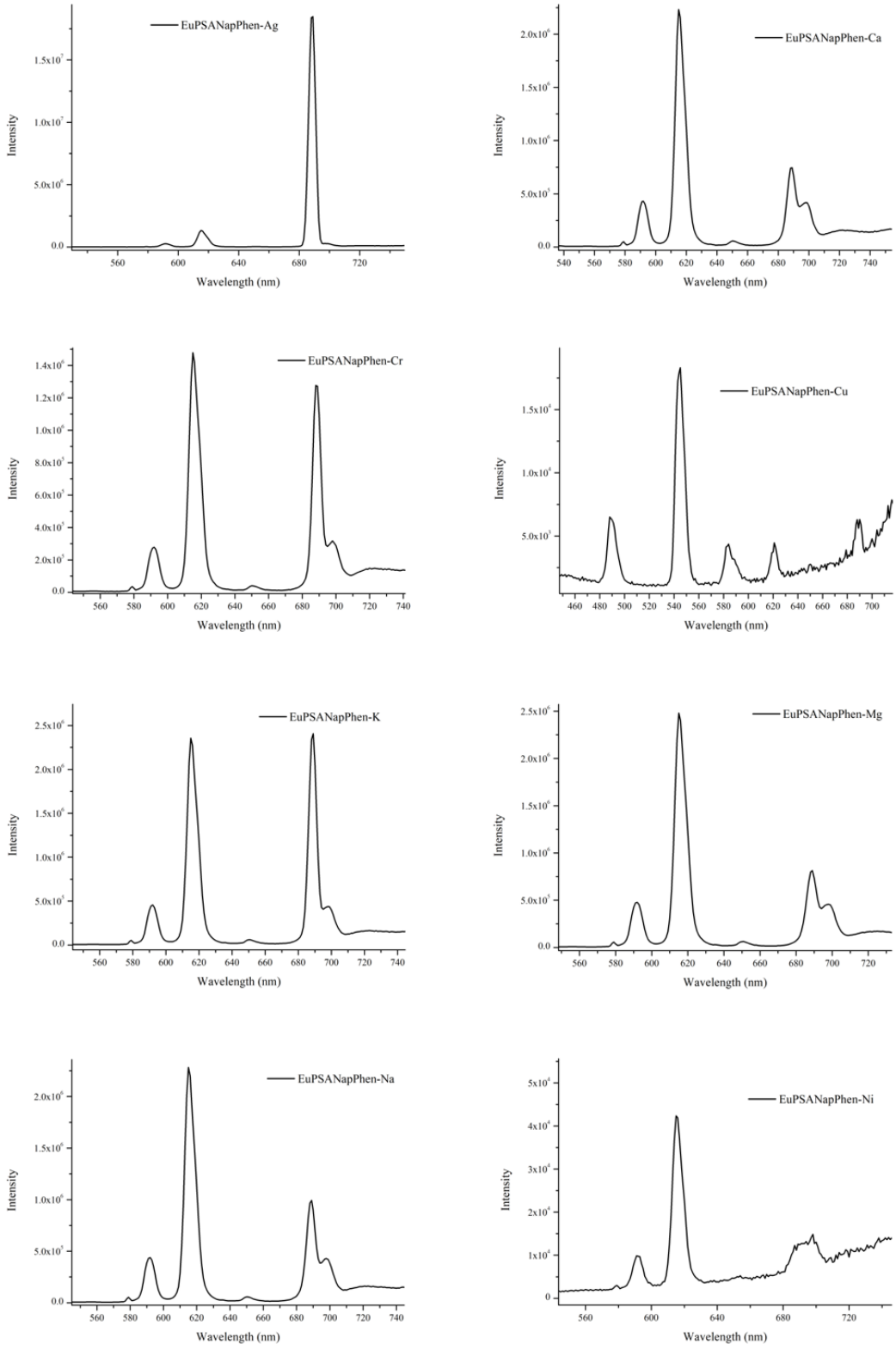

Figure S 5. Emission spectra of EuPSANapPhen-metals (Ag, Ca, Cr, Cu, K, Mg, Na and Ni, respectively) (EtOH:H_2O) solutions (λexc = 344 nm).

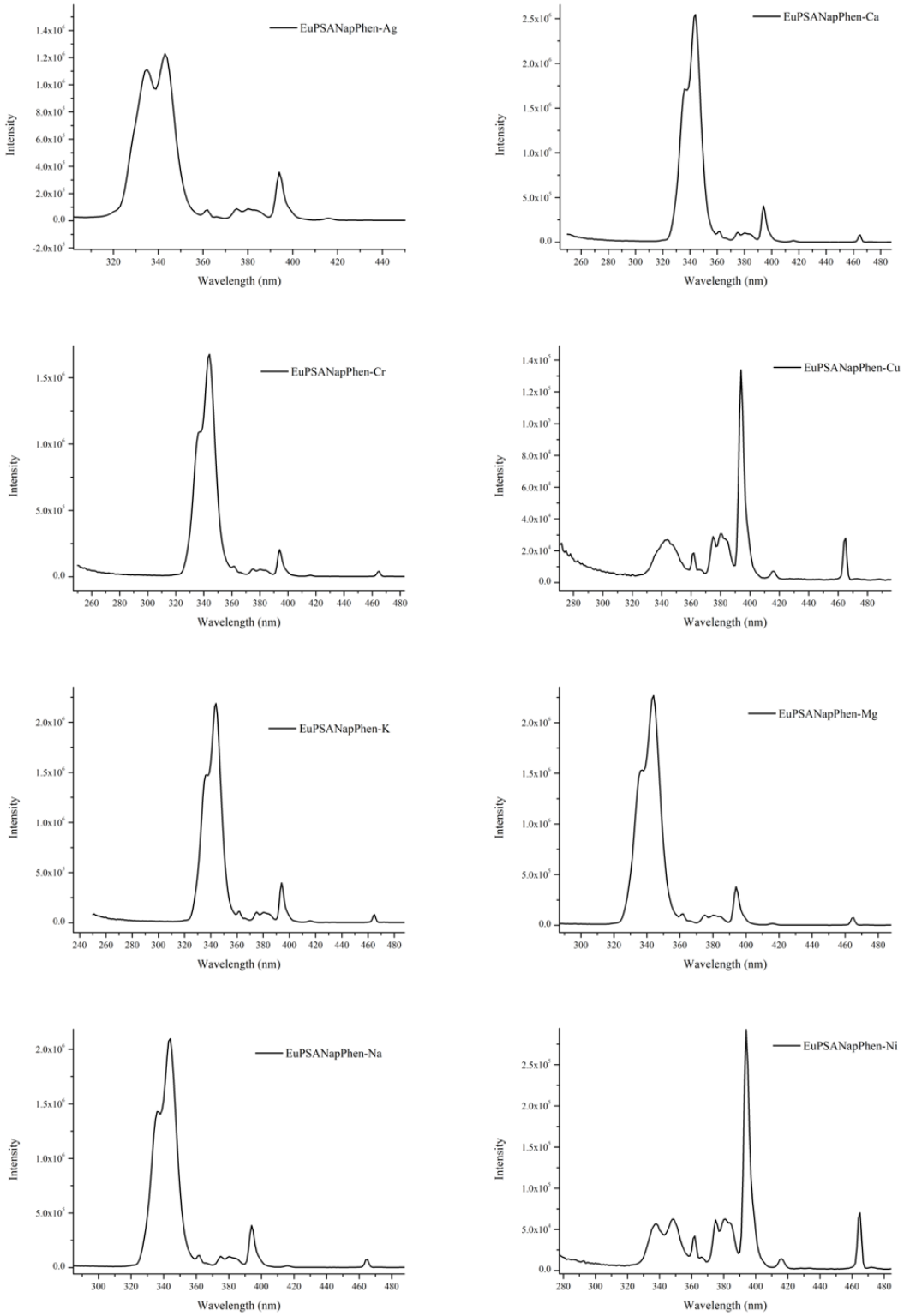

Figure S 6. Excitation spectra of EuPSANapPhen-metals (Ag, Ca, Cr, Cu, K, Mg, Na and Ni, respectively) (EtOH:H_2O) solutions (λem = 616 nm).

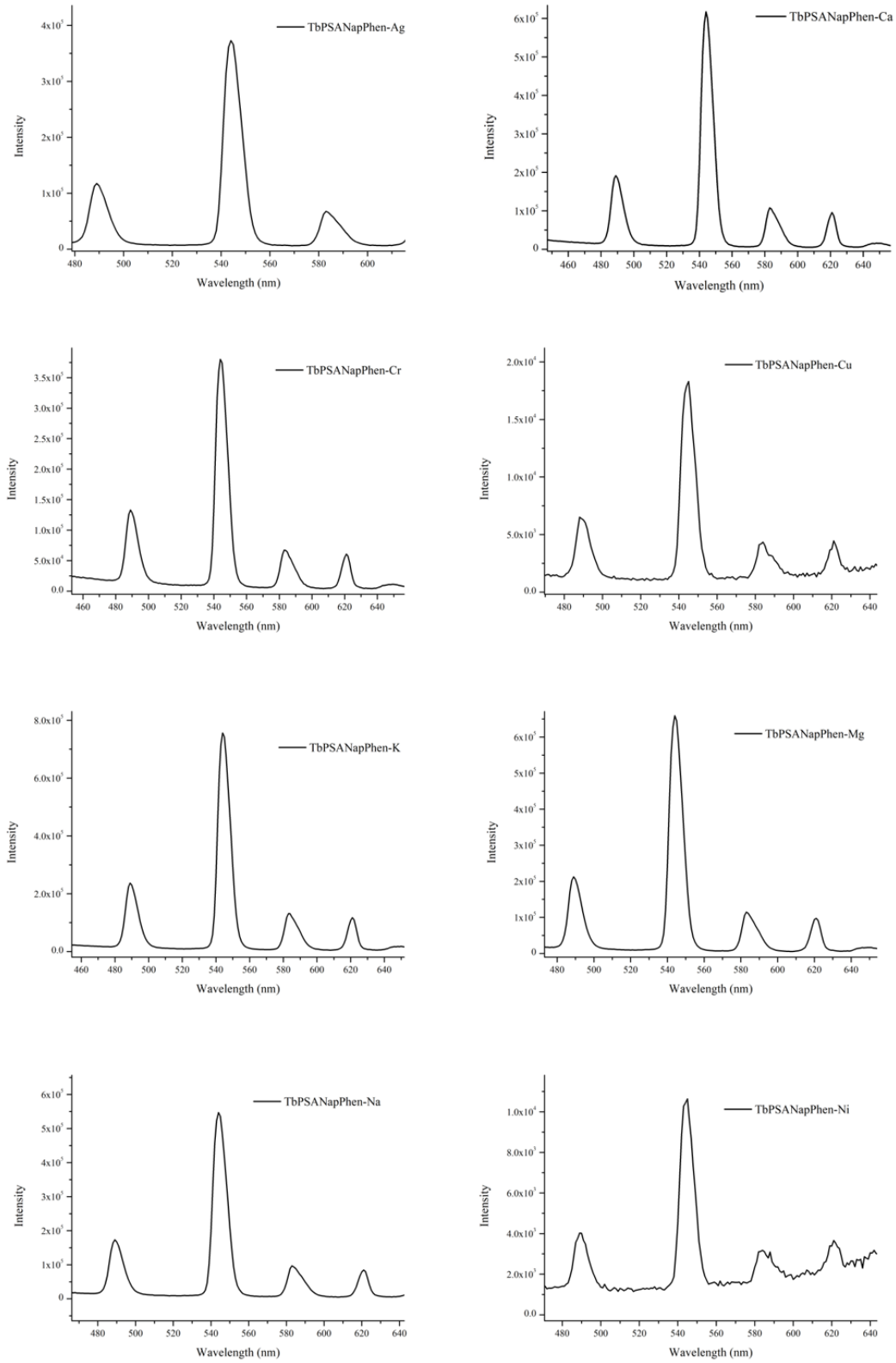

Figure S 7. Emission spectra of TbPSANapPhen-metals (Ag, Ca, Cr, Cu, K, Mg, Na and Ni, respectively) (EtOH:H_2O) solutions (λexc = 344 nm).

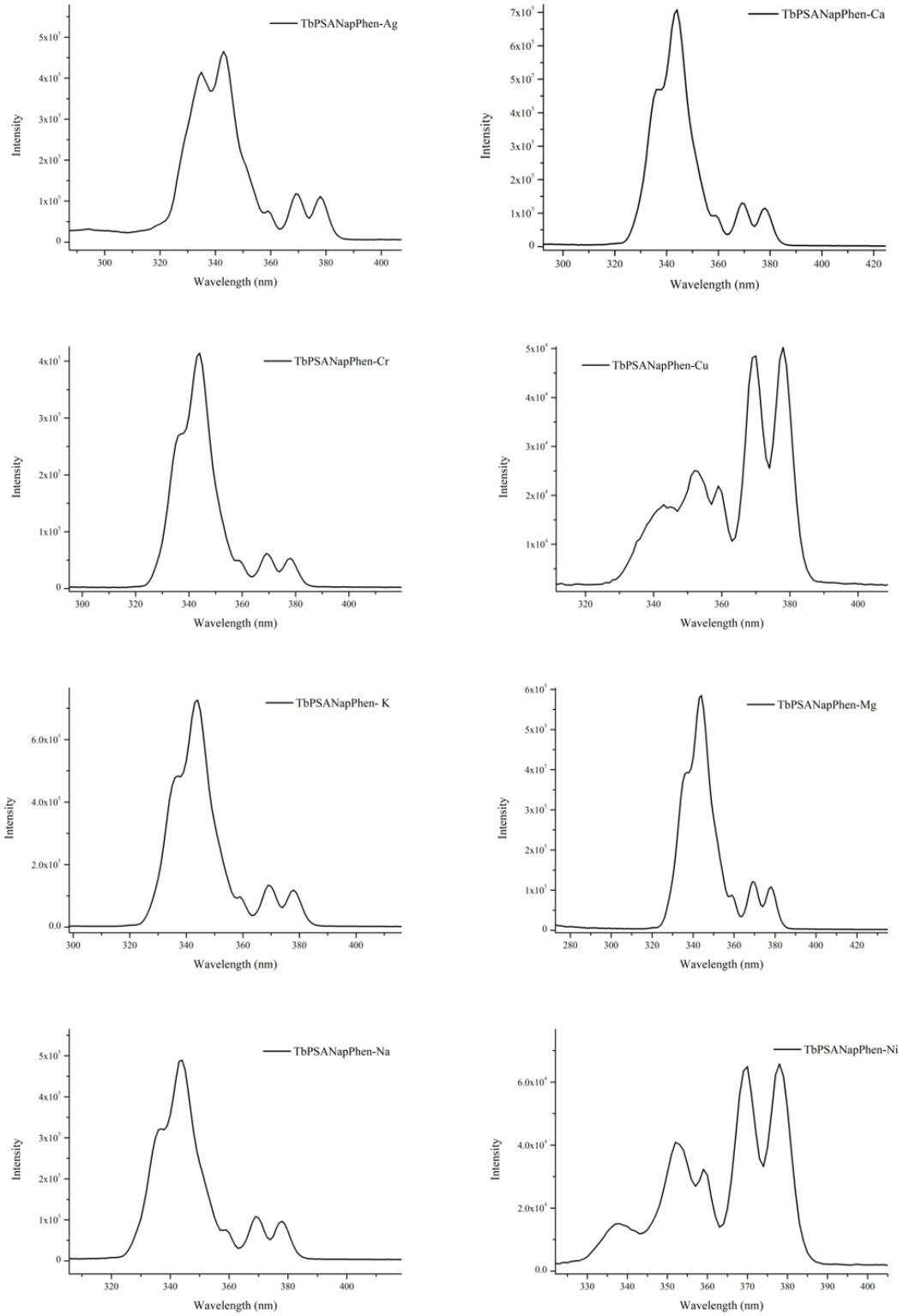

Figure S 8. Excitation spectra of TbPSANapPhen-metals (Ag, Ca, Cr, Cu, K, Mg, Na and Ni, respectively) (EtOH:H_2O) solutions (λem = 543 nm).

7.4 Influence of the anion on the emission of Lanthanide polymer complex solutions

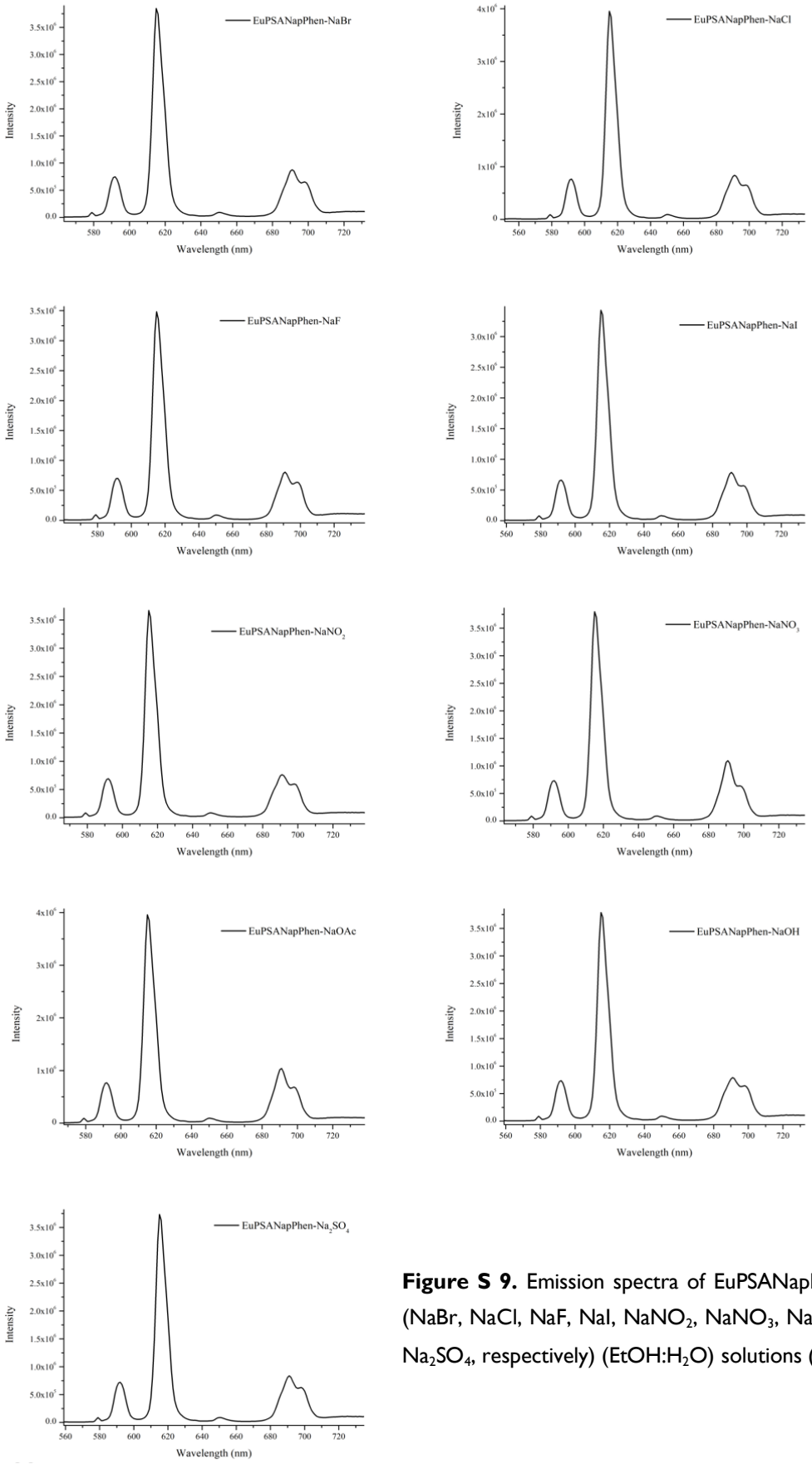

Figure S 9. Emission spectra of EuPSANapPhen-sodium salts (NaBr, NaCl, NaF, NaI, $NaNO_2$, $NaNO_3$, NaOAc, NaOH, and Na_2SO_4, respectively) (EtOH:H_2O) solutions (λexc = 344 nm).

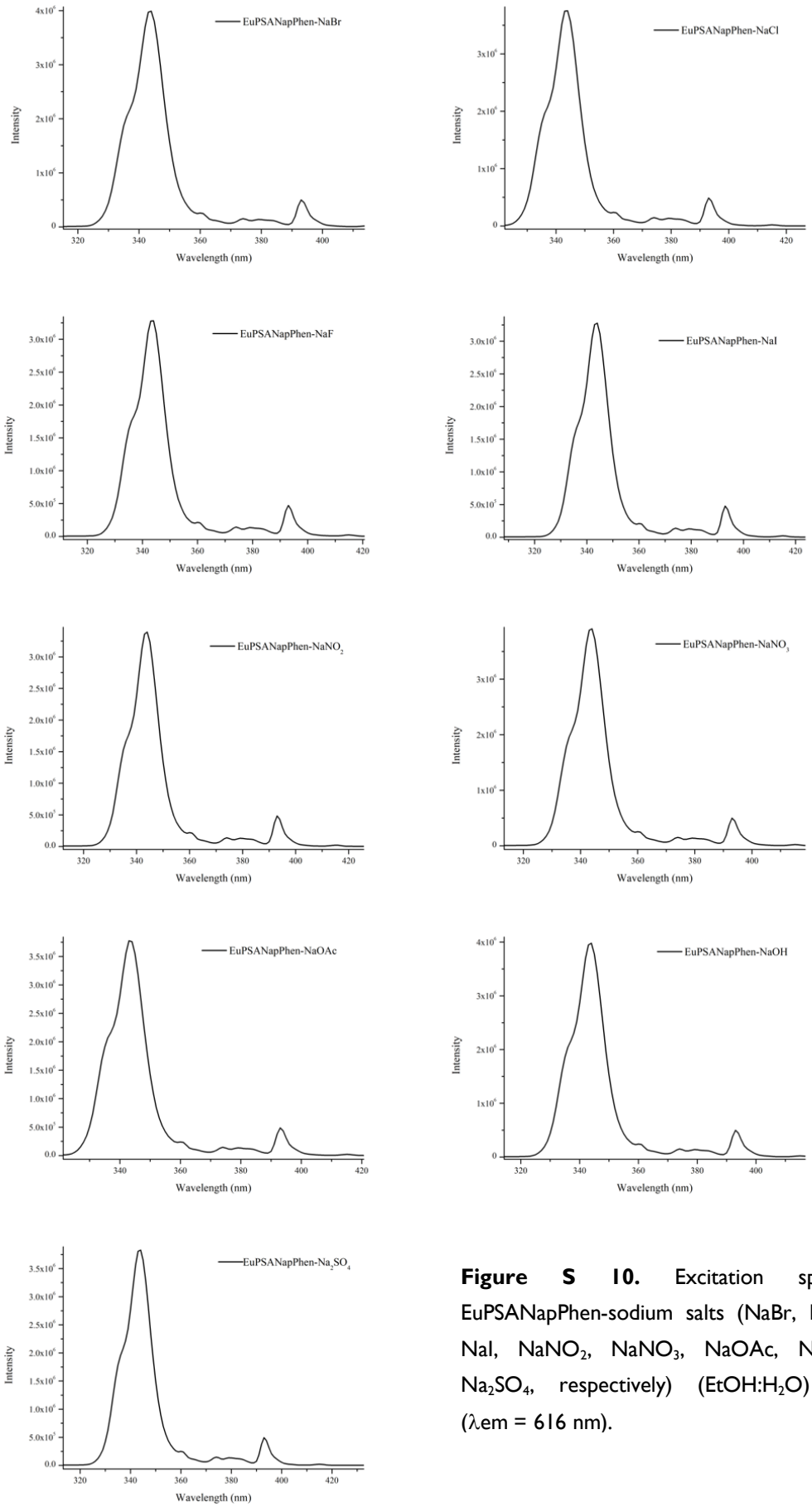

Figure S 10. Excitation spectra of EuPSANapPhen-sodium salts (NaBr, NaCl, NaF, NaI, $NaNO_2$, $NaNO_3$, NaOAc, NaOH, and Na_2SO_4, respectively) (EtOH:H_2O) solutions (λem = 616 nm).

7.5 Detection limit of copper and nickel solutions

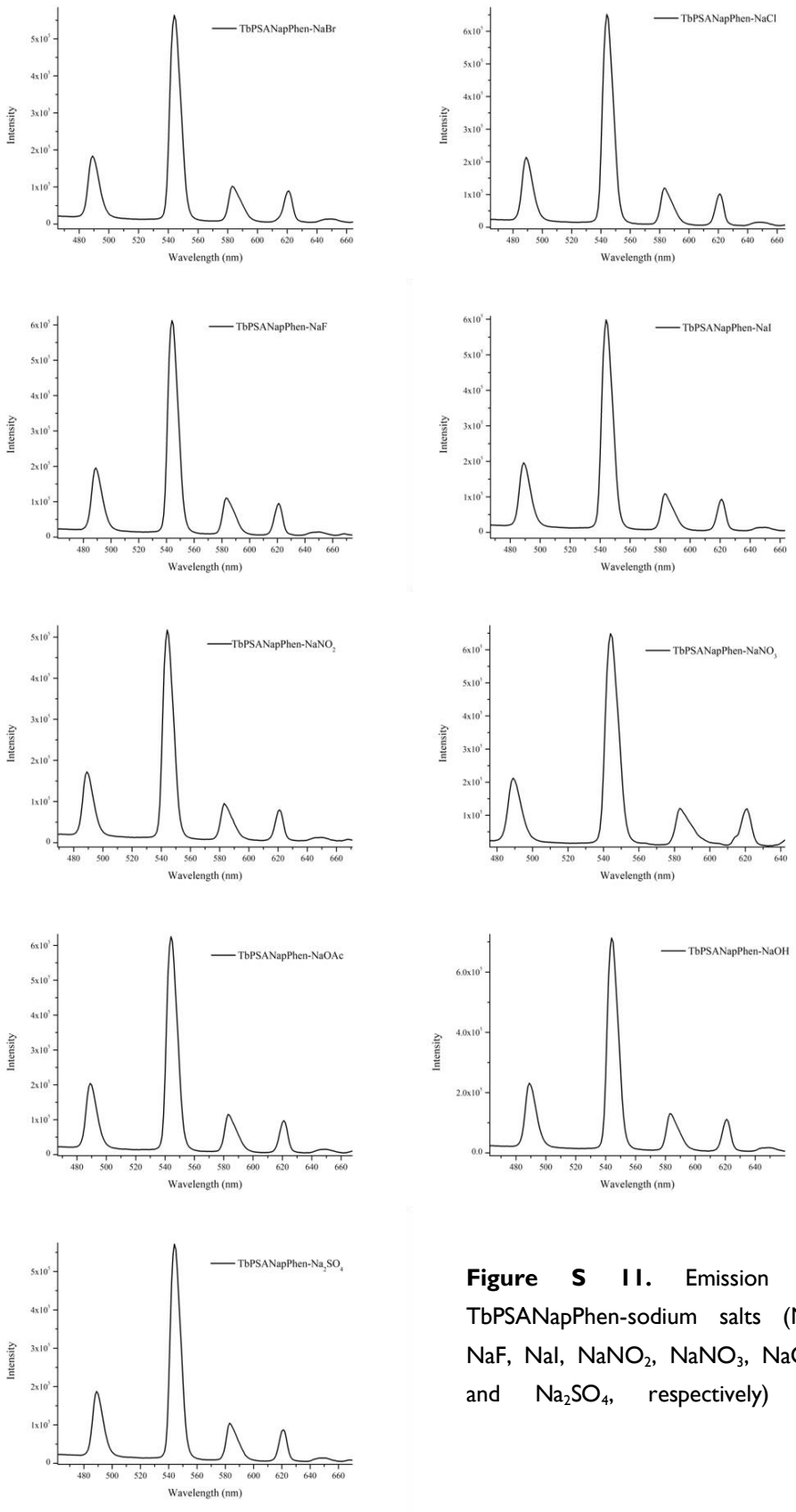

Figure S 11. Emission spectra of TbPSANapPhen-sodium salts (NaBr, NaCl, NaF, NaI, $NaNO_2$, $NaNO_3$, NaOAc, NaOH, and Na_2SO_4, respectively) (EtOH:H_2O)

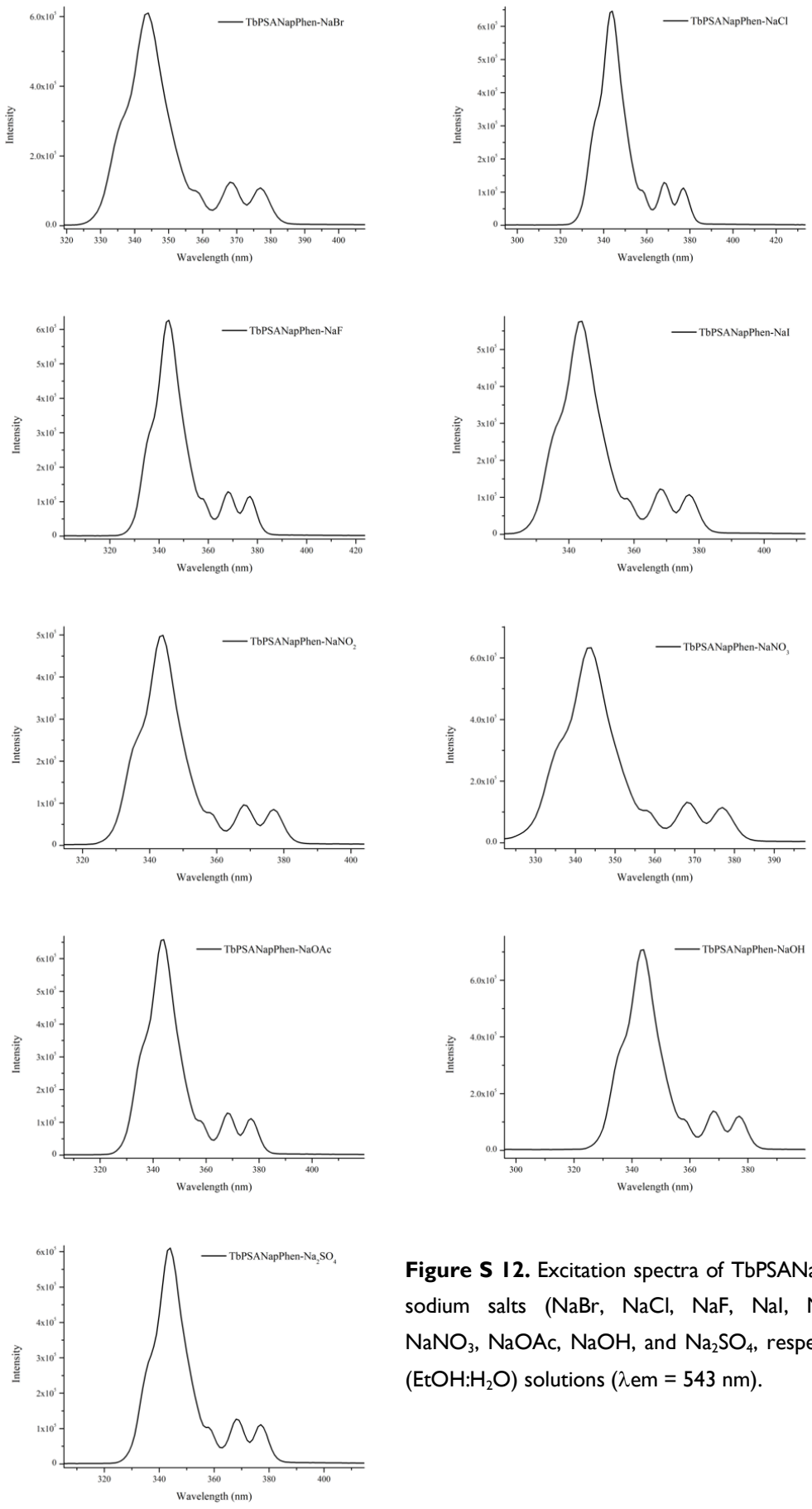

Figure S 12. Excitation spectra of TbPSANapPhen-sodium salts (NaBr, NaCl, NaF, NaI, $NaNO_2$, $NaNO_3$, NaOAc, NaOH, and Na_2SO_4, respectively) (EtOH:H_2O) solutions (λem = 543 nm).

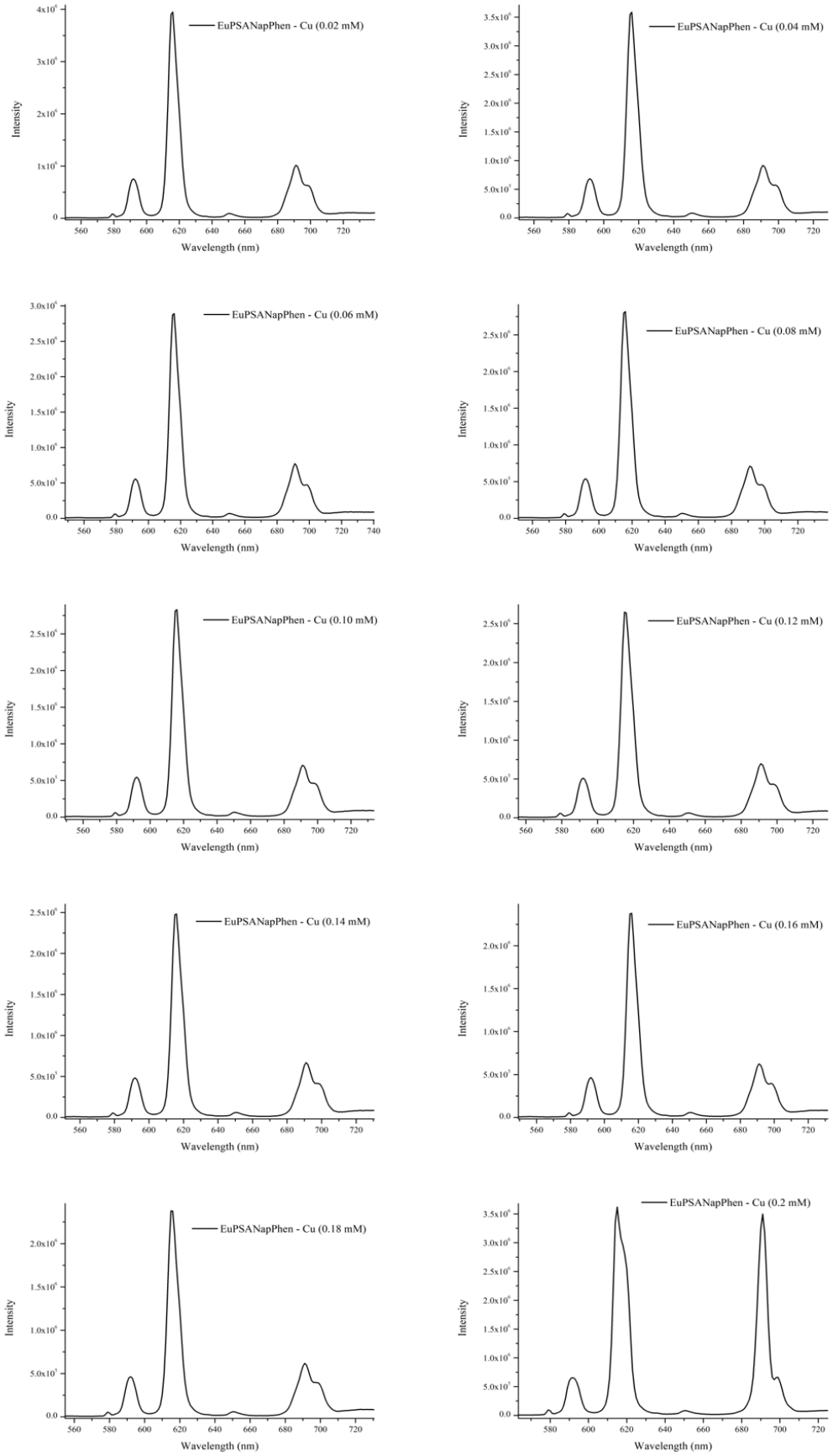

Figure S 13. Emission spectra of EuPSANapPhen-Cu (EtOH:H_2O) in a range of concentrations between 0.02 and 0.2 mM, (λ_{exc} = 344 nm).

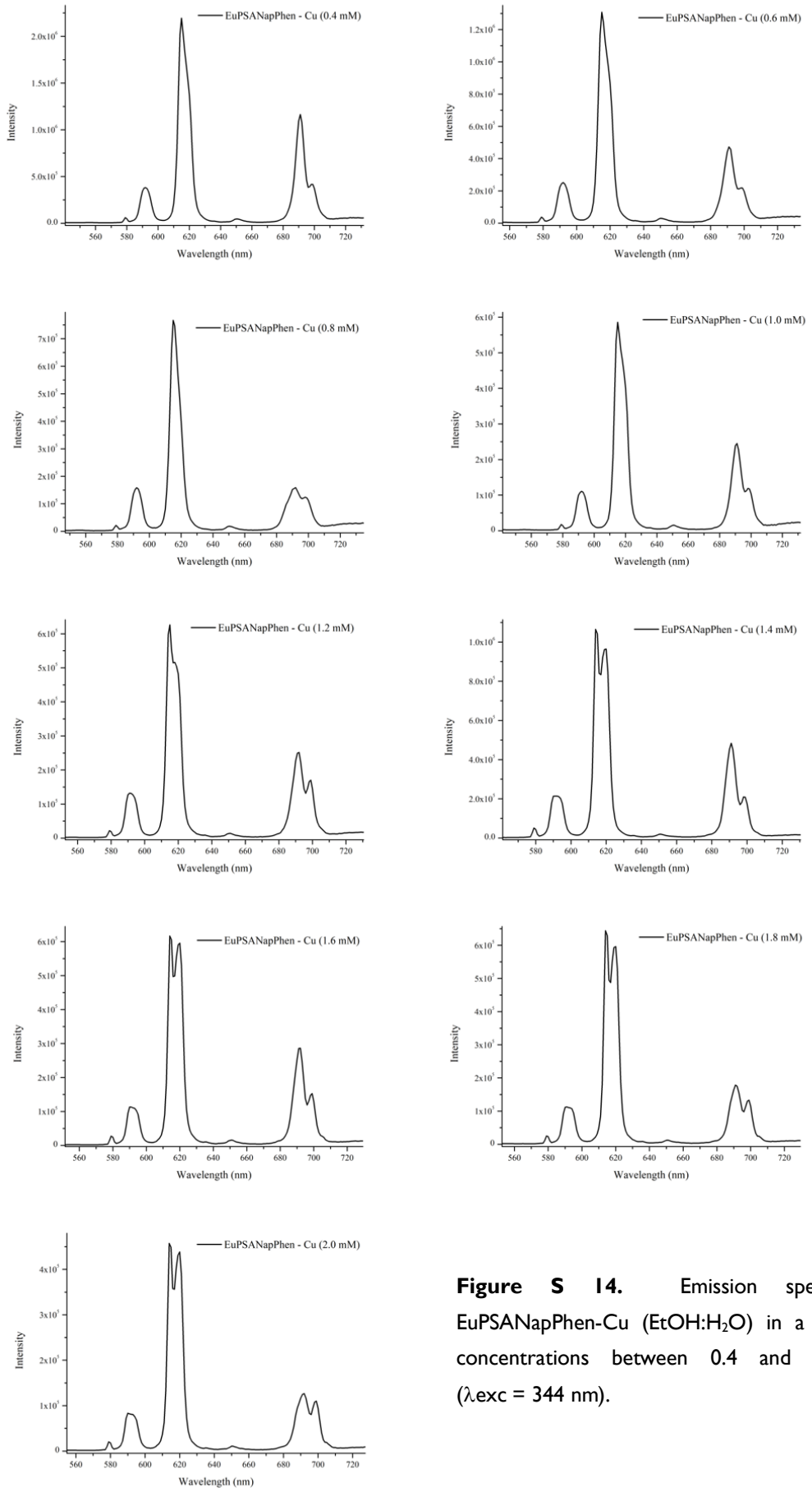

Figure S 14. Emission spectra of EuPSANapPhen-Cu (EtOH:H_2O) in a range of concentrations between 0.4 and 2.0 mM (λexc = 344 nm).

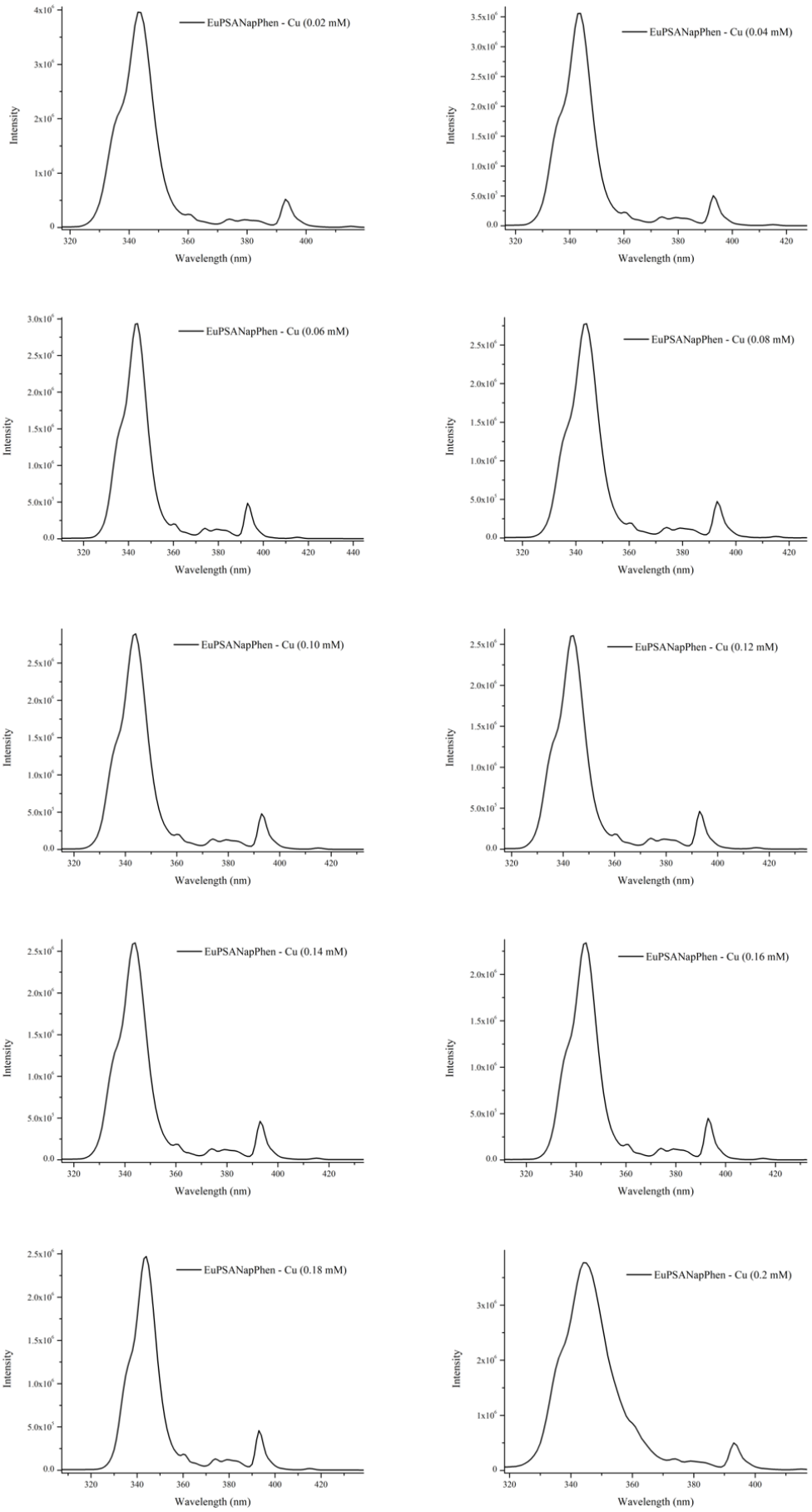

Figure S 15. Excitation spectra of EuPSANapPhen-Cu (EtOH:H_2O) in a range of concentrations between 0.02 and 0.2 mM (λem = 616 nm).

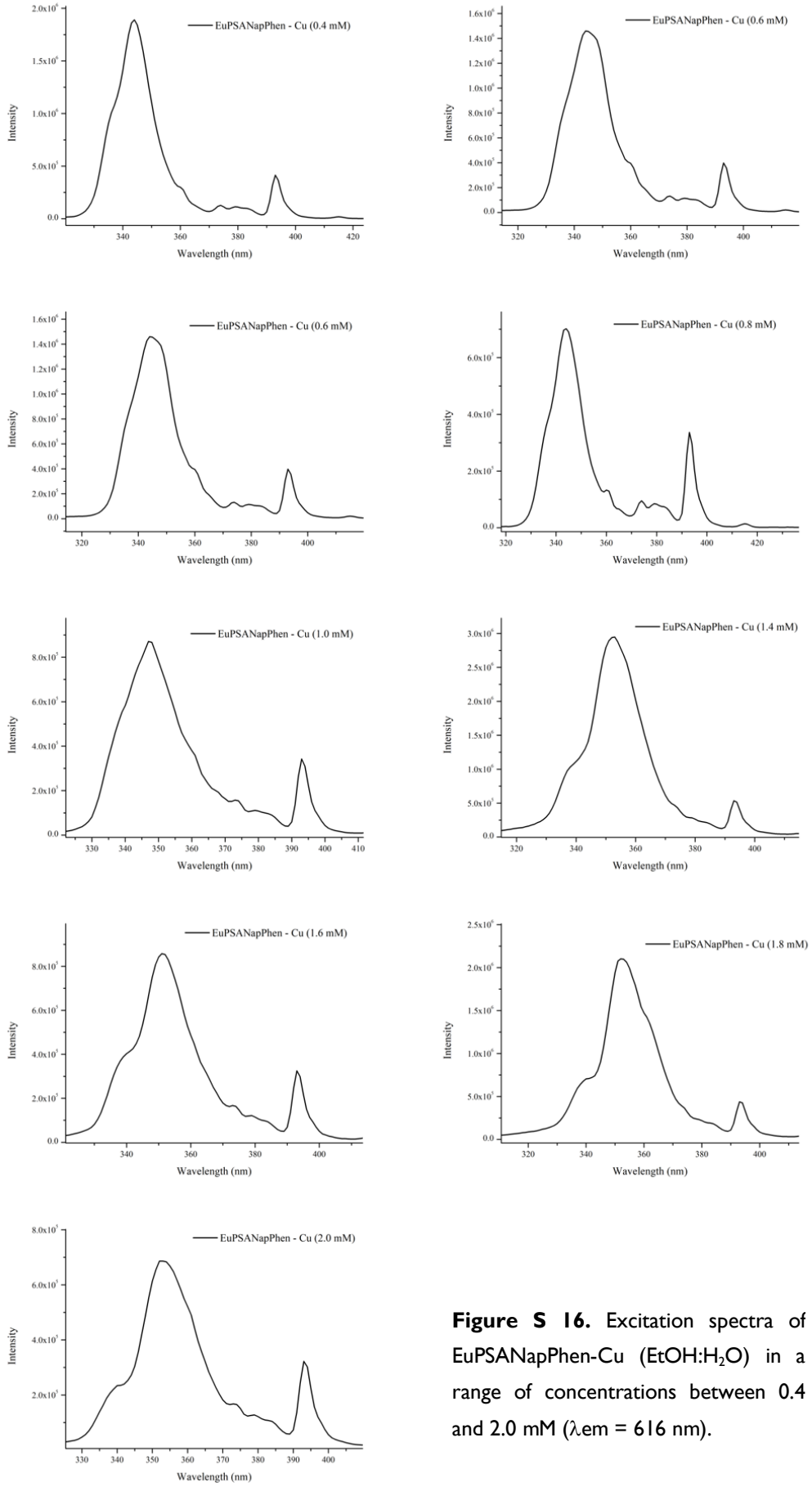

Figure S 16. Excitation spectra of EuPSANapPhen-Cu (EtOH:H_2O) in a range of concentrations between 0.4 and 2.0 mM (λem = 616 nm).

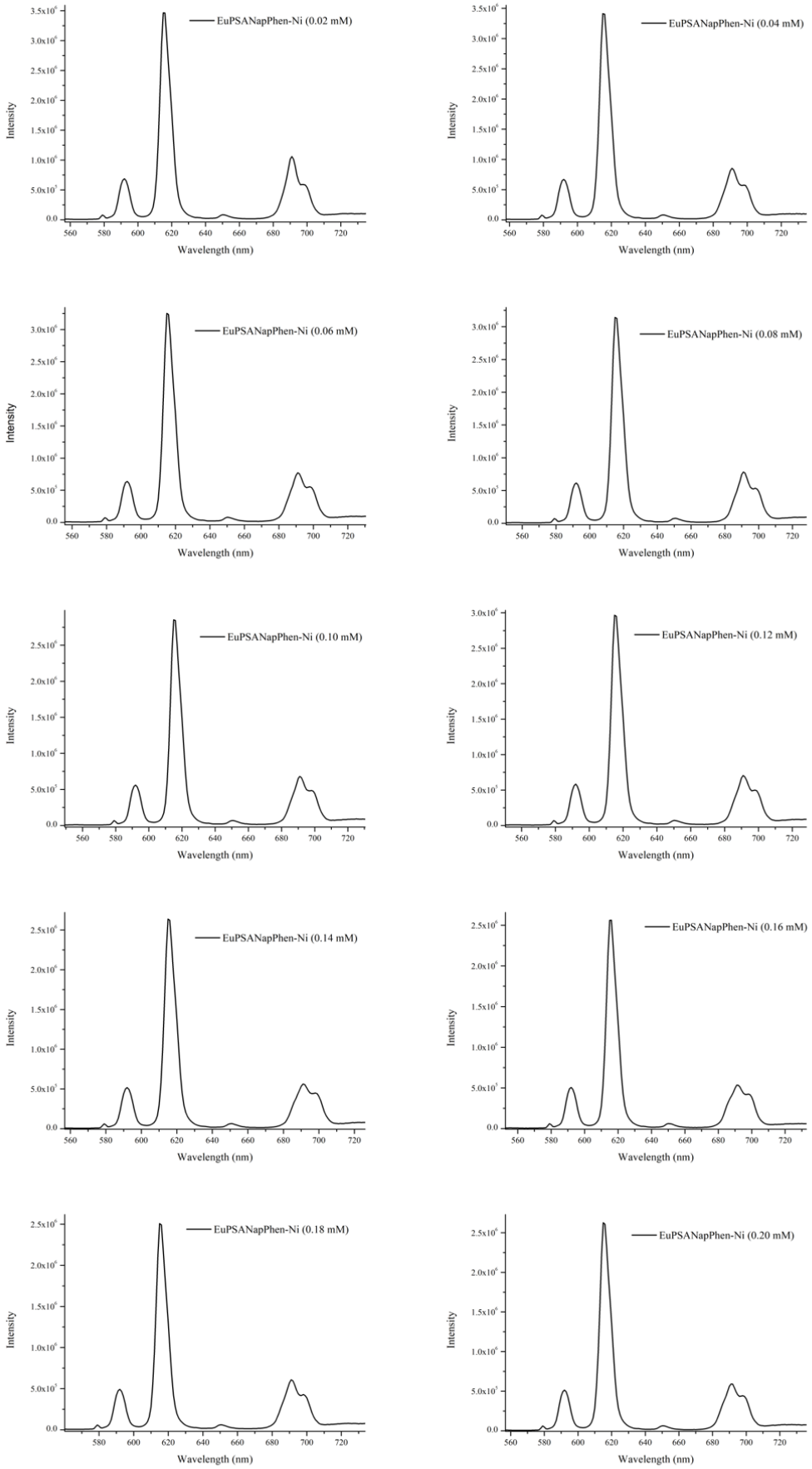

Figure S 17. Emission spectra of EuPSANapPhen-Ni (EtOH:H_2O) in a range of concentrations between 0.02 and 0.2 mM (λexc = 344 nm).

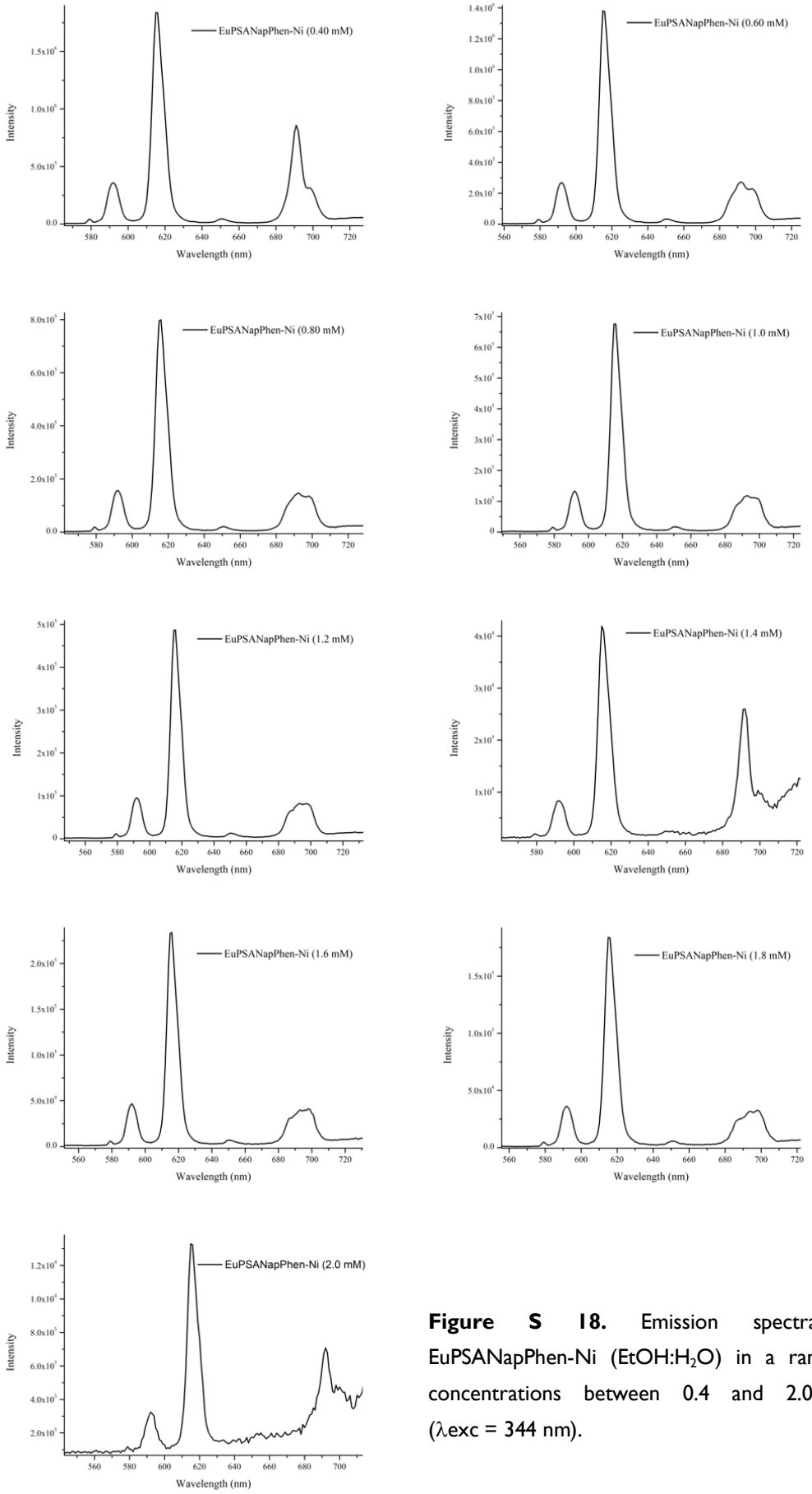

Figure S 18. Emission spectra of EuPSANapPhen-Ni (EtOH:H_2O) in a range of concentrations between 0.4 and 2.0 mM (λexc = 344 nm).

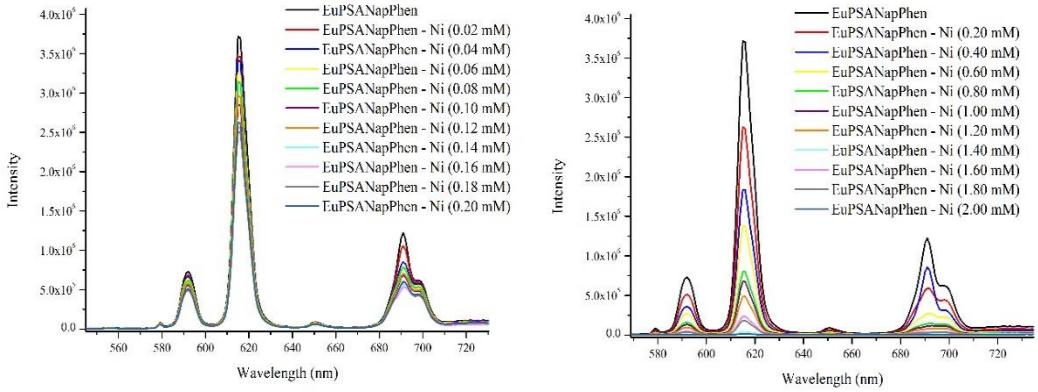

Figure S 19. Emission spectra of EuPSANapPhen solutions (EtOH:H_2O) in the presence of $Ni(NO_3)_2.6H_2O$ in the concentrations from 0.02 mM to 2 mM (λexc = 344 nm).

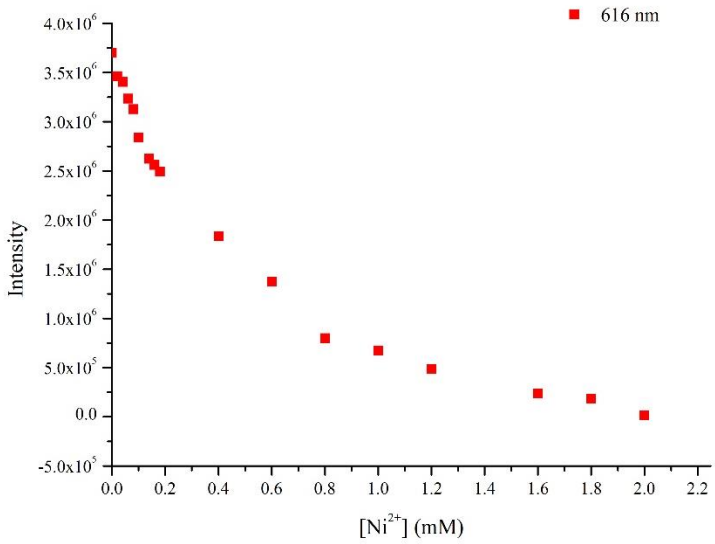

Figure S 20. Dependence of the emission intensity of EuPSANapPhen ($^5D_0 \rightarrow {}^7F_2$ transition) / Ni(II) mixed solutions on the Ni(II) concentration.

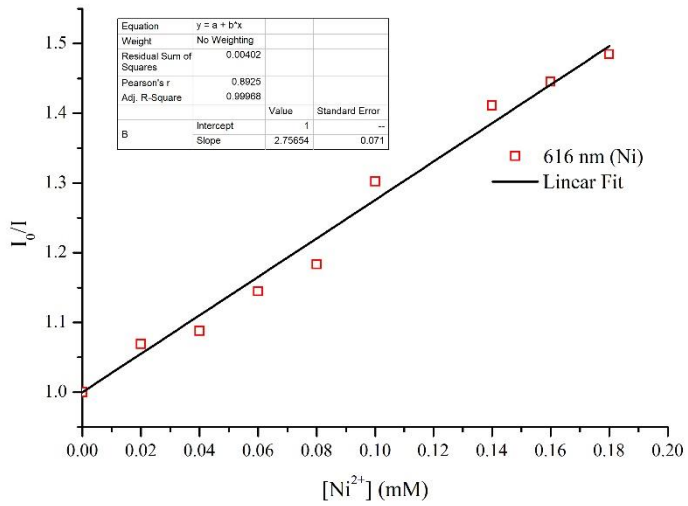

Figure S 21. Stern-Volmer plot of EuPSANapPhen-Ni $^5D_0 \rightarrow {}^7F_2$ transition (616 nm), ranging Ni(II) concentration.

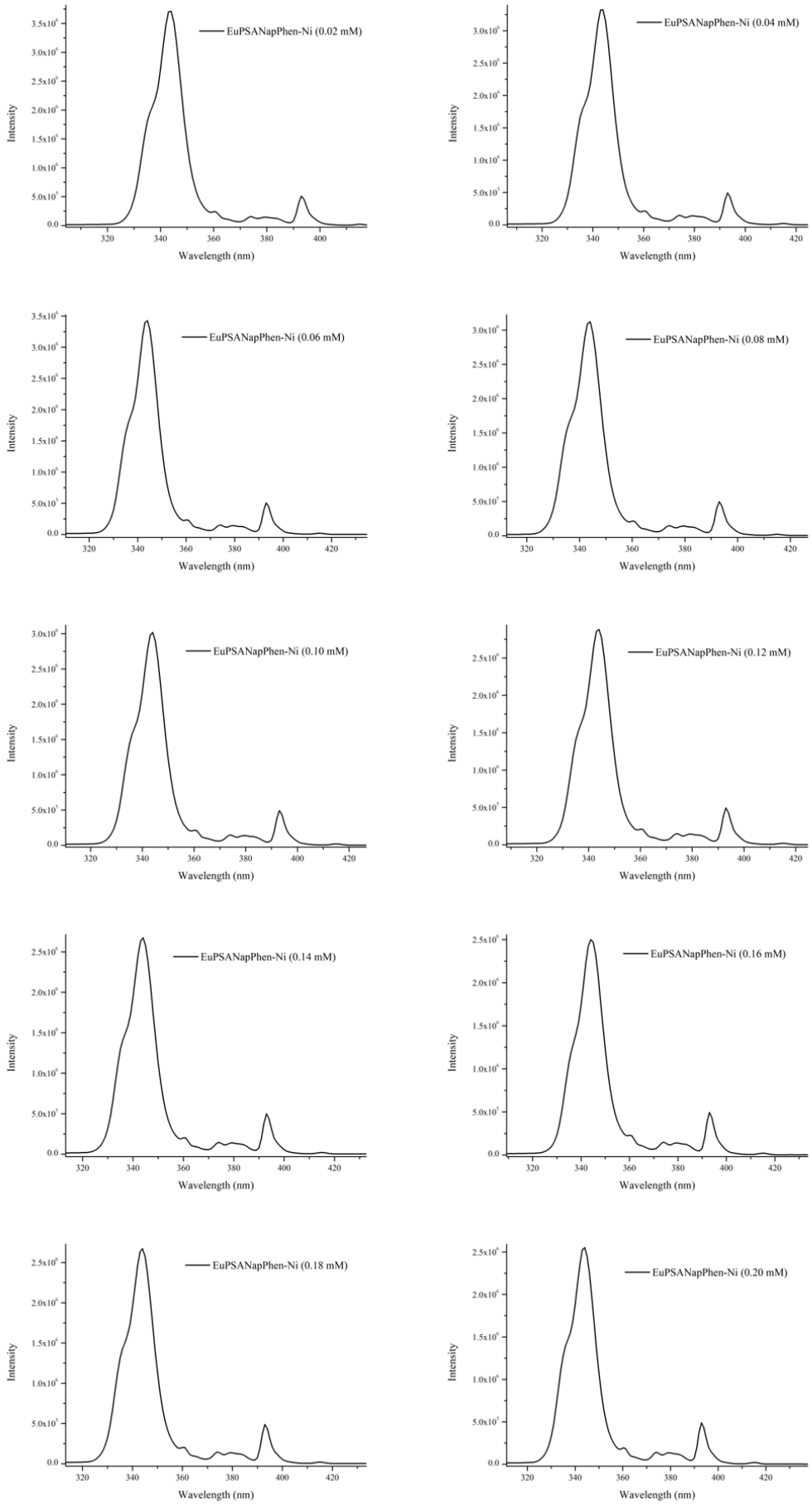

Figure S 22. Excitation spectra of EuPSANapPhen-Ni (EtOH:H_2O) in a range of concentrations between 0.02 and 0.2 mM (λem = 616 nm).

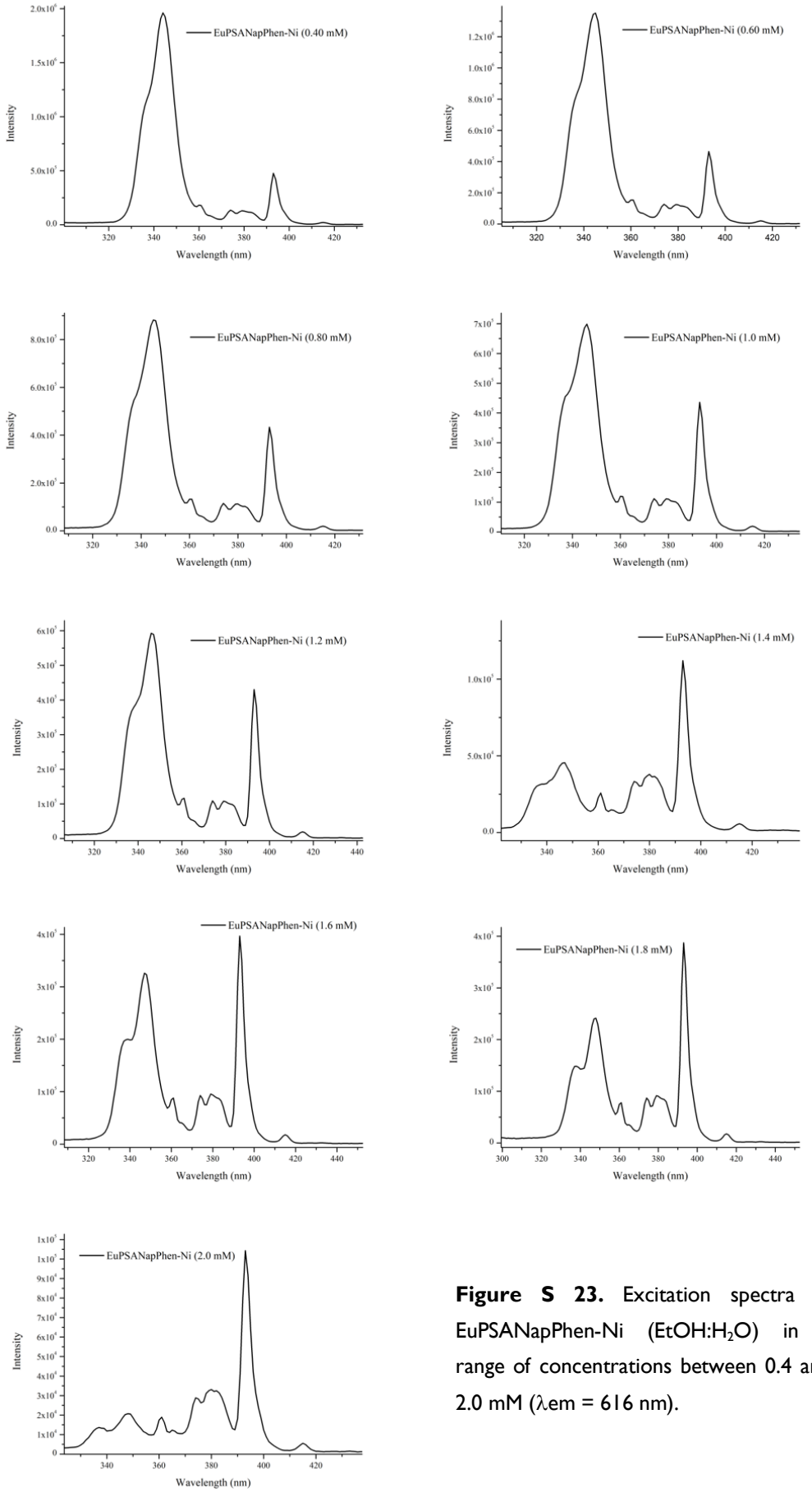

Figure S 23. Excitation spectra of EuPSANapPhen-Ni (EtOH:H_2O) in a range of concentrations between 0.4 and 2.0 mM (λem = 616 nm).

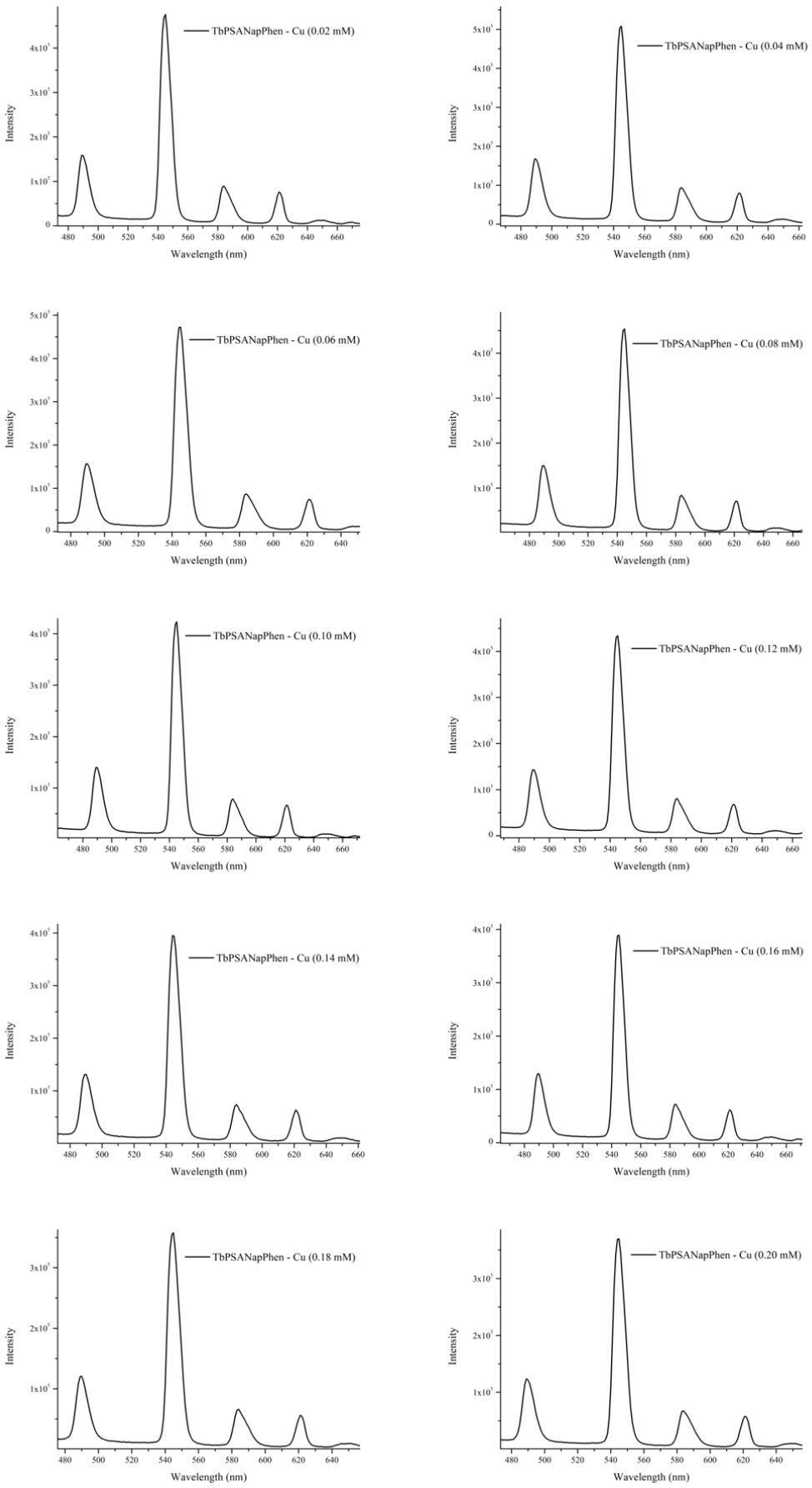

Figure S 24. Emission spectra of TbPSANapPhen-Cu (EtOH:H_2O) in a range of concentrations between 0.02 and 0.2 mM (λexc = 344 nm).

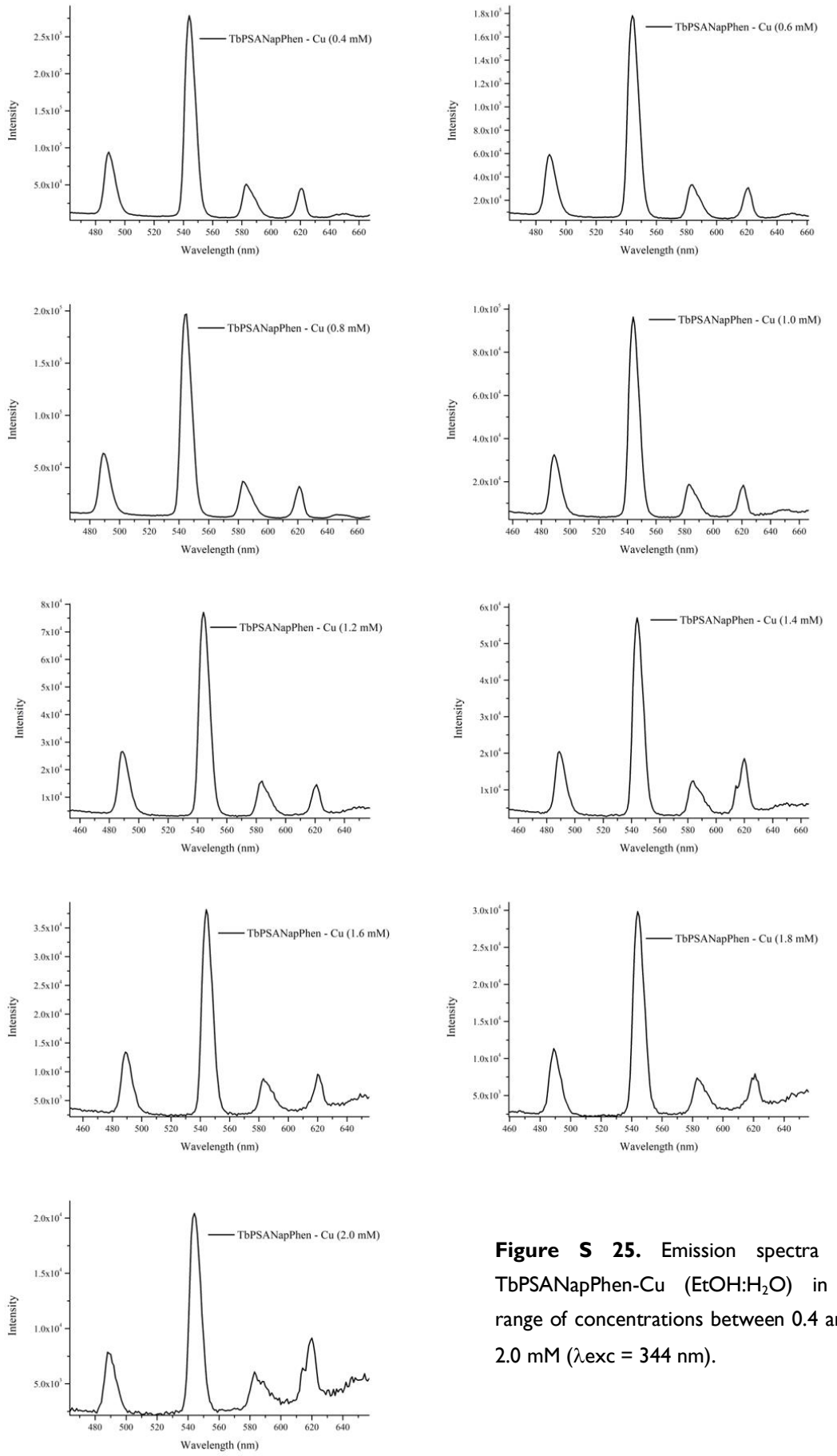

Figure S 25. Emission spectra of TbPSANapPhen-Cu (EtOH:H_2O) in a range of concentrations between 0.4 and 2.0 mM (λexc = 344 nm).

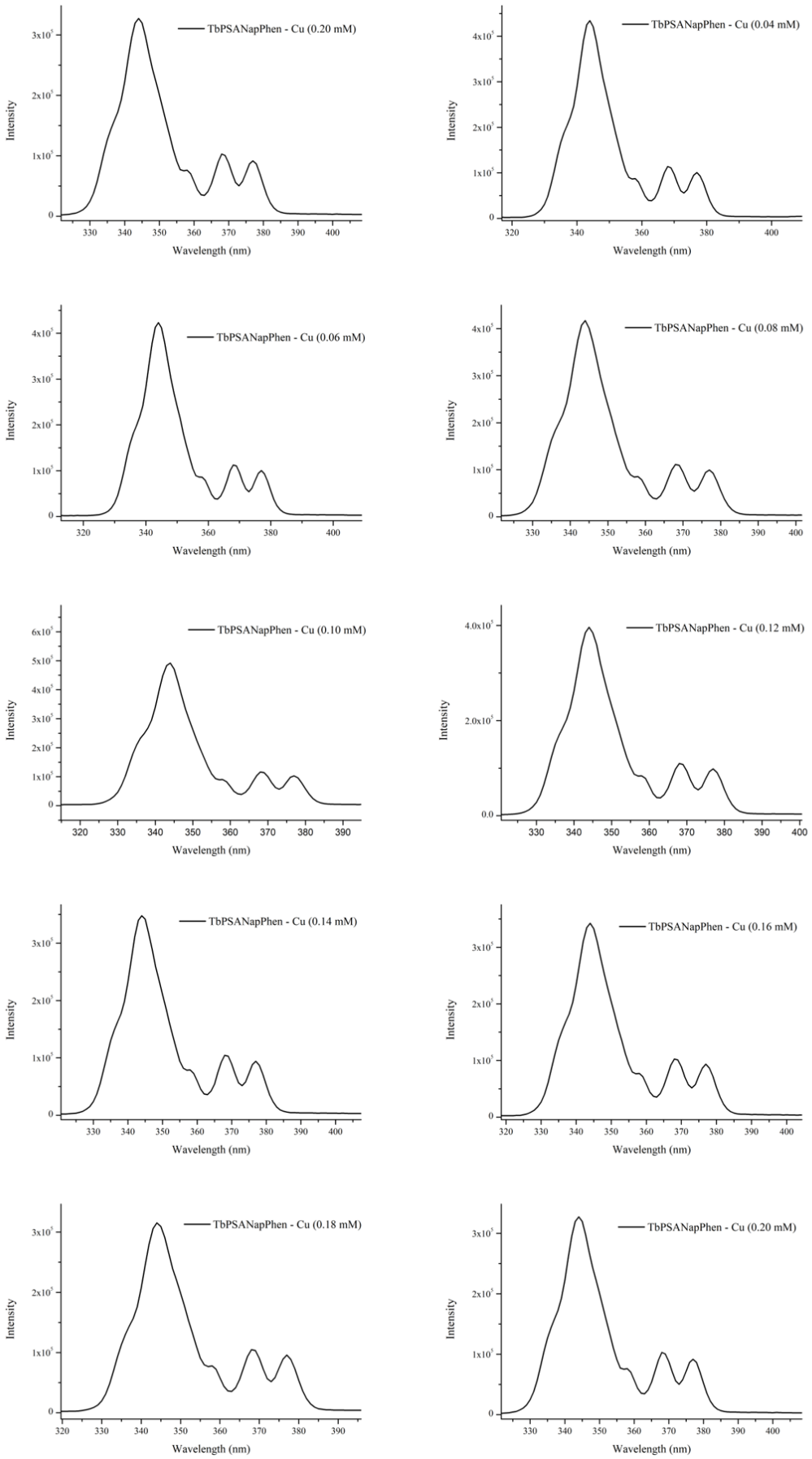

Figure S 26. Excitation spectra of TbPSANapPhen-Cu (EtOH:H_2O) in a range of concentrations between 0.02 and 0.2 mM (λem = 543 nm).

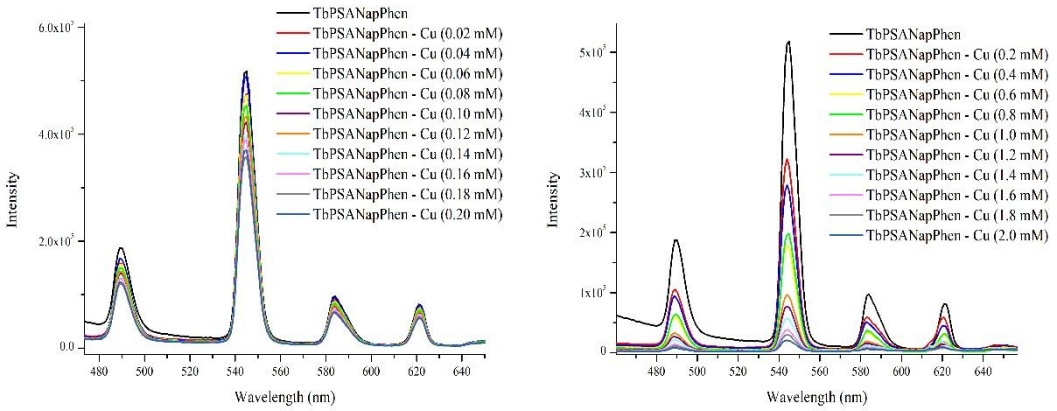

Figure S 27. Emission spectra of TbPSANapPhen solutions (EtOH:H_2O) in the presence of $Cu(NO_3)_2$ in the concentrations from 0.02 mM to 2 mM (λexc = 344 nm).

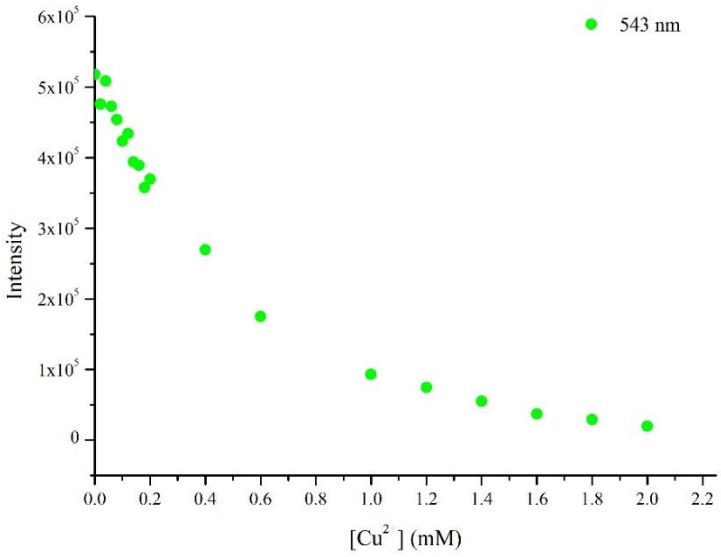

Figure S 28. Dependence of the emission intensity of TbPSANapPhen ($^5D_4 \rightarrow {}^7F_5$ transition) / Cu(II) mixed solutions on the Cu(II) concentration.

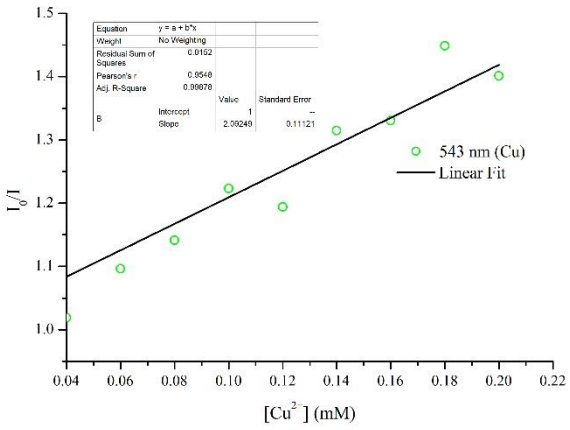

Figure S 29. Stern-Volmer plot of TbPSANapPhen-Cu $^5D_4 \rightarrow {}^7F_5$ transition (543 nm), ranging Cu concentration.

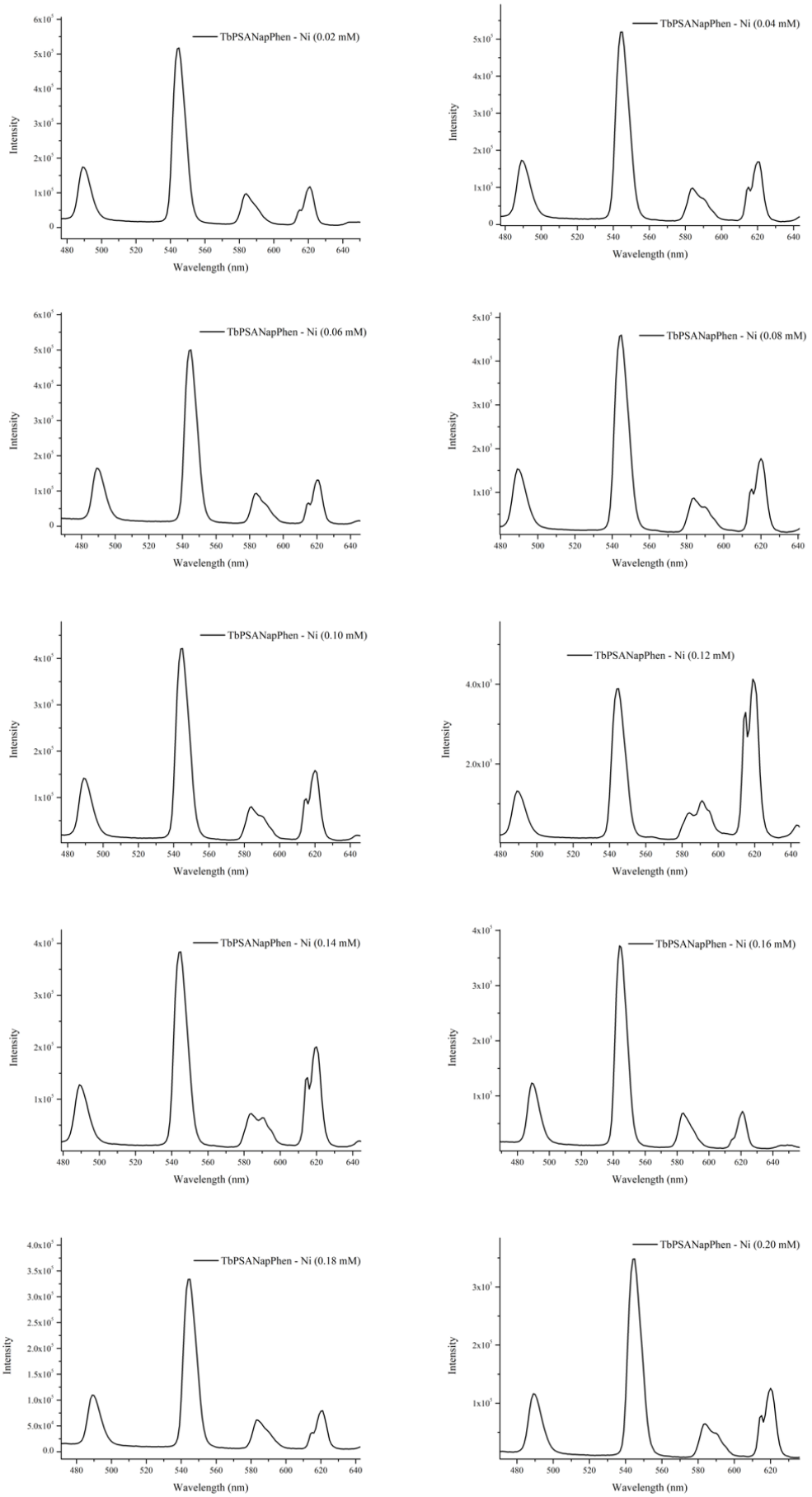

Figure S 30. Emission spectra of TbPSANapPhen-Ni (EtOH:H_2O) in a range of concentrations between 0.02 and 0.2 mM (λexc = 344 nm).

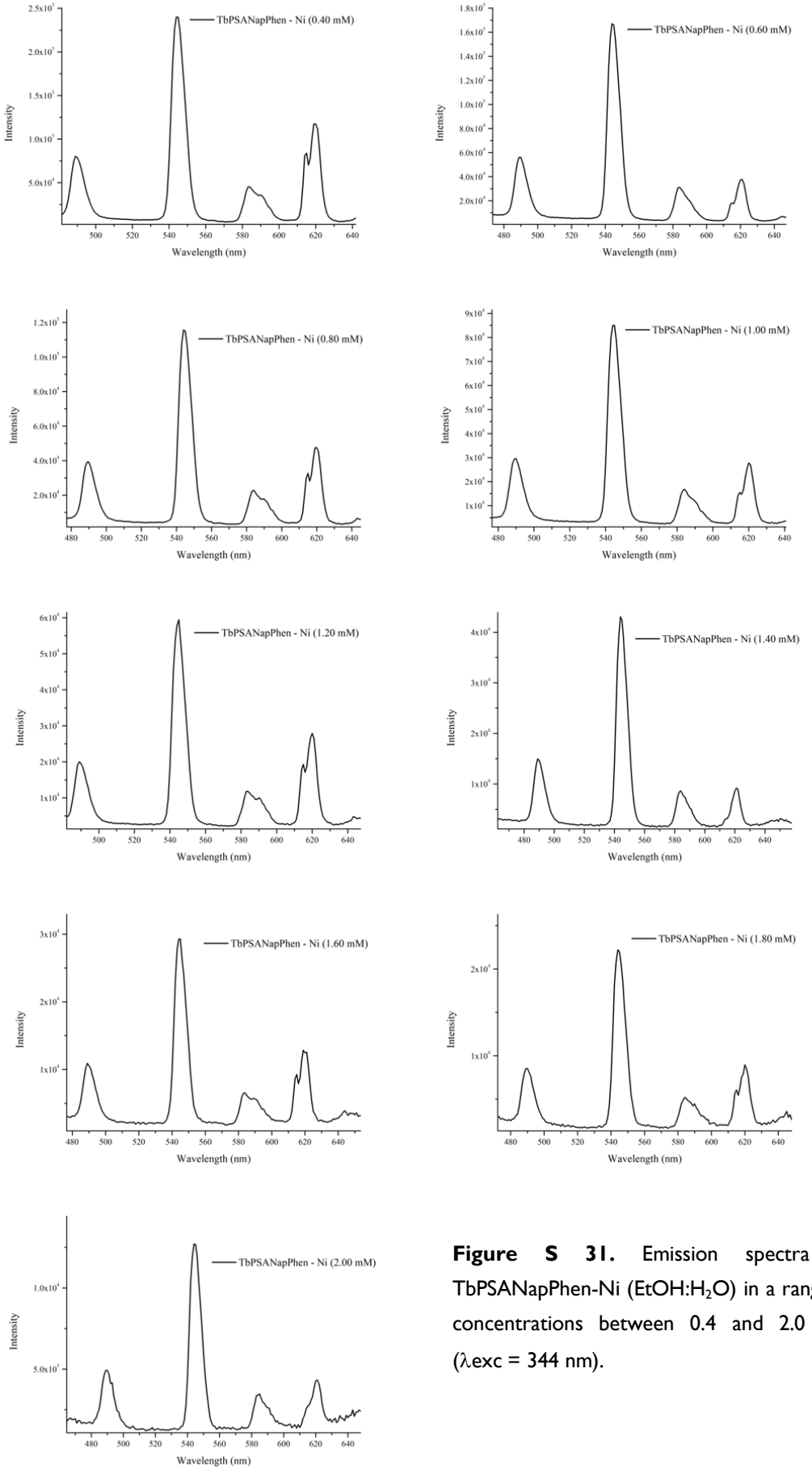

Figure S 31. Emission spectra of TbPSANapPhen-Ni (EtOH:H_2O) in a range of concentrations between 0.4 and 2.0 mM (λexc = 344 nm).

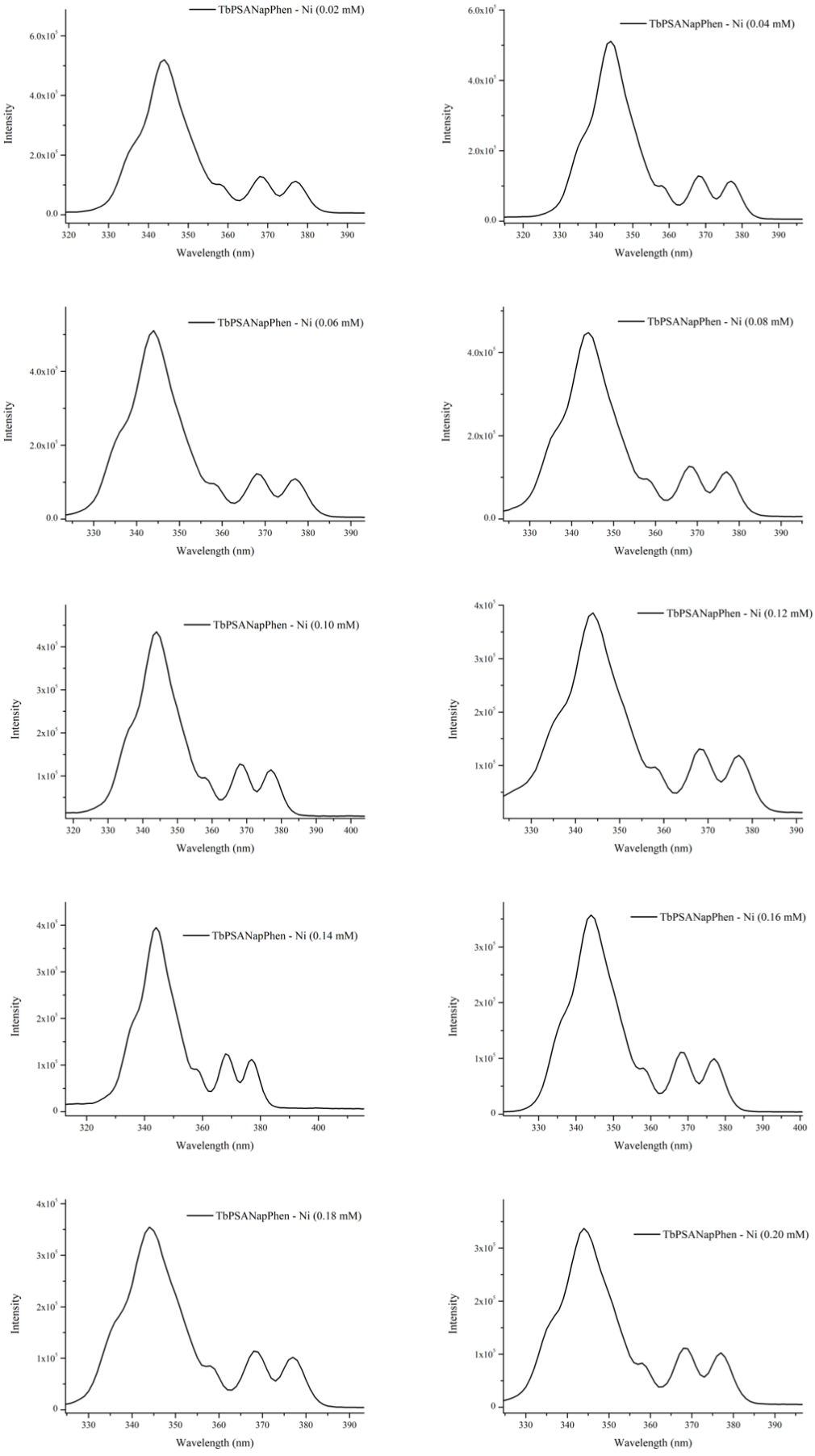

Figure S 32.Excitation spectra of TbPSANapPhen-Ni (EtOH:H_2O) in a range of concentrations between 0.02 and 0.2 mM, (λem = 543 nm).

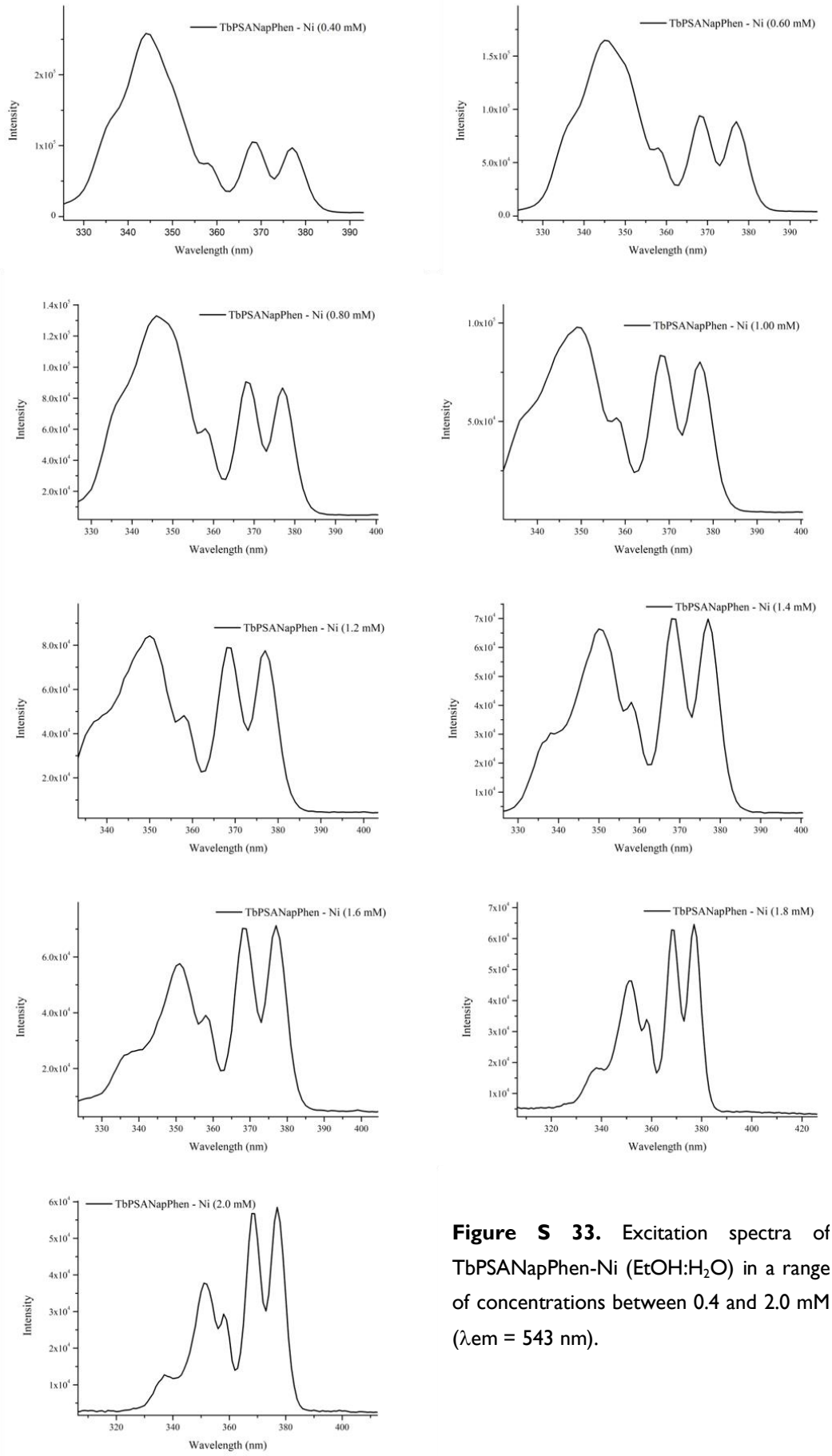

Figure S 33. Excitation spectra of TbPSANapPhen-Ni (EtOH:H_2O) in a range of concentrations between 0.4 and 2.0 mM (λem = 543 nm).

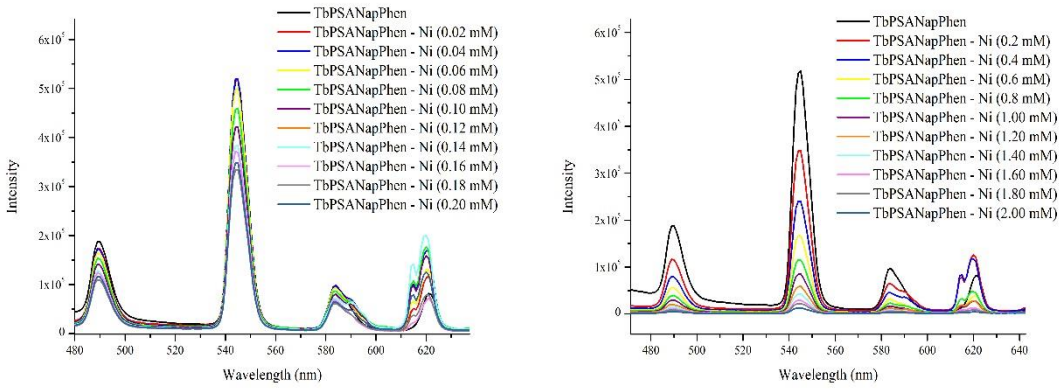

Figure S 34. Emission spectra of TbPSANapPhen solutions (EtOH:H_2O) in the presence of $Ni(NO_3)_2.6H_2O$ in the concentrations from 0.02 mM to 2 mM (λexc = 344 nm).

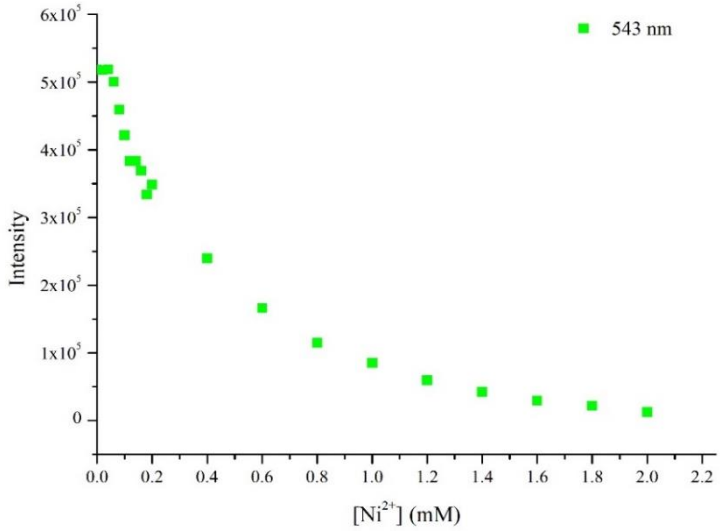

Figure S 35. Dependence of the emission intensity of TbPSANapPhen ($^5D_4 \rightarrow {}^7F_5$ transition) / Ni(II) mixed solutions on the Ni(II) concentration.

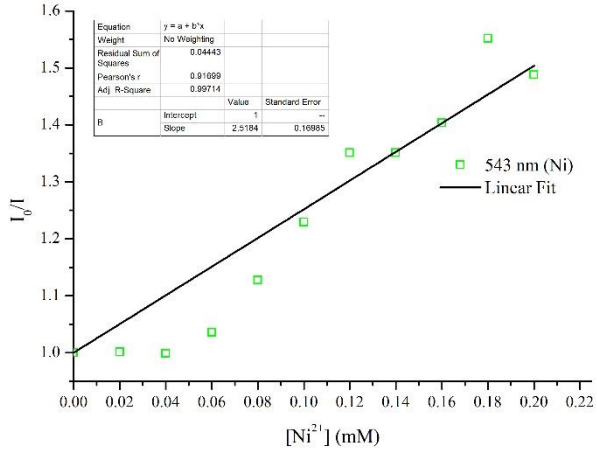

Figure S 36. Stern-Volmer plot of TbPSANapPhen-Ni $^5D_4 \rightarrow {}^7F_5$ transition (543 nm), ranging Ni concentration.

7.6 Costs Information

In the following table can be observed the prices of the all of the reagents used in this master thesis.

Table S 1. Prices of all the reagents used in this master thesis.

$EuCl_3.6H_2O$	Sigma Aldrich	5g – 78.10 €	15.62 €/g
		25g – 464.00 €	18.56 €/g
$TbCl_3.6H_2O$	Sigma Aldrich	5g – 66.40€	13.28 €/g
		25g – 288.00€	11.52 €/g
PSA	Sigma Aldrich	100g – 75.70€	0.76 €/g
		500g – 193.00€	0.39 €/g
Nap	Sigma Aldrich	25g – 24.10€	0.95 €/g
Phen	Sigma Aldrich	2.5g – 34.60€	13.84 €/g
		5g – 49.90 €	9.98 €/g
		25g – 174.00 €	6.96 €/g
		100g – 367.00 €	3.67 €/g

To prepare 50 mL of solution of EuPSANapPhen and TbPSANapPhen, which is the volume used for each step of incorporation of the lanthanide polymer complex in the paper, and the same volume which is freeze-dried for the use in the coating process, the amount of reagents necessary and the most expensive costs are explicit on Table S2 and Table S3, respectively.

Table S 2. Specific costs for the production of a 50 mL EuPSANapPhen solution.

$EuCl_3.6H_2O$	0.229 g	4.25 €
PSA	1.313 g	0.99 €
Nap	0.108 g	0.10 €
Phen	0.113 g	1.56 €
TOTAL		6.90 €

Table S 3. Specific costs for the production of a 50 mL TbPSANapPhen solution.

$TbCl_3.6H_2O$	0.233 g	3.09 €
PSA	1.313 g	0.99 €
Nap	0.108 g	0.10 €
Phen	0.113 g	1.56 €
TOTAL		5.74 €